APPLICATION OF STATISTICAL PHYSICS IN HUMAN PHYSIOLOGY:

HEART-BRAIN DYNAMICS

Gyanendra Bohara

Dissertation Prepared for the Degree of

DOCTOR OF PHILOSOPHY

UNIVERSITY OF NORTH TEXAS

August 2018

APPROVED:

Paolo Grigolini, Major Professor
Gary A. Glass, Committee Member
Duncan Weathers, Committee Member
Yuri Rostovtsev, Committee Member
Michael Monticino, Interim Chair of the Department of Physics
Su Gao, Dean of the College of Science
Victor Prybutok, Dean of the Toulouse Graduate School

Bohara, Gyanendra. *Application of Statistical Physics in Human Physiology: Heart-Brain Dynamics*. Doctor of Philosophy (Physics), August 2018, 98 pp., 1 table, 34 figures, 117 numbered references.

This dissertation is devoted to study of complex systems in human physiology particularly heartbeats and brain dynamics. We have studied the dynamics of heartbeats that has been a subject of investigation of two independent groups. The first group emphasized the multifractal nature of the heartbeat dynamics of healthy subjects, whereas the second group had established a close connection between healthy subjects and the occurrence of crucial events. We have analyzed the same set of data and established that in fact the heartbeats are characterized by the occurrence of crucial and Poisson events. An increase in the percentage of crucial events makes the multifractal spectrum broader, thereby bridging the results of the former group with the results of the latter group. The crucial events are characterized by a power index that signals the occurrence of 1/f noise for complex systems in the best physiological condition.

These results led us to focus our analysis on the statistical properties of crucial events. We have adopted the same statistical analysis to study the statistical properties of the heartbeat dynamics of subjects practicing meditation. The heartbeats of people doing meditation are known to produce coherent fluctuations. In addition to this effect, we made the surprising discovery that meditation makes the heartbeat depart from the ideal condition of 1/f noise.

We also discussed how to combine the wave-like nature of the dynamics of the brain with the existence of crucial events that are responsible for the 1/f noise. We showed that the anomalous scaling generated by the crucial events could be established by means of a direct analysis of raw data. The efficiency of the direct analysis procedure is made possible by the fact that periodicity and crucial events is the product of a spontaneous process of self-organization. We argue that the results of this study can be used to shed light into the nature of this process of self-organization.

TABLE OF CONTENTS

LIST OF TABLES

LIST OF FIGURES

CHAPTER 1

INTRODUCTION

This chapter intends to provide a general outline of the present dissertation. It gives a general thought of comprehension about my research work and how the dissertation is sorted out. It additionally clarifies some essential ideas that we have to know to comprehend the entire work specified in this document. All of the studies to be discussed based on various complex systems so we need to know about complex systems first.

1.1. Complex Systems

A complex system is neither a perfectly ordered nor a chaotic system. It is actually an intermediate condition between them. If the system is perfectly ordered or chaotic, then it is easy to formulate them numerically and the future is deterministic. However, in most complex systems mathematical formulation isn't simple and what's to come isn't well known. We have to follow a probabilistic approach to forecast the future. A unified definition of complexity is not yet well established. But there is common agreement between investigators that a complex system is a system which comprises of an extensive number of particles, components or constituents and the interaction between them generates nonlinear dynamics which is frequently portrayed by a power law distribution.

$$\psi(\tau) \propto \frac{1}{\tau^{\mu}} \tag{1.1}$$

Where $\psi(\tau)$ is the waiting time distribution (WTD), τ is the distance between two consecutive events of a nonlinear system and μ is the complexity index. A Complex system may also be characterized by different scaling of self-organized and self similar patterns resulting from the interaction between its constituents.

The essence of statistical physics is that it deals with the complex systems, which exist everywhere. There are several examples of complex systems in the real world, e.g., the dynamics of Stock Markets, Earthquakes, Human Brains, Heartbeat dynamics, Internet

networks, High- way traffic and etc. This dissertation is devoted to study of complex systems in human physiology particularly Heartbeats and Brain dynamics. We recommend readers [1, 2, 3, 4, 5] for more insight about complex system studies.

1.2. History

"the Second Law of Thermodynamics only applies in an equilibrium state. And we've now demonstrated the universe is in a radically non-equilibrium state. The universe is not falling apart. Its enthralling, creative, participating. And life is a natural outcome of a creative universe. We are part of an unfolding universe of increasing complexity in which living things have co-evolved with other living things, mutually make livings together, are functionally coupled and mutually unfolding " Stuart Kauffman [6].

" You cannot reverse the evolution of the universe, even theoretically. And you cannot predict its future, except in terms of scenarios that depend on never-ending series of crossroads in the chain of causality " Ilya Prigogine [6].

Complexity is a very broad interdisciplinary subject. It covers many fields like *Physics*, *Biology*, *Chemistry*, *Sociology*, *Ecology*, *Geology* etc. However, there is no long history of complexity studies compare to other natural sciences. Theoretical modeling and quantitative investigation of it has been ascending since 20th century with the advent of advanced digital and analog computers. Complexity theory is also called Post Newtonian Paradigm theory. As indicated by Newton our universe is steady and predictable, which we know now no true any longer. Poincare in 1910 found that three body problem can't be solved, which implies that our universe is a million- body system in an out of equilibrium condition, which is not predictable. Investigators in the 19th century likewise discovered that the Second law of thermodynamics is only applicable to closed and isolated systems. It doesn't hold true for open systems. These two ideas drive the world to think toward complexity theory [6]. Numerous inteligent individuals devoted their lives to the study of complexity. Mainly, there were three uderlying foundations of complexity in 20th century [7]. American Cybernetics shaped by splendid individuals in Mathematics (Norbert Wiener, John von

Neumann, Walter Pitts), Engineering(Julian Bigelow, Claude Shannon) and Neurobiology (Rafael Lorente de No, Arturo Rosenblueth, Warren McCulloch) in 1946. Causality, feedback networks, artificial intelligence, and communication were among its main themes. Similarly, General systems theory, considered as an European counterpart to American Cybernatics headed by Ludwig von Bertalanffy was evolving since 1920. Afterward, Von Bertalanffy, moved to North America and formed the Society for General Systems Research (SGSR) in 1956 at Stanford, with Ralph Gerard, Kenneth Boulding, and Anatol Rapoport. System dynamics is another foundation of complexity which is a branch of mathmatics which established chaos theory along with the discovery of digital and analog computers.

1.3. Thesis Structure

The next chapter focuses on the fundamental theories, basic terms and some mathmatical concepts require to study complexity. Chapter 3 explains the analytical techniques applied in our studies. In Chapter 4, we exhibit the outcomes from the analysis of heartbeat data using Diffusion Entropy Analysis (DEA) and Multi-fractal Detrended Fluctuation Analysis (MFDFA) techniques. Chapter 5 is devoted to meditation effect on heartbeat dynamics . Chapter 6 is based on brain dynamics with EEG data analysis . Finally, Chapter 7 ends with conclusion and future works .

CHAPTER 2

FUNDAMENTAL THEORIES AND PROBABILISTIC APPROACH

This chapter concentrates on fundamental theories and some mathmatical concepts in the study of complex systems. It likewise provides an intuitive idea regarding the characteristics of complexity for the individuals who are new to this field. I attempt to make it more tutorial for those who don't have any mathematical background or knowledge.

2.1. General Characteristics of Complexity

The definition of complex system alongside its historical studies are already mentioned in Chapter 1. The properties of complexity are very essential to know while studying complex systems. For that propose, general characteristics of complexity are described as follows.

2.1.1. Nonlinearity

Complex systems are *nonlinear* in nature. In other words, the interactions between its constituents don't follow linear behavior. A Complex system contains a very large number of constituents. The interactions and connectivity between the constituents are very high. There is no direct relation between cause and effect like in other simple linear systems. That is the reason we call this system a nonlinear system which is a key characteristic of complex systems. This can produce sudden change from one regime to another regime. There is a brisk transition from a stable to an unstable condition. We can see several examples of nonlinearity in complex systems in our real life like *human brain, heartbeat dynamics, stock market fluctuations, political revolutions, internet networks* etc.

2.1.2. Self-Organization

Self organization is another key feature of complexity. It arises due to the interactions between the elements of a complex system. When the elements within the system interact,

they organize themselves giving rise to self-similar sturctures or patterns. This is a spontaneous appearance of order from a bottom up process also referred to as global coordination out of local level interactions.

The term *'self-organization'* was introduced by one of the pioneers of cybernetics and renowned psychiatrist William Ross Ashby in 1947 [8] . Later on, in 1977, Nobel laureate Ilya Prigogene found "order out of chaos", in other words *'self-organization'*, in many non-equilibrium physical and chemical systems [9]. His discovery implies that the 2nd law of thermodynamics is no longer applicable in open systems due to reduction of entropy in such systems.

2.1.3. Self Similarities

When *self-organization* is achieved in complex sytems, we see similar patterns with nice structures. These are also called scale-invarianct structures. Mathematically it can be written as

$$f(\lambda x) = \lambda^{\alpha} f\,(x)$$

which is a homogeneous function of degree α. Where λ is an arbitrary real number. This distribution follows the *power law* (see Eq.1.1).

2.1.4. Emergence

Complex systems show *emergent* behaviour. These behaviours emerge at the level of the systems as wholes, as a result of interactions between the individual components in the systems. This sort of behaviour cannot simply be derived by aggregating the behaviour of a system's components. The whole is more than the sum of its parts which is also known as non-reductive property of complex systems. Most often the emergent behaviors of systems are more intricate and less predictable than the behavior of their individual constituents. *Emergence* is a necessary but not sufficient condition for a system to be complex. We are

stating this because an ideal gas may show emergent behaviour but it is not a complex system.

One example of a complex system whose emergent properties have been studied extensively is cellular automata [10]. In almost all cases, cellular automaton evolution is irreversible. In a cellular automaton, a grid of cells, each having one of finitely many states, evolves over time according to very simple rules. These very simple rules create complex emergent phenomenon through the 'interactions' of each cell with its neighbor cells. Although the rules are defined locally, they are capable of producing global behavior, for instance in Conway's Game of Life devised by John Horton Conway in 1970.

2.1.5. Stochastic

Complex systems are *stochastic* in nature. They change over time in a random way. Mathematically, *stochastic process* can be defined as a set of random variables $\{Xt\}t \in T$, indexed by T, Where T is a subset of $(0, \infty)$. $\{Xt\}t \in T$ is said to be a discrete-time process and continuous time process when $T = (0, 1, 2, 3.....N)$ and $T = (0, \infty)$ respectively.

The concept of a *stochastic processes* is very important both in mathematical theory and its applications in science, engineering, economics, etc. It is used to model a large number of various phenomena where the quantity of interest varies discretely or continuously through time in a random fashion.

Fig. 2.1 shows the stochastic characteristics in *heartbeats* and *brain signals*.

2.1.6. Non-Deterministic

Complex systems often are *not deterministic*. In other words, complex systems are not well predictable. That's why we use a probabilistic approach to study the behavior of complex systems. Because of the interconnection of large numbers of elements within a system, a small change in a local entity will change the global behavior of the complex system.

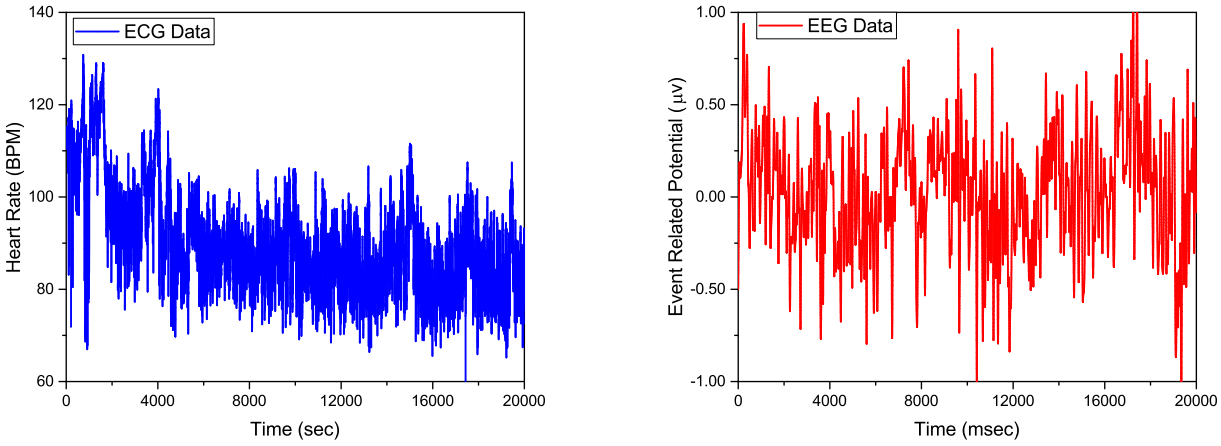

(A) Heartbeat dynamics

(B) Brain dynamics

FIGURE 2.1. Stochastic process

2.2. Probabilistic Approach

We already described in the previous section that complex systems are not deterministic. In order to make predictions we have to use a *probabilistic approach*. Probabilistic theories are based on events. Let us discuss about events first.

2.2.1. Events

Events are noticed when there are significant changes from the normal trend in a system. The definition of *events* also depends on the system under consideration. For example, it may be an *earthquake in a geological system, a crash in a stock market, avalanches on a mountain*, etc. These events are the most important ingredients in probability theory as well as in complex system studies to predict future consequences.

2.2.2. Crucial Events

Crucial events are also known as renewal events. These events are totally uncorrelated with each other. In other words, the events which are going to occur will be totally indepedent from whatever occured earlier. We adopt the theoretical perceptive of ref [11] to define

crucial events on the basis of the time interval between the occurance of two consecutive events.

The WTD (see 2.2.3) of Crucial events follow the asymptotic inverse power law (IPL) structure:

$$\psi(\tau) \propto \frac{1}{\tau^{\mu}} \tag{2.1}$$

with $\mu < 3$. The time intervals between two different pairs of consecutive events are totally uncorrelated:

$$\langle \tau_i \tau_j \rangle \propto \delta_{ij}. \tag{2.2}$$

Where δ_{ij} is the Kronecker delta. By definition

$$\delta_{ij} = \begin{cases} 1, & \text{if } i = j, \\ 0, & \text{if } i \neq j. \end{cases} \tag{2.3}$$

Crucial events play an important role in the transport of information from one complex network to another [12].

It is important to discuss the dynamical origin of crucial events. These events are the product of cooperative interactions between the elements of a complex network; they are expected to lead to a spontaneous organization process, usually called Self Organized Criticality (SOC)[13]. Numerous studies have been made regarding SOC since the original work of Bak *et al.*.

2.2.3. Waiting Time Distribution

Let us suppose τ is the time distance between two consecutive events. This is also called the waiting time. The probability density function (PDF) of τ is called the waiting time distribution (WTD) $\psi(\tau)$. Mathematically, the probability that an event occurs in the short time interval $[\tau, \tau + d\tau]$, is given by PDF $\psi(\tau)d\tau$, which must be ≥ 0. Also, the waiting time PDF must satisfy the normalization condition

$$\int_0^\infty \psi(\tau)\, d\tau = 1. \tag{2.4}$$

Studies of the waiting time distribution suggesting long range temporal correlations in different complex systems can be found elsewhere. .

2.2.4. Survival Probability

The probability that an event of interest such as a failure, break or something else has not occured by the time t is called the survival probability. Mathematically, it can be written as

$$\Psi(t) = \int_t^\infty \psi(\tau)\, d\tau \tag{2.5}$$

Using *Eq.* 2.4 , *Eq.* 2.5 can be written as

$$\Psi(t) = 1 - \int_0^t \psi(\tau) d\tau \tag{2.6}$$

Now, it is clear that at $t = 0$, $\Psi(0) = 1$. Also, at $t = \infty$, using *Eq.* 2.5, *Eq.* 2.6 gives $\Psi(\infty) = 0$.

Also, the waiting time distribution is the negative of the derivative of the survival probability density (SPD). This can be written as

$$\psi(t) = -\frac{d\Psi(t)}{dt} = -\Psi'(t) \tag{2.7}$$

2.2.5. Events Rate

Rate of events is defined as the number of events occur per unit time. Let us suppose $R(t)$ is the rate of events, the probability for an event to occur in the short interval of time $(t, t+dt)$ is $R(t)dt$. Where t is measured from the begining of the observation. It can be expressed in terms of WTD as follows.

$$R(t) = \sum_{1}^{\infty} \psi_n(t). \tag{2.8}$$

Where,

$$\psi_n(t) = \int_0^t \psi_{n-1}(t')\psi(t-t')\,dt' \tag{2.9}$$

is the probability density for $n-th$ event to occur in time t.

2.2.6. Aged Events Rate and Poisson Distribution

The age-dependent rate of events, often called the hazard function $g(t)$, is defined as

$$g(t) = \lim_{dt\to 0} \frac{Pr(t \le T < t+dt \mid T \ge t)}{dt} \tag{2.10}$$

The term in the numerator of above equation is the conditional probability that the event will occur in the interval $(t, t+dt)$ given that it has not occurred before, and the term dt in the denominator is the interval width.

Also, the rate of occurrence of the event at duration t equals the waiting time distribution $\psi(t)$ of the events at t , divided by the survival probability to that duration without experiencing the event. It can be expressed as,

$$g(t) = \frac{\psi(t)}{\Psi(t)}. \tag{2.11}$$

Substituting $\psi(t)$ from eq. 2.7 in eq. 2.11 we get:

$$g(t) = -\frac{\Psi'(t)}{\Psi(t)}. \tag{2.12}$$

Again,

$$g(t) = -\frac{\Psi'(t)}{\Psi(t)} = \frac{d\left(\log[\Psi(t)]\right)}{dt} \tag{2.13}$$

This implies that,

$$d\log(\Psi(t)) = -g(t)\,dt \tag{2.14}$$

which results the final equation as,

$$\log[\Psi(t)] - \log[\Psi(0)] = \log\left[\frac{\Psi(t)}{\Psi(0)}\right] = -\int_0^t g(t')\,dt',$$

$$\Psi(t) = \Psi(0)e^{-\int_0^t g(t')\,dt'} = e^{-\int_0^t g(t')\,dt'}, \tag{2.15}$$

Where $\Psi(0)$ is equal to 1 because It is sure that there is no occurance of event during time 0.

When $g(t) = g$, i.e.constant over time, the *survival distribution* of eq. 2.15 becomes,

$$\Psi(t) = e^{-\int_0^t g(t)\,dt} = e^{-gt}, \tag{2.16}$$

This distribution is called the Poisson (or negative exponential) distribution with parameter g. Fig. 2.2 shows the poisson distribution plot in log log scale.

Poisson distribution is also a very popular distribution and has several relevant applications in real life such as number of decay of atoms in radioactive process , the number of arrivals at a car wash in one hour, the number of network failures per day and etc. [14].

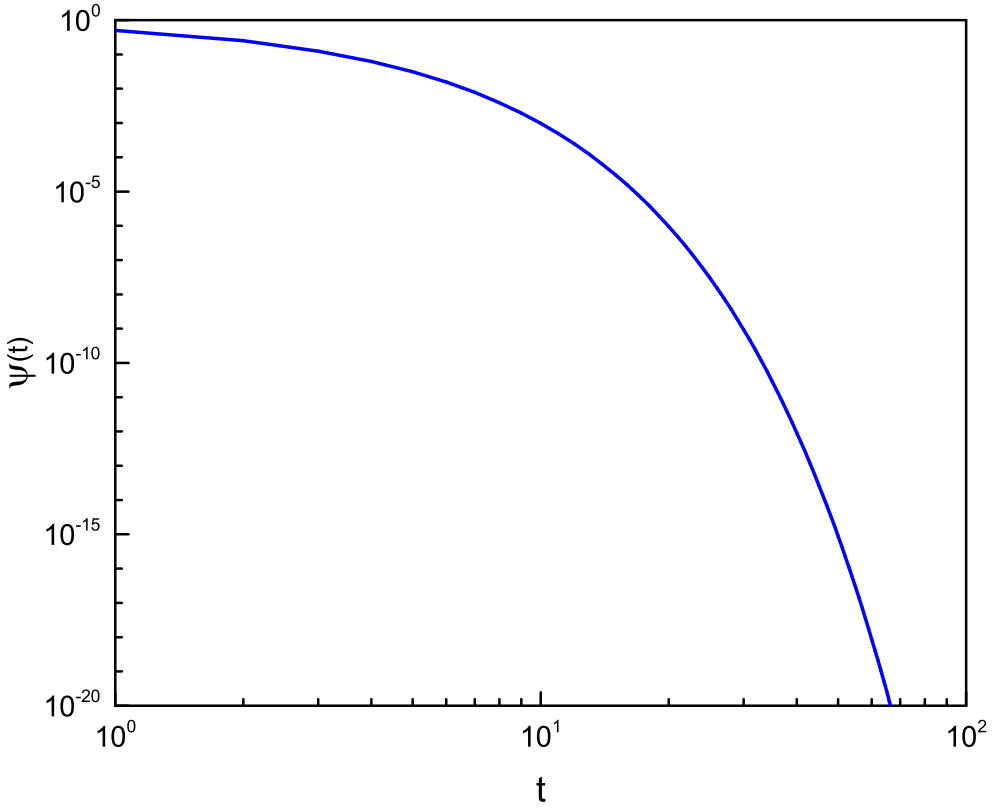

FIGURE 2.2. Exponential

2.2.7. Aged Waiting Time Distribution

Aging phenomena are very common in a number of complex systems like spin glasses, high-temperature superconductors, and charge density wave systems. Experimentally, these systems appear to be in equilibrium if observed over short period of time, while longer time observations reveal that they are out of equilibrium [15].

Let us consider a system which is prepared in such a way that an event occur at $t = 0$. Let's start to observe the system at time ta for an event to occur at time t after the preparation event. The probability density we obtain in this case is given by

$$\psi(t_a, t) = \psi(t) + \int_0^{t_a} R(t')\psi(t - t')\, dt' \tag{2.17}$$

is called the *aged waiting time distribution.*

Similarly, the *aged survival probability* is given by

$$\Psi(t_a, t) = \Psi(t) + \int_0^{t_a} R(t')\Psi(t - t')\, dt' \tag{2.18}$$

2.2.8. Power Laws

When the probability of finding a particular value of some quantity varies inversely as a power of that value, the qunatity is said to obey a *power law*. *Power laws distribution* often called Pareto distribution which was named after the Italian engineer, economist and sociologist Vilfredo Pareto. Pareto first noticed the power law in the income weatlth distriubtion in 1897 which is considered as a real hallmark of complexity. Since that time several studies reveal that *power laws* appear widely in *physics, chemistry, biology, ecology, sociology, economics finance and several other interdisciplinary areas* [16, 17].

Mathmatically it can be defined as,

$$\psi(t) \propto t^{-\mu}.$$

power law is also a linear relationship between logarithms, of the form

$$log\psi(t) = \alpha logt + logK$$

where K is propotionality constant. Many studies of critical phenomena in different systems suggest that power laws emerge close to special critical or bifurcation points separating two different phases or regimes of the system.

Power law distributon also obeys the symmetry of scale invariance.

$$f(\lambda x) = \lambda^{\alpha} f\,(x)$$

Fig. 2.3 shows the power law distribution plot in log log scale.

Initially the ubiquity and significance of scale invaraiance was pointed out by Mandelbrot. He invented the term *'fractals'* to explain the nondifferentiable geometric objects that follow power law scaling when α is not equal to an integer value. Fractals have the

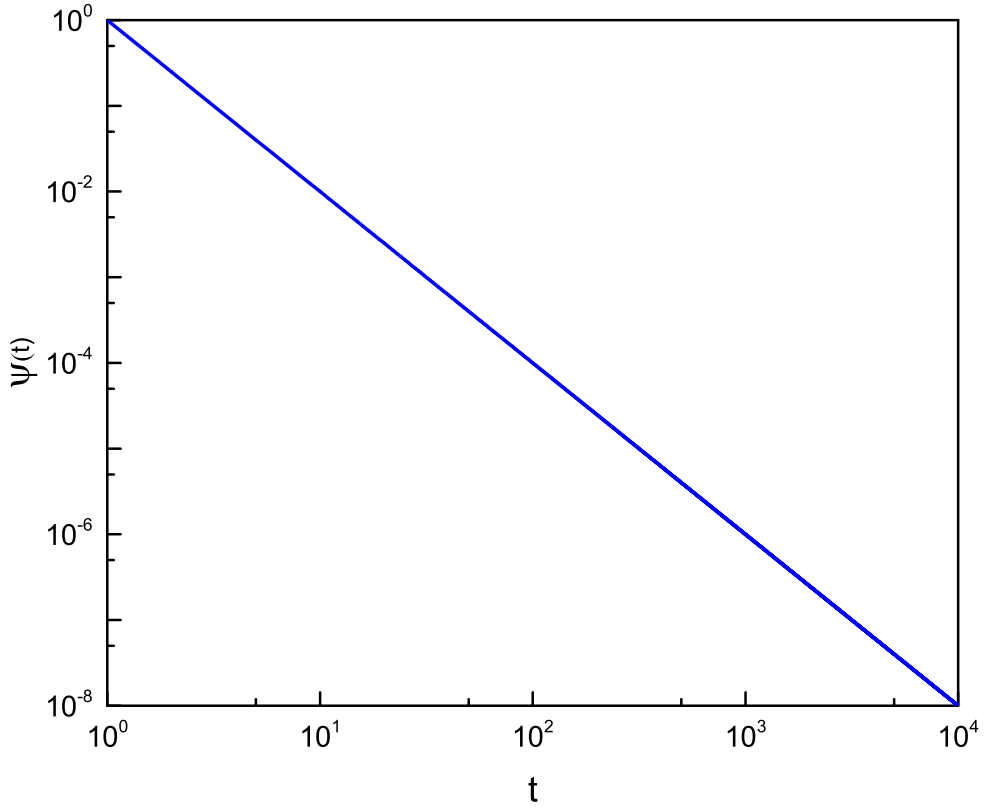

FIGURE 2.3. Power Law

property that the system or structure keeps the same behavior interms of different scalings while we zoomed it. Mandelbrot illustrated that fractals are pervasive in nature, e.g. *coastlines, clouds, floods, earthquakes, financial returns, and fundamental inaccuracies in clocks* [18].

The moments of the power law distriution diverge when $m > \mu - 1$. Mathamatically, mth moment $< \tau^m >$ of the power law distribution is given by,

$$< \tau^m >= \int_0^\infty \tau^m \psi(\tau)\, d\tau \tag{2.19}$$

In the ergodic regime $2 < \mu < 3$, the second moment of the distribution diverges. Where as in non-ergodic regime $1 < \mu < 2$, the first moment (mean) diverges.

2.2.9. Entropy

Entropy is the most influential concept in statistical physics, information theory and complexity theory. It was Clausius who coined the term entropy in mid 19 th century. He found very important relation between heat , temperature and entropy as follows.

$$S = \frac{dQ}{T} \tag{2.20}$$

where S denotes entropy, dQ stands for change in heat and T is absolute temperature of the system. Most often it is known as a quantitative measurement of disorderness in the systems. Earlier invention of entropy by Clausius didn't mention it as a measure of order or disorder in the systems. Later Boltzman related entropy to the disorder. Mathmatically Boltzman entropy can be expressed as,

$$S = k_{\mathrm{B}} ln\Omega$$

Where k_{B} is Boltzmanns constant and Ω is the thermodynamical probability in which each possible microstate of a macrostate is equaly probable. This shows entropy as a measure of distribution of atoms and molecules in the thermodynamic system. Perfectly arrangement of particles in crystals have more ordered which tells us the fact that entropy is zero or minimum where as the arrangement of particles in gases have more disordered where entropy is maximum.

Second law of thermodynamics is also related to entropy. The second law of thermodynamics states that the entropy of an isolated system is always increasing. But for open systems entropy not always increase, it also decreases.

After a century since the invention of Boltzmann entropy, Shannon in 1949, invented fascinating formula 2.21 in information theory.

$$S(t) = -\int_{-\infty}^{+\infty} dx p(x,t) \ln\left[p(x,t)\right]. \tag{2.21}$$

Boltzmann entropy is a special case of the Shanon entropy. Shannon entropy gives the wonderful idea to quantify uncertainty which is also called a lack of information about a system. For eg. if you toss a fair coin, the outcome of it is either head or tail with equal probability of 1/2. This means that we have some uncertainty about the outcome of each experiment. It can be quantified using Shannon equation. Now, if we modified a coin in such a way that it's outcome is tail all time. Then the probability of occurance of tail is 1 with entropy 0 which means that we don't have any uncertainty in the outcome of the experiment. The entropy in Information theory has also an important role in shaping theories of perception, cognition, and neural computation [19].

2.3. Chaos Theory

Chaos theory is a mathematical tool to study complex and nonlinear dynamical systems. It can be called as a branch of physics which deals with the non-linear systems. While talking about the chaos theory there are several researchers who made significant contributions to this field recently.

However, the brilliant Lorentz comes first in mind who made a profound discovery in *chaos theory*. In 1961, Lorentz was developing a weather prediction mathematical model using three coupled differential equations. He was running the model in powerful computer to make prediction accurate. One day, he decided to review his forecasts. He decided to save time starting from halfway through the first run cconsidering that as a initial condition. After some time, he found the final result was drastically deviated from the previous run. He was thinking what had gone wrong? He printed out the result which was showing to three decimal places, it was actually crunching the original six decimal places. So, in the second run he used the number 0.506 which was originally 0.506127. The result of the second run turned out drastically different with minor change in intial state although the difference was one part in a thousand. He found seeds of chaos [20]. This means tiny differences produce huge effects which is a remarkable hallmark of chaotic system.

Lorenz explained this effect with the famous analogy of a butterfly flapping its wings

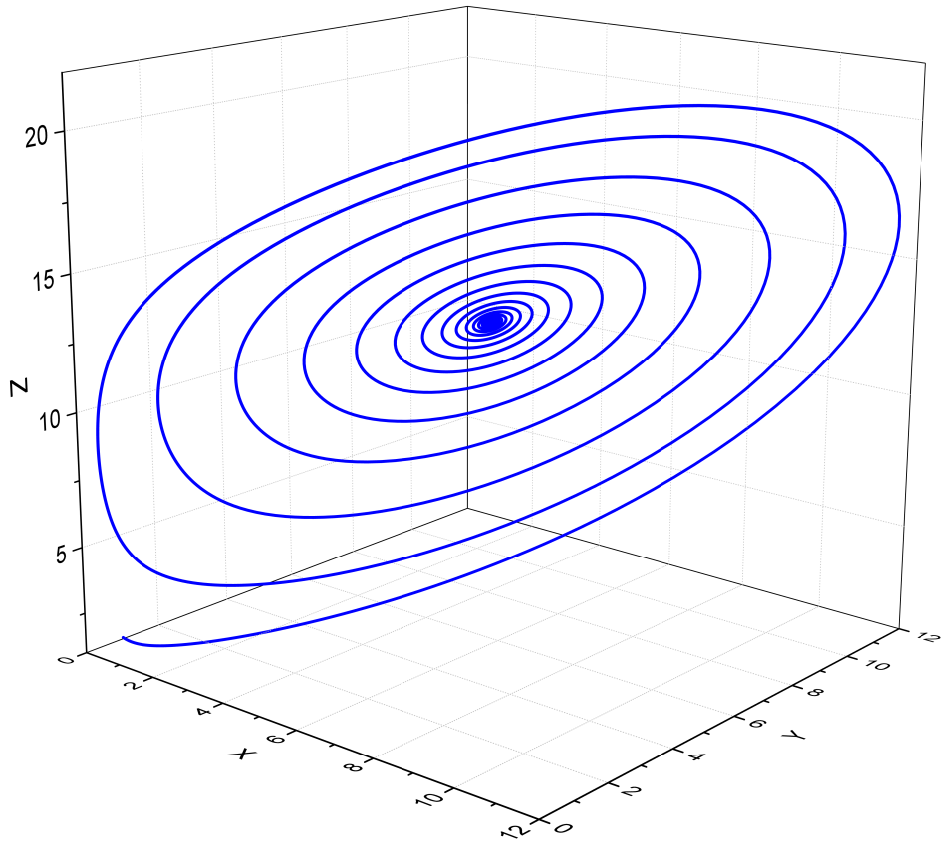

FIGURE 2.4. Single attractor

and thereby causing the formation of a hurricane or huge disaster half a world away. "Butterfly effect" was just an anology to explain real small effect in an initial condition to produce large effect in the final.

Another famous term in chaos theory is an "attractor". An attractor can be a point, a set of points, a curve or even a complicated structure towards which dynamical systems evolve. This helps a lot to predict the final state of the system. Fig. 2.4 is an example of single attractor towards wihich dynamical system evolves.

But some time system evolves towards strange attractors too. Strange attractors are the new attractors toward which systems evolve leaving previous attractor. Fig. 2.5 is an example of strange attractor where the system evolves leaving previous attractor.

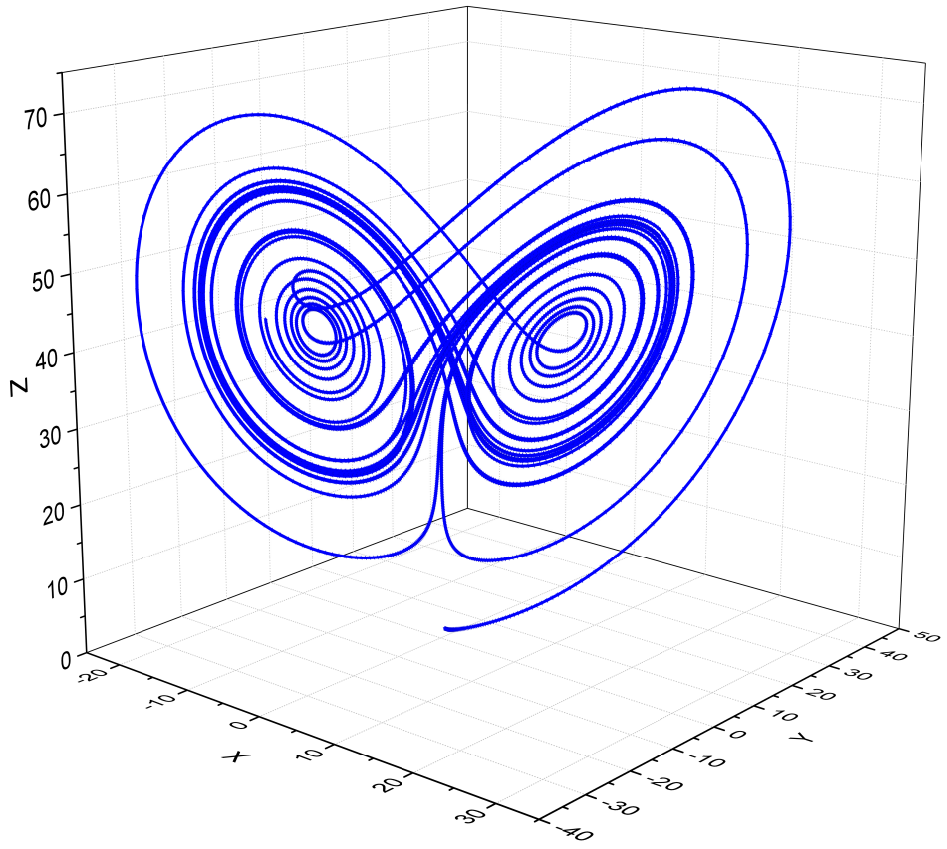

FIGURE 2.5. Strange attractor

Chaos theory is applicable in many fields such as *physics, biology, sociology, economics, psychology and etc.*

2.4. Brownian Motion

History of *Brownian motion* begins with the Dutch physician Jan Ingenhausz who observed the zigzag motion of powdered charcoal on an alcohol surface in 1785. But the phenomenon was labelled as "Brownian motion" under the name of Botanist Robert Brown who reported the "rapid oscilatory motion" of pollen particles in water through a microscope while studying the fertilization process in a species of flowers in 1828. A satisfactory explaination of "Brownian motion" was not possible until 1905. World renowned scientist

Einsten was the one who made it possible to explain "Brownian motion" [21].

According to Einstein, Brownian motion generates in the continual bombardment of the pollen particles by the molecules of the surrounding water. He argued that the pollen particles had the same average kinetic energy as the molecules of surrounding water as a result of continuous bombardment. Einsten's explaination regarding Brownian motion was much more important that it was showing the theoretical evidence about the existance of atoms. From his mathmetical derivation of the mean squared displacement of the Brownian particle with linear dependence on time (see 2.22)

$$< x^2 > \approx 2Dt \tag{2.22}$$

Jean Perrin was able to measure Avogadro's number. Perrin won the 1926 Nobel Prize in Physics from that invention.

Brownian motion follows the normal distribution with mean 0 and variance linear with time t.

Development of Brownian motion process studies and its many generalizations and extensions occur in numerous and diverse fields such as *economics, communication theory,biology,management science,and mathematical statistics* [22].

CHAPTER 3

ANALYTICAL TECHNIQUES

In this chapter we discuss the analytical techniques used to study heart-brain dynamics. Predominantly we used two analytical techniques, one is *Diffusion Entropy Analysis (DEA)* and the other is *Multifractal Detrendred Fluctuation Analysis (MFDFA)*. Brief introduction, procedure and the importance of these analytical techniques are presented as follows.

3.1. Diffusion Entropy Analysis

Since we already discussed about the fact that *scale invariance* is one of the fundamental properties of Complex systems, finding the correct scaling of such systems is equally important. It is also evident that these systems can't be described by the ordinary statistical physics. Ordinary statistical physics strictly related with central limit theorem which can't go beyond Gaussian distribution. Therefore, one can say that the search for the correct *scaling exponents* has the connection with the discovery of deviations from ordinary statistical mechanics.

There are several methods that have been developed recently to find correct scaling of complex systems. Many of them can produce correct scaling for Gaussian distribution but fail to determine the correct scaling for non-Gaussian distribution such as *Levy statistics*. Grigolini and his group in 2002 invented *Diffusion Entropy Analysis (DEA)* method [23]. The DEA let the correct scaling of a diffusion process, regardless of whether the Gauss condition applies or not.

To introduce an algorithm to find *scaling exponent* δ using DEA, let us consider a sequence of N numbers ξ_i, $i = 1, ..., N$. At first, let us choose an integer number t, satisfying the condition $1 \leq t \leq N$. This integer number is referred as time. For any given time t we can get $N - t + 1$ sub-sequences given by

$$\xi_i^{(s)} \equiv \xi_{i+s}, with\ s= 0, \ .\ .\ ., \ N\text{-}t. \tag{3.1}$$

Now, we have a diffusion trajectory, with index s, defined by position

$$x^{(s)}(t) = \sum_{i=1}^{t} \xi_i^{(s)} = \sum_{i=1}^{t} \xi_{i+s}. \tag{3.2}$$

Let us suppose that we have a stochastic particle which has the position as defined above and it's movement is characterized by Eq. 3.1. Now we need to evaluate the PDF $p(x,t)$. It can be done by dividing the x-axis into many cells of size $\Delta(t)$. After this we count how many particles are there in the same cell at a given time t. Let us suppose there are $N_i(t)$ no. of particles. Now the probability that a particle can be found in the $i-th$ cell at time t is given by

$$p_i(t) \equiv \frac{N_i(t)}{(N-t+1)}. \tag{3.3}$$

So, the entropy of the diffusion process is given by,

$$S_d(t) = \sum_i p_i(t) \ln\left[p_i(t)\right]. \tag{3.4}$$

Now, Let us follow the continuous assumptiion for simplicity where Shannon entropy of the diffusion process becomes

$$S(t) = -\int_{-\infty}^{+\infty} dx p(x,t) \ln\left[p(x,t)\right]. \tag{3.5}$$

Also, PDF $p(x,t)$ takes the form,

$$p(x,t) = \frac{1}{t^{\delta}} F\left(\frac{x}{t^{\delta}}\right), \tag{3.6}$$

where $F(y)$ is a function for crucial events which doesn't follow ordinary Gaussian form.

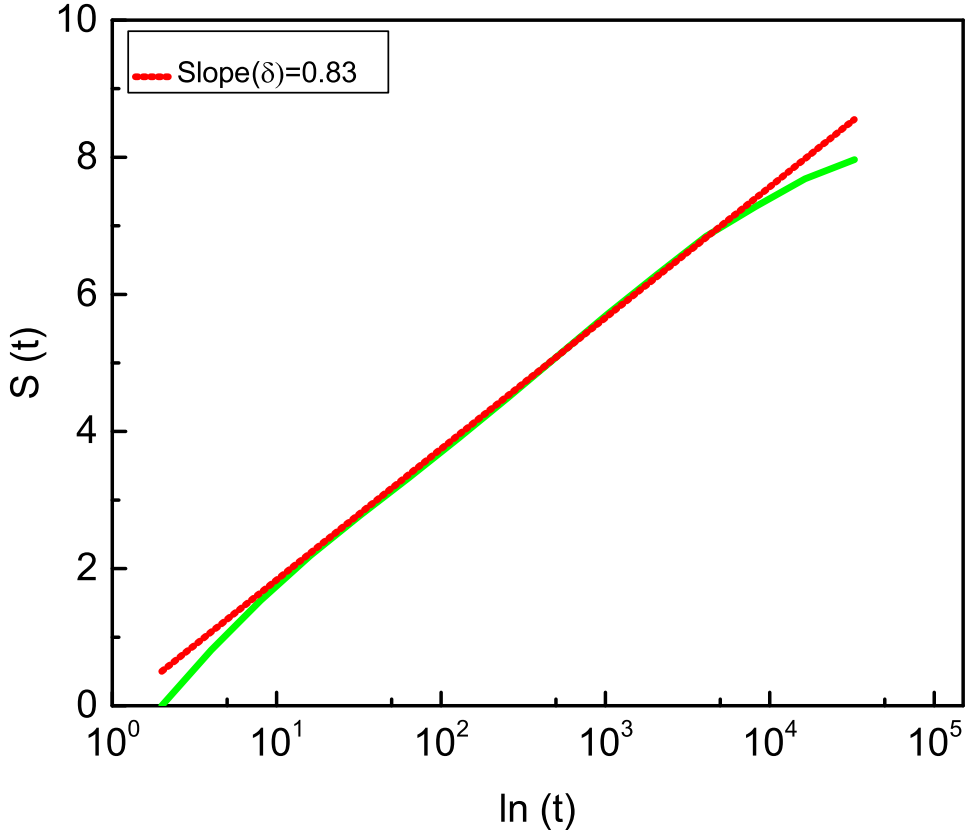

FIGURE 3.1. DEA example

From Eq. (3.5) and Eq. (3.6), and replacing the integration variable x by the other integration variable $y = x/t^{\delta}$, we get

$$S(t) = A + \delta \ln(t), \tag{3.7}$$

where,

$$A \equiv -\int_{-\infty}^{+\infty} dy F(y) \ln\left[F(y)\right]. \tag{3.8}$$

The slope of the straight line resulting from Eq. (3.7) is the scaling coefficient δ. An illustrative example is shown below in Fig. 3.1.

3.2. Multifractal Dentrendred Fluctuation Analysis

Multifractal Detrendred Fluctuation Analysis (MFDFA) is based on a generalization of the *detrended fluctuation analysis (DFA)* technique. Peng and his group in 1994 invented DFA method. They used this method to study the correlation properties in heart beat time series and DNA sequences [24, 25].

After that it became a very popular technique for the determination of (mono-) fractal scaling properties and the detection of long-range correlations in noisy, nonstationary time series. It has been widely used in diverse fields such as *neuron spiking, human gait, long-time weather records, cloud structure, geology, ethnology, economics time series and so on.* One of the main reason to apply this method is to avoid spurious detection of correlations that are artifacts of nonstationarities in the time series.

DFA calculates a fluctuation function $F(t)$ as a function of log (t). The logarithmic plot of $F(t)$ vs t gives a straight line if there exists long range temporal- correlation. The slope of the logarithmic plot is also called α *scaling exponent* which provides the following information depending on their values.

TABLE 3.1. Scaling Exponent and Corrrelation

Scaling Exponent	Corrrelation
$\alpha \sim 0.5$	Uncorrelated sequence
$0 < \alpha < 0.5$	Anti-correlated sequence
$0.5 < \alpha < 1$	Long-range temporal correlations
$\alpha > 1$	Strong correlations that are not of a power-law form

Complex systems in general do not exhibit a single scaling exponent or simple monofractal behavior. In such systems multiscaling behavior can be observed in many subsets of the time series.

Kantelhardt developed a MFDFA method in 2002 to study the multifractal characteristics of nonstationary time series, which is based on a generalization of the DFA method

[26].

Let us suppose that x_k is a series of length N. Our aim to find the spectrum of singularities $f_q(s)$ for the series x_k. MFDFA procedure consists of the following steps.

Step 1: Determine the profile

$$Y(i) \equiv \sum_{k=1}^{i} [x_k - < x >], i = 1, ..., N \tag{3.9}$$

Subtraction of the mean $< x >$ is not necessary, it can be eliminated by detrending in the third step.

Step 2: Divide the profile $Y(i)$ into $Ns \equiv int(N/s)$ nonoverlapping segments of equal length s. Since the length N of the series is often not completely divisible by time scale s, a short part sometime remain as remainder. In order to account that remainder, the same procedure is followed starting from the opposite end there by obtaining $2N_s$ segments in total.

Step 3: This step is focused to detrend the profile in each segment of length s separately. The least-square fit of the series for each of the $2N_s$ determines the variance as,

$$F^2(s, \upsilon) \equiv 1/s \sum_{i=1}^{s} \{Y[(\upsilon - 1)s + i] - y_\upsilon^n(i)\}^2 \tag{3.10}$$

for each segment υ, $\upsilon = 1, ..., 2N_s$, the corresponding variances are given by

$$F^2(s, \upsilon) \equiv 1/s \sum_{i=1}^{s} \{Y[N - (\upsilon - N_s)s + i] - y_\upsilon^n(i)\}^2 \tag{3.11}$$

for $\upsilon = N_s + 1, ..., 2N_s$ where $y_\upsilon^n(i)$ is the fitting polynomial in segment υ with order n. Eq. 3.11 shows that the detrending of the time series is done by the subtraction of the polynomial fits from the profile. The different order DFA varies in their ability of removing trends in the time series. This is called the MFDFA of order n.

Step 4: We define qth order fluctuation function as

$$Fq(s) \equiv \left\{ 1/2N_s \sum_{\upsilon=1}^{2N_s} [F^2(s, \upsilon)]^{q/2} \right\}^{1/q} \tag{3.12}$$

where, the index variable q can have any real value except zero. The standard DFA procedure is retrieved when $q = 2$. Here, $F_q(s)$ depend on the time scale s for different values of q so we must repeat steps 2 to 4 for several time scales s. By construction, $F_q(s)$ is only defined for $s \geq n + 2$.

Step 5: Now we determine the scaling behavior of the fluctuation functions by analyzing log-log plots $F_q(s)$ versus s for different values of q. If the time series x_i have long range correlation, it follows the power law as,

$$F_q(s) \sim s^{h(q)} \tag{3.13}$$

where the exponent $h(q)$ depend on q. For stationary time series, $h(2)$ is identical to the well-known Hurst exponent H. Thus, we will call the function $h(q)$ generalized Hurst exponent.

We also define the exponent

$$\tau(q) = qh(q) - 1 \tag{3.14}$$

Fig. 3.2 gives the straight line if the time series is monofractal. Similarly the plot gives curved line if the time series is multifractal.

Finally the singularity spectrum $f(\alpha)$ vs α gives the multifractal spectrum as shown in Fig. 3.3, where $f(\alpha)$ and α are related to τ via a Legendre transformation as

$$\alpha = \tau'(q) \tag{3.15}$$

and

$$f(\alpha) = q\alpha - \tau(q) \tag{3.16}$$

.

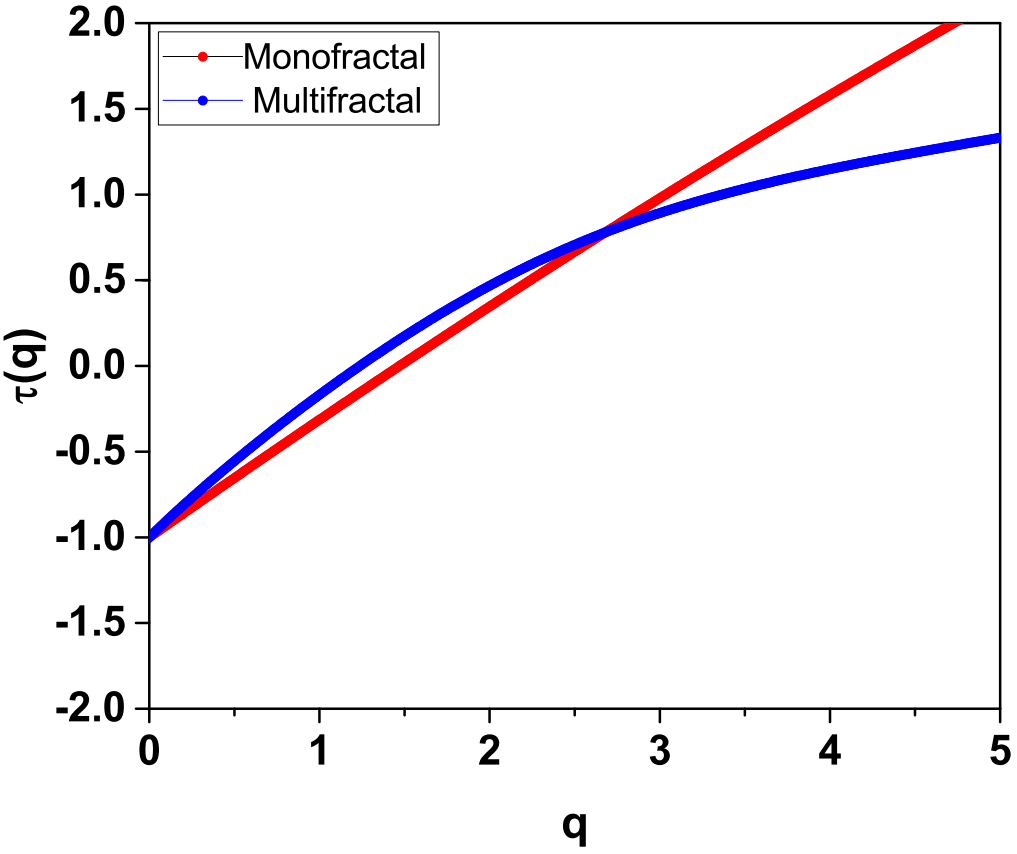

FIGURE 3.2. $\tau(q)$ vs q

Here, α is the singularity strength or exponent, while $f(\alpha)$ denotes the dimension of the subset of the series that is characterized by α.

Using equation 3.14 in 3.15 and 3.18 we have,

$$\alpha = h(q) + qh'(q) \tag{3.17}$$

.

and

$$f(\alpha) = q[\alpha - h(q)] + 1 \tag{3.18}$$

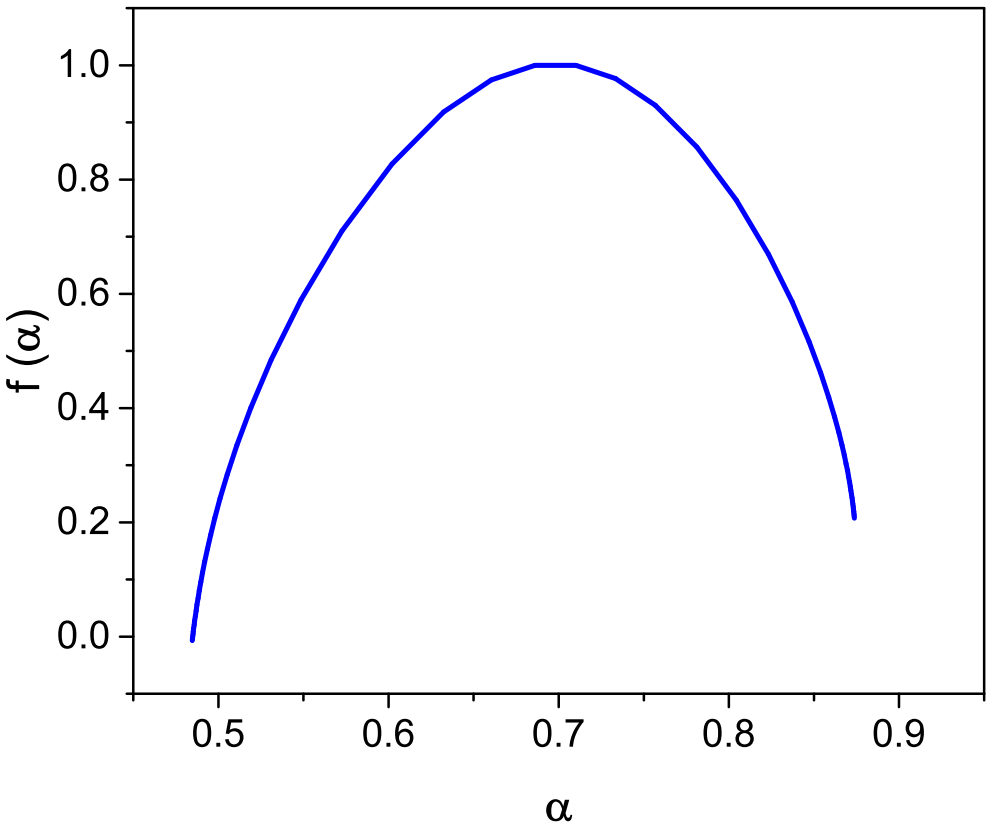

FIGURE 3.3. MFDFA example

.

CHAPTER 4

CRUCIAL EVENTS AND MULTIFRACTALITY IN HEARTBEATS

This chapter is devoted to present the results of heartbeat data analysis. Following [27] and [28], we used the ECG records of the MIT-BIH Normal Sinus Rhythm Database and of the BIDMC Congestive Heart Failure Database, for healthy and congestive heart failure patients, respectively. We made an investigation to study the relationship between the multi-fractal property and crucial events in the case of heart beat variability from both healthy and pathologic subjects. Over the last twenty years two apparently different diagnostic techniques have been established: the first is based on the observation that the multi-fractal spectrum of healthy patients is broader than the multi-fractal spectrum of pathologic subjects; the second is based on the observation that heartbeat dynamics are a superposition of crucial and uncorrelated Poisson-like events, with pathologic patients hosting uncorrelated Poisson-like events with larger probability than the healthy patients. In this study, we prove that increasing the percentage of uncorrelated Poisson-like events hosted by heartbeats has the effect of making their multi-fractal spectrum narrower, thereby establishing that the two different diagnostic techniques are compatible with one another and, at the same time, establishing a dynamic interpretation of multi-fractal processes that had been previously overlooked. This study might be of a broad interest to not only physicists, but also to biologists and medical doctors.

4.1. Introduction

The hypothesis that multi-fractality is a significant property of physiological processes picked up a consideration in the writing of the most recent two decades. Ivanov *et al* [29] admitted this attention using wavelet transform method to analyze the heartbeat time series of several patients, some healthy and some suffered by congestive heart failure.

This chapter is reproduced from Bohara, Gyanendra and Lambert, David and West, Bruce J and Grigolini, Paolo, "Crucial events, randomness, and multifractality in heartbeats", published on Dec 29, 2017 in Journal of Physical Review E,Vol. 96, 062216, with permission from APS.

They discovered that the distinction between the healthy and non-healthy is that the healthy subjects have a significantly wider multi-fractal spectrum. The multi-fractal technique [29] is an efficient tool to study cardiovascular *variability* [30], referred to as heart rate variability (HRV), the proper treatment of which is still the object of intense discussions [31].

The statistical probe of heartbeat variabilities in addition to that of other physiological phenomenon, is often accomplished by preparing proper time series. Each time series is special which generates the problem to establish a connection with the Gibbs ensemble perspective, where mean values have to be taken over indistinguihable copies of the same system. This difficulty is solved with the assumption that different sections of the individual time series can be explained as indistinguishable copies of the same process, corresponding to different initial conditions. A notable analysis procedure of this type is *Detrended Fluctuation Analysis* (DFA), [32, 25]. Due, to some degree, to the expanding enthusiasm in multi-fractality [33], Kantelhardt *et al.* [26] stretched out DFA to make it conceivable to extricate from it multi-fractal information, by means of the spectral density $f(\alpha)$ which frequently has the form of a wide inverted parabola that is expected to become very thin and centered on the scaling index $\alpha = 0.5$ in the conventional Poisson case. We refer to the procedure developed by Kantelhardt *et al.*[26] as Multi Fractal Detrended Fluctuation Analysis (MFDFA). MFDFA is embraced to talk about the transmission of multi-fractality from a complex network stimulus to another complex network [34], both being described by a broad $f(\alpha)$ spectrum.

The fundamental motivation behind the investigation is to reveal the dynamical origin of a wide $f(\alpha)$ range by moving from the particular instance of HRV to the general properties of non-Poisson time series. To accomplish this, we follow the scan for a diagnostic distinction between healthy and pathological subjects. The objective, in any case, is to get a superior comprehension of the dynamical root of multi-fractal variability. Huge bits of knowledge about this dynamic origin would attract general interest to the enhancement of diagnostic techniques. One possible road to the arrangement of this issue can be found by noticing that

in 2002 Allegrini *et al* [28] used the detection of crucial events as the main tool to distinguish healthy (with a broad $f(\alpha)$ spectrum) from unhealthy (with narrow $f(\alpha)$ spectrum) patients. For a proper definition of crucial events we adopt the theoretical point of view built up in earlier work, see for example [11], defining the *crucial events* on the basis of the time interval between the occurrence of two consecutive events.

4.2. Origin of Crucial Events

It is vital to talk about the dynamical root of crucial events. Crucial events are an indicatiion of agreeable interactions between the units of a complex network that is relied upon to lead to a spontaneous organization process, usually called Self Organized Criticality (SOC). Huge advance has been made in understanding SOC since the first work of Bak *et al.* [13]. The development of SOC is motioned by the births of anomalous avalanches, see [35, 36] for recent work along these lines.

There exists a new approach to SOC emphasizing temporal rather than intensity anomalous distributions [37, 38]. The authors of Ref. [38] characterized their way to deal with self-organization as *Self-Organized Temporal Criticality* (SOTC). As indicated by SOTC the crucial events characterized before with the assistance of Eqs. (1.1) and (2.2), to be specific the events that the authors of [28] could discover in heartbeats, occur on an intermediate time scale, after an initial transient regime to the condition of intermediate asymptotics. The inverse power law (IPL) nature of crucial events is tempered by an exponential relaxation in the long-time limit. This elucidation enables us to encourage our way to deal with the connection between the diagnostic techniques of Ref. [29] and of Ref. [28]. In fact, the three time regimes of SOTC are a type of variability that we subsequently connect to the physiological variability that drove the authors of Ref. [29] to their diagnostic insight.

To rundown judgment the crucial events are responsible for the complexity of the intermediate asymptotics regime, as it will be more broadly pointed out in Section 4.4. Furthermore, we must consider that as stated by Ref. [28] the definition of crucial events must be extended to consider the case where the time interval between the occurrence of

the crucial events defined by Eq. (1.1) and Eq. (2.2) is filled with events with memory. The initial crucial event triggers the generation of the filling events and the occurrence of the next crucial event ends this arrangement and activates a new sequence of strongly correlated filling events. The events filling the time interval between two crucial events must not be confused with the Poisson-like events disturbing the healthy physiological condition of the heartbeats. In Ref. [28] the events filling the time distance between two consecutive crucial events were responsible for a phenomenon called *memory beyond memory effect*. The intuitive idea of this effect is that the crucial events with $\mu < 3$ are responsible for slowly decaying correlation functions, thereby implying a form of memory. The filling events have an additional memory preventing them from disturbing the healthy physiological condition signaled by the crucial events. Those actual heartbeat process will be a superposition of two time series, the former relating of the healthy function and the later being given by a sequence of completely uncorrelated events.

In this investigation the surrogate time series are produced adopting for the healthy time series two different prescriptions. The first prescription fits the direction of Ref. [28]. For effortlessness' purpose, we set up the exceedingly correlated nature of the filling events with the assumption that time distance τ between two consecutive pseudo events is constant. The distribution of τ is an inverse power law with μ essentially bigger than 3 including $\mu = \infty$, namely an ordinary Poisson process. Obviously, for this situation, the crucial renewal condition of Eq. (2.2) is violated. The later time series, of perturbing Poisson-like events, is generated by deriving the time distance between two consecutive events from a distribution density with $\mu > 3$ indistinguishable to that of the filling events of the previous. As we shall see, these perturbing Poisson-like events reproduce very well the disturbing process responsible for heart failure. We adopt also the second prescription, where the healthy time series hosts only crucial events and the wide laminar region between two consecutive crucial events is left empty. This straightforward prescription makes it possible for us to delineate the efficiency of the technique of Diffusion Entropy Analysis (DEA) [23] to determine the scaling generated by the crucial events, however it can't be utilized to disclose how to establish the

percentage of disturbing Poisson-like events. The straightforward prescription, however, is advantageous to demonstrate that crucial events alone can produce the multifractal distribution. We shall refer to the first prescription as generating *dressed crucial events* and to the second as generating *bare crucial events*.

4.3. Crucial Events and Multifractality

The search for crucial events is made troublesome by the way that crucial events are often imbedded in billows of uncorrelated and irrelevant events. The authors of [28] utilized a procedure of measurable investigation, called DEA [23], to detect the anomalous scaling index δ, which these crucial events would create were they not imbedded in a billow of non-crucial events, specifically, when they are visible. Nonetheless, to establish a connection with the results of Ivanov *et al* [29] it is important to address an issue that goes beyond the merely diagnostic goal of both [29] and [28]. The issue is to reveal the physical mechanism creating the multifractality uncovered by MFDFA. This issue has been the subject of many research papers and we devote this Section to a short review of the consequences of that exploration.

A key component of this debate is the DEA, which was appeared to be the right approach to decide the scaling produced by crucial events while DFA isn't [39, 40, 41]. This is a result of the fact that DFA determines the scaling of the second moment of a distribution that can be divergent for non-Gaussian distribution densities. Therefore many endeavors have been made to consolidate the right scaling assessment with the evaluation of multifractality [40, 41, 42, 43, 44, 45]. However, these fascinating papers leave unanswered the focal inquiry of the multifractal significance of crucial events, since these authors applied the new method of analysis to real data with no discussion of surrogate data hosting only crucial events.

It is advantageous, for lucidity, to mention some papers from the field of experimental psychology [46, 47, 48, 49]. For our purposes, the value of these publications is that they set up, through their investigation of real data, a connection between multifractality and the

transport of information. Along these lines they imply a connection between multifractality and the crucial events uncovered by the best possible utilization of DEA, in accordance with the observation that crucial events play a vital role in the transport of information from one complex network to another [12].

Finally, it is vital to say that [50] and [51] inspect a non-stationary human network by means of DEA that empowers them to uncover the presence of periodicity and complexity simultaneous. Sarkar and Barat [51] apply DEA to analyze heartbeats before and after meditation, with the astounding revelation of a distinct oscillatory behavior of diffusion entropy. We shall come back to talk about the results of [51] in section 4.8. Here we restrict ourselves to properly addressing the connection between crucial events and multifractality by using surrogate sequences with a mixture of Poisson-like and crucial events, including the situation where only crucial events are hosted in the sequence. Such surrogate arrangements enable us to assess how crucial events are perceived by MFDFA. This is the case where it is useful to utilize the prescription for bare crucial events.

As indicated by the measurable examination of [28] the distinction between healthy and pathologic subjects is set up by noting that the heartbeat dynamics of pathologic subjects host a critically large number of uncorrelated Poisson-like events. An essential result of this study is the observation that uncorrelated Poisson-like events have the impact of lessening HRV. The largest HRV is figured it out in the ideal case of cardiac dynamics uniquely determined by the SOTC process, with its complete time evolution including the transient regime, intermediate asymptotics with its crucial events of Eqs. (1.1) and (2.2), and the final tempered asymptotic regime. The dressed crucial events are a type of randomness flagging the healthy physiological function of heartbeats, while the uncorrelated Poisson-like events represent a disturbance of this healthy physiological function and therefore we refer to them either as randomness or strong randomness, when they reach the high concentration revealed by our analysis in the case of heart failure. In addition to results of diagnostic approach, this investigation starts down the road to a more profound comprehension of the dynamical origin of multifractality.

4.4. Intermediate Asymptotics

In his book on intermediate asymptotics [52] Barenblatt adopts a visual art metaphor to illustrate the idea of intermediate asymptotics: "... We need to take a look at paintings at a distance far enough not to see the brush-strokes, but rather in the meantime sufficiently enough to enjoy not only the painting as a whole but also its important details: think of van Gogh's work, for example. ...". Goldenfeld [53] delineates the renormalization group rules that we need to adopt to eliminate the divergences generated by the perturbation approach. This representation is based on the assumption that the physical condition of intermediate asymptotics is a type of perennial transition to equilibrium.

There is a wide conviction that this is a simplifying however valuable glorification of reality. A remarkable example is managed by the work of Mantegna and Stanley [54]. These authors noticed that although a finite size-actuated truncation is an unavoidable outcome of the dynamics of real physical processes, the time duration of the transition to the Gaussian statistics prescribed by the central limit theorem may turn out to be extremely extended, in accordance with the idealized condition of perennial intermediate asymptotics of Goldenfeld. However, for practical purposes a complex system can likewise be seen on so extensive a time scale as to see dynamical impacts that for straightforwardness might be deciphered as types of ordinary fluctuation-dissipation processes. Essential work has been done to get analytical results for both short- and long-time regimes, see for example [55], which activated noteworthy enthusiasm in the appropriate mathematical formalism of transient anomalous diffusion [56], including the exponential type of tempering [57, 58]. It is advantageous to point out that tempering might be an impact of representing real physical processes by means of finite length time series, an unavoidable consequence of observation. We accept [38] that tempering is a bona fide property of self-organization process itself, since it rises up out of the cooperation of a finite number of units and that the heartbeat dynamics belongs to this class of self-organizing processes, thereby involving tempering.

4.5. DEA and Crucial Events

The DEA technique [23] was initially acquainted to properly analyze time series assumed to be driven by crucial renewal events. It is essential to stress that the renewal events speculated [28] for the analysis of heartbeats are the subject of an extended literature concentrating on the phenomenon of renewal aging [59]. For an agreeable delineation of the main results of this study, we remind the readers about an algorithm used to produce non-Poisson renewal events. It is given by [12]

$$\tau = T\left(\frac{1}{y^{\frac{1}{\mu-1}}} - 1\right), \tag{4.1}$$

where y is a real number selected with uniform probability on the interval $(0, 1)$. The times τ produced by this method are completely uncorrelated and obey the waiting time PDF

$$\psi(\tau) = (\mu - 1)\frac{T^{\mu-1}}{(\tau + T)^{\mu}}. \tag{4.2}$$

Note that to be as close as possible to the tempering prescriptions of SOTC [38], we should adopt a survival probability $\Psi(t)$ with the structure

$$\Psi(t) = \left(\frac{T}{t+T}\right)^{\mu-1} \exp(-\lambda t), \tag{4.3}$$

with the transient regime to intermediate asymptotics being determined by the parameter T and defined by the time region $0 < t < T$. The time region of intermediate asymptotics corresponds to $T < t < \frac{1}{\lambda}$ and the tempered region is given by $t > \frac{1}{\lambda}$. For the sake of simplicity, surrogate sequences hereby utilized are established using Eq. (4.1), which would correspond to $\lambda \to 0$, the tempered action being exerted by the finite size of the time series, L. We make the assumption that $\lambda \propto 1/L$.

In this chapter, following the results of earlier work [28], we restrict our analysis to the IPL index range:

$$2 < \mu < 3. \tag{4.4}$$

It is important to notice that the Poisson events correspond to $\mu = \infty$, but events generated using $\mu = 5$ are sufficienctly far from the crucial condition which can be used as generators of non-crucial events. The algorithm of Eq. (4.1) can be applied to describe in an intuitive way the different nature of the randomness of $\mu < 3$ as compared to that of $\mu \gg 3$. The time interval between two consecutive events of the random number y in Eq. (4.1) has the mean value

$$\langle \tau \rangle = \frac{T}{(\mu - 2)}, \tag{4.5}$$

as can be easily determined using the waiting time PDF $\psi(t)$ of Eq. (4.2) to find the average. If $\langle \tau \rangle < \Delta t$, where Δt is the integration time step, we see a process that is totally random. In the limiting case of $\mu < 2$, $\langle \tau \rangle \gg \Delta t$, since in this case $< \tau >$ is divergent; the randomness is sporadic. In the region $2 < \mu < 3$ randomness is not as sporadic as for $\mu < 2$. However, $< \tau^2 >$ is divergent and as a consequence randomness remains distinctly intermittent. We assume that the sporadic randomness of crucial events is better for the healthy function of cardiac dynamics and that an excess of randomness is risky.

To talk about the joint activity of frequent and sporadic randomness let us generate resonable surrogate time series, namely a proper sequence of times $\tau_1, \tau_2, ...\tau_i, \tau_{i+1}, ...$. This arrangement is produced by a repeated random selection of y in Eq. (4.1) so as to generate either a sequence of crucial events, with $\mu < 3$, or a sequence of non-crucial events, with $\mu > 3$. More accurately, in the applications of the present study we choose $3 > \mu > 2$ for crucial events and $\mu = 5$ for non-crucial events.

Each of these two time sequences has to be converted into a corresponding suitable fluctuation $\xi(t)$. For that we apply the Asymmetric Jump Model (AJM) [28]. The reason of choosing this model is that this random walk rule helps DEA to find the correct scaling established by the generalized central limit theorem (GCLT) [60] in the entire crucial event region $\mu < 3$, including the region $\mu < 2$. This random walk rule is obtained by setting $\xi = 0$ when there are no events, and $\xi = 1$ when either a crucial or uncorrelated Poisson event occurs.

Thus we generate two time series, one corresponding to $\mu < 3$ and the other corresponding to $\mu > 3$. The surrogate time series used here for the analysis corresponds to the superposition of both time series,

$$\xi(t) = (1- \in)\xi_{\mu>3}(t)+ \in \xi_{\mu<3}(t). \tag{4.6}$$

The parameter $\in< 1$ is the probability that the observed heartbeat signal, detected according to the prescription of the next section is generated by a genuine SOTC process. The prescription chosen to produce the complex time series is the prescription earlier mentioned as generating bare crucial events. In Section 4.6 we illustrate how to obtain $\in$ from the analysis of real heartbeat data, with the help of surrogate time series when we apply the prescription to create dressed crucial events.

In the case where SOTC events are visible, specifically $\in= 1$, DEA leads to the detection of the scaling index

$$\delta = \frac{1}{\mu - 1} \tag{4.7}$$

after an initial transient corresponding to the micro-time regime, where complexity process is not yet perceived. Keep in mind that the transition from the Lévy to the Gauss regime occurs at $\mu = 3$. However, as mentioned earlier, the surrogate time series of this study rest on $\mu = 5$, namely a condition well imbedded in the Gaussian basin of attraction.

Figs. 4.1, 4.2 and 4.3 show the results of applying DEA to a different data sets through the linear-log representation, which is used, according to Section 3.1, to detect the scaling index δ, the slope of the linear portion of $S(t)$ in this representation.

Fig. 4.1 shows the case where $\in= 1$, specifically the condition where the bare crucial events are fully visible, with $\mu = 2.2$. The corresponding crucial scaling should be $\delta = 0.83$. However, in the short time regime the scaling has the larger value $\delta = 1.5$ and the scaling $\delta = 0.83$ of crucial events appears in the intermediate time regime. For this reason, the proper scaling, as shown in this figure, is optimal in the intermediate time regime. Actually, we see that in the region around $t \propto 10^5$ a tempering deviation from the crucial scaling of Eq. (4.7) occurs. Note that this is not the tempering of the SOTC defined in [38]. The

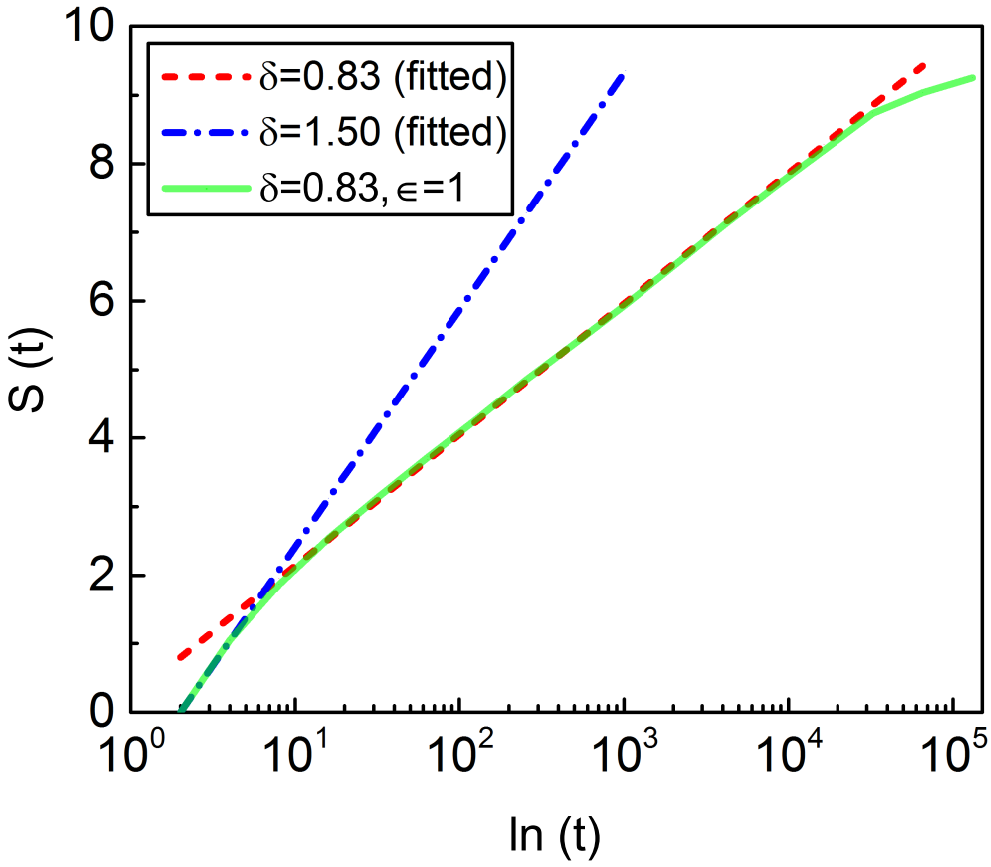

FIGURE 4.1. Entropy of the time series versus the logarithm of time from the micro-time to the asymptotic time scale with $\in = 1$. The solid line (green) is numerical. Numerical constants are $T = 0.5$ and length of time series $L = 1.5(10^5)$. We use the prescription generating bare crucial events.

theoretical study of that physical tempering of the process is beyond the scope of this study, but we make the plausible assumption that heartbeat dynamics fit it as a consequence of being itself a self-organized process.

Fig. 4.2 illustrates the more important case where the crucial events are hidden by a billow of noncrucial events. In this case, too, according to previous analysis [28], the precise scaling obtained by the bare crucial events appears in the intermediate time regime. However, in this case the reason for the initial transient is quite different from the SOTC

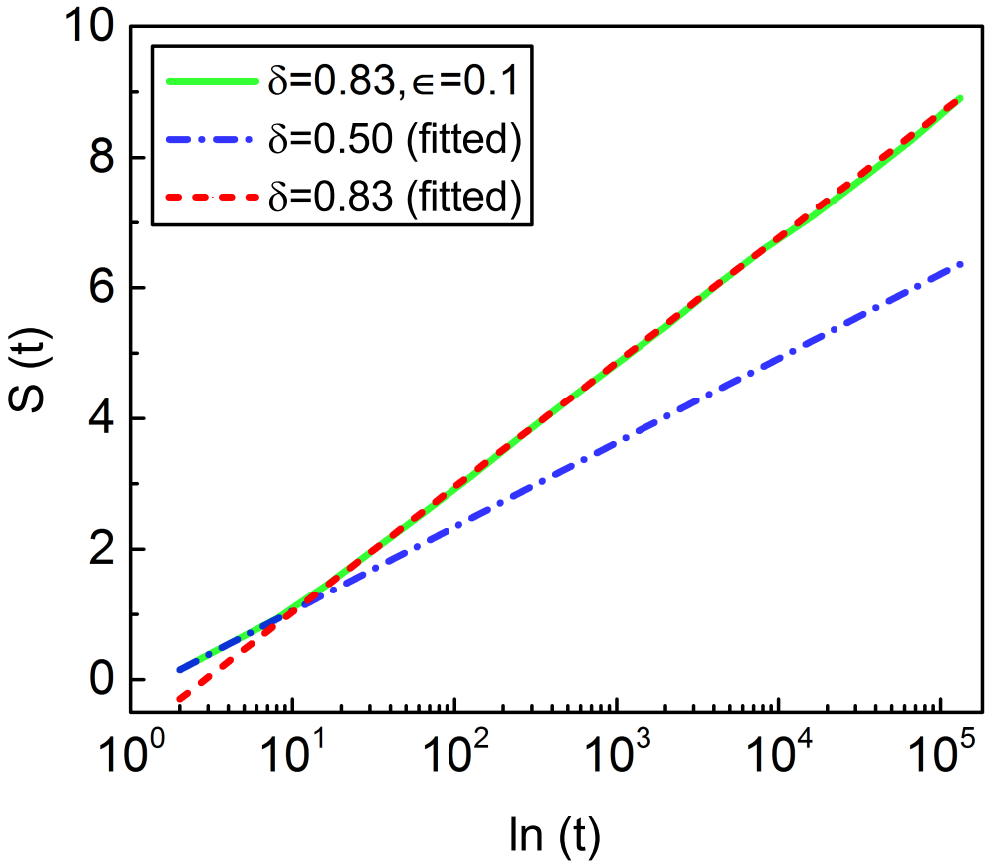

FIGURE 4.2. Entropy of the time series versus the logarithm of time from the micro-time Gaussian basin of attraction to the asymptotic time scale with $\in = 0.1$. The solid line (green) is numerical. Numerical constants are $T = 0.5$ and length of time series $L = 1.5(10^5)$. We use the prescription generating bare crucial events.

initial transient. In this case the initial short-time regime characterized by the conventional scaling $\delta = 0.5$, corresponds to the scaling of uncorrelated Poisson-like events. In the long-time limit, when the SOTC intermediate asymptotic emerges, the faster scaling of the crucial events with $\mu < 2$ leads them to crossover to ordinary diffusion. The overlap of the Poisson-actuated transient regime and transient SOTC make the derivative of the diffusion entropy non-monotonic. For the sake of simplicity we don't demonstrate this complicated behavior,

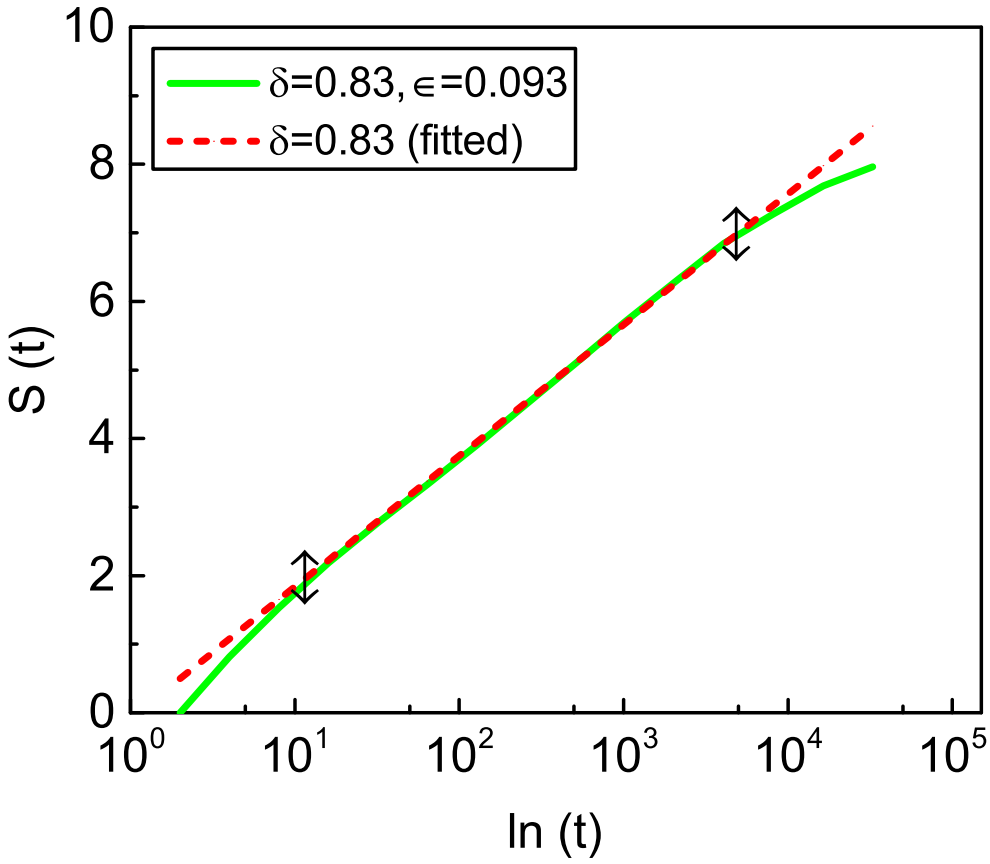

FIGURE 4.3. DEA determines the scaling of invisible crucial events in the intermediate asymptotic time. The solid line (green) is produced from real heartbeat data of healthy individual. The scaling index δ is the slope of the straight line between the two vertical arrows.

rather we concentrate on the complexity of the intermediate asymptotics. Notice that, although the stretched out transient to the intermediate asymptotic regime actuated by a large percentage of uncorrelated Poisson-like events can be confused with the transient SOTC regime, the corresponding physical impacts are the inverse of each other. The SOTC transient creates a wide multi-fractal spectrum, while the long transient actuated by a large percentage of uncorrelated Poisson-like events has the impact of making the multi-fractal spectrum narrower.

To wrap up this section we make a few remarks concerning Fig. 4.3. In Section 4.6 we disclose how to get this figure from real data on heartbeats. Here we constrain our observation to the scaling index δ, representing the indicator of the occurrence of crucial events. The IPL index is obtained by observing the intermediate asymptotics region, the short- and long-time limit of which are meant by vertical arrows. In this case, the deviation from Eq. (4.7) of the tempering region is most likely due the properties of heartbeats, as opposed to the finite size L of the sequence under investigation.

In brief, it is imperative to emphasize that based on late advances made concerning SOTC [38], the time series produced by complex processes are described by three regimes: the short-time regime, where the genuine complexity of the process is not yet perceived; an intermediate time regime driven by the crucial events; and a long-time regime where the process can be mistaken for an ordinary statistical process. The long time regime is, on the contrary, a tempering effect generated by self-organization.

4.6. Detecting Events in Heartbeat Time Series

Following [27] and [28], we use the ECG records of the MIT-BIH Normal Sinus Rhythm Database and of the BIDMC Congestive Heart Failure Database, for healthy and congestive heart failure patients, respectively.

The fundamental issues experienced in demonstrating that SOTC is the procedure driving the phenomenon under investigatiion has to do with the detection of the crucial events, in particular, events with a waiting time PDF yielding a diverging second moment. Fig. 6.7 demonstrates the approach we adopt, following that utilized before [28]. The experimental signal is generated by assigning to each beat a value corresponding to the time interval in the vicinity of one and the following.

We partition the inter-beat time axis into proper stripes of size ΔT. We take after the results of the investigation done in [61] to define ΔT. These authors recommend $\Delta T \cong$ 30 msec and we set $\Delta T = 33$ msec. We identify the occurrence of an event when the experimental signal crosses the stripes. We observe that the heartbeat trajectory may stay

in a particular strip for an extended time, suggesting the typical intermittent behavior that led to the finding of crucial events. However, the experimental signal crossing the border between two bordering stripes isn't necessarily a crucial event. The crucial events are renewal and thus the times τ_i should be uncorrelated. To assess the breakdown of the renewal condition we find the time-average correlation function, where the time average is given by an overbar

$$C(t) = \frac{\sum\limits_{|i-j|=t} \overline{(\tau_i - \overline{\tau})(\tau_j - \overline{\tau})}}{\sum\limits_{i} \overline{(\tau_i - \overline{\tau})^2}}. \tag{4.8}$$

This correlation function is properly normalized yielding $C(0) = 1$, and in the case of actual renewal events must satisfy the condition $C(t) = 0$ for $t > 0$. On the other hand we get

$$C(1) \approx \in^2, \tag{4.9}$$

where $\in$ is the probability of selecting ξ, see Eq. (4.6). This result is theoretically well explained. According to [61] the correlation function $C(t)$ must read

$$C(t) = (1- \in^2)\delta_{t,0} + \in^2 \Lambda(t), \tag{4.10}$$

where $\delta_{t,0}$ refers to the Kronecker unit step function, namely a function equal to 1 for $t = 0$ and equal to 0 otherwise, and $\Lambda(t)$ is a slowly decaying smooth function with the property $\Lambda(0) = 1$. This theoretical approach results Eq. (4.9).

In short, we must use $C(1)$ to define $\in$. The investigation of real data as appeared in Fig. 4.5 drives to conclusions that qualitatively match with this theoretical approach, with some cautionary remarks, however. Fig. 4.5 demonstrates that the correlation function $C(t)$ makes a sudden jump from 1 to a little, but non-vanishing value of $\in^2$, affirming that the examination we apply to uncover events actually does not detect only genuine renewal events, but a blend of renewal and non-renewal events. Moreover, as depicted from Fig. 4.5, in the case of pathological individuals, $C(t)$, after the fall experiences quick exceptional fluctuations that may stop us from defining $\in^2$ through $C(1)$. In this situation, and in the case where $C(1) < 0$ as well, we alternatively define $C(1)$ through the average over the first one

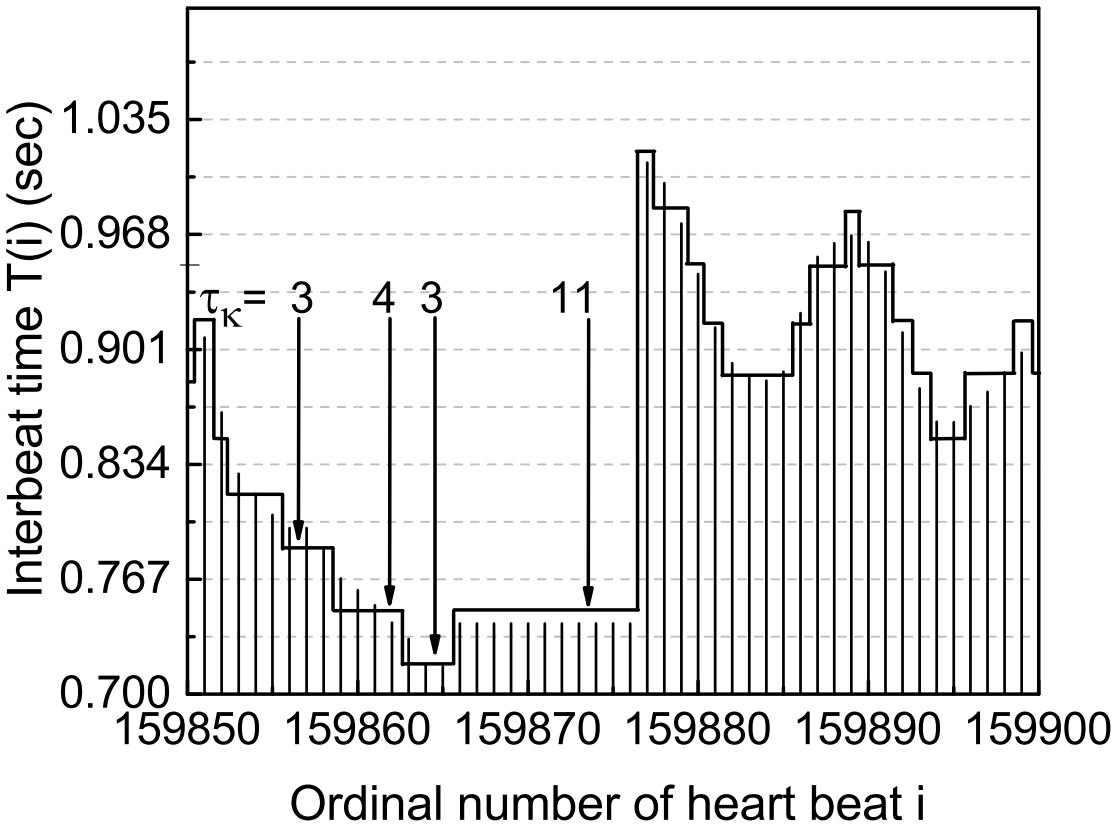

FIGURE 4.4. Rule applied to define events. An event is defined as the experimental curve, thick black line, crossing the border between two nearest stripes. The symbols τ_k represent the time distance, as number of beats, between two consecutive events, characterized as the black line crossing from one strip to one of the neighbor stripes The size of the stripes is $\Delta T = 1/30$ sec.

hundred events. In the case of fluctuations of moderate intensity, we utilize $C(1)$ to define $\in^2$. We likewise utilize Fig. 4.5 to characterize the border between strong and weak randomness. Estimations of $\in^2$ larger than 0.05, $\in >$ 0.22, are considered as weak randomness and values of $\in^2$ smaller than 0.05, $\in <$ 0.22, are considered as strong randomness.This definition is suggested by the observation of the healthy and pathological individual of Fig. 4.5, however this definition must be used with caution because the distinction between healthy

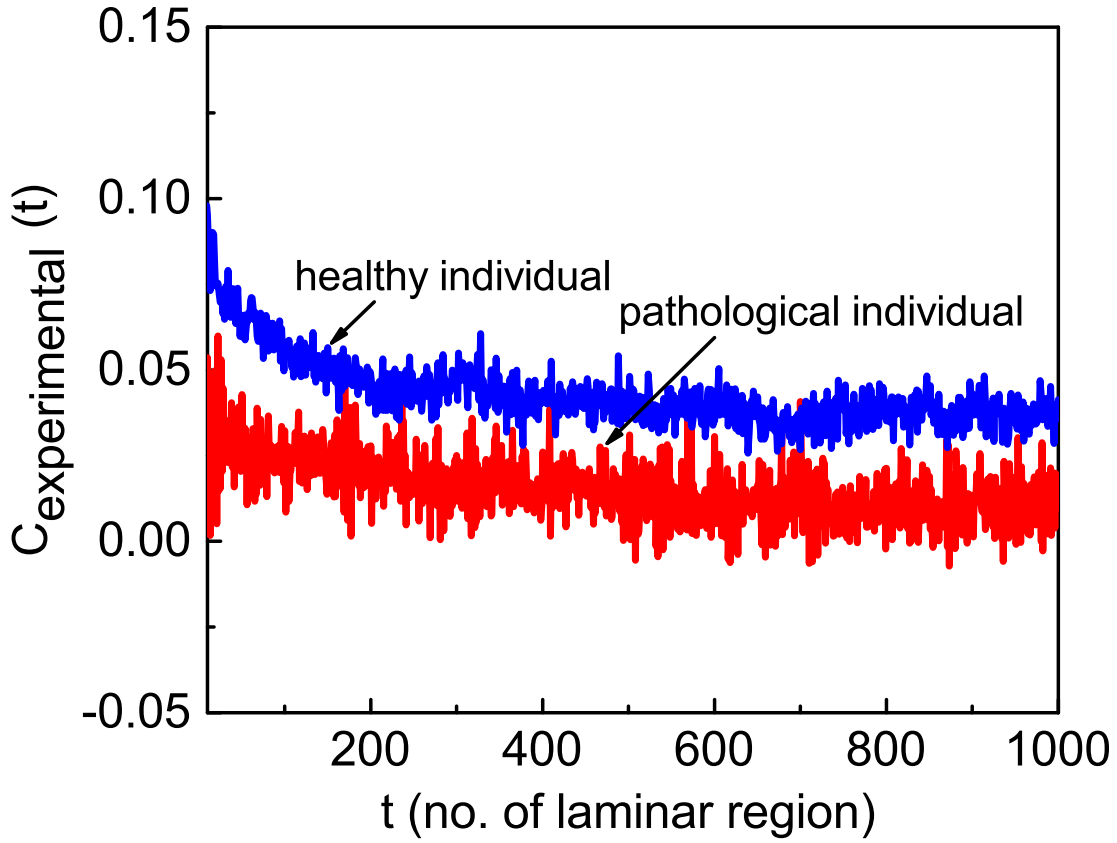

FIGURE 4.5. Correlation function $C(t)$ for two typical patients, one healthy and one pathological.

and pathological individuals, as shall we observe with Fig. 4.8, requires the knowledge of the scaling index δ and in addition that of $\in^2$.

To show signs of improvement in the comprehension of the significance of $\in^2$, and to clarify the theoretical motivation behind why we can utilize Eq. (4.9), we interrogate the surrogate sequences defined by Eq. (4.6), for the situation when the sequence of crucial events is generated by the prescription to create dressed crucial events. With the assistance of Fig. 4.6 and Fig. 4.7 we build up that the intensity $\in^2$ is the square of the probability that an event is a crucial event. This is the motivation behind why we choose the symbol $\in^2$ to signify the estimation of the correlation C(t) instantly after the sudden jump down

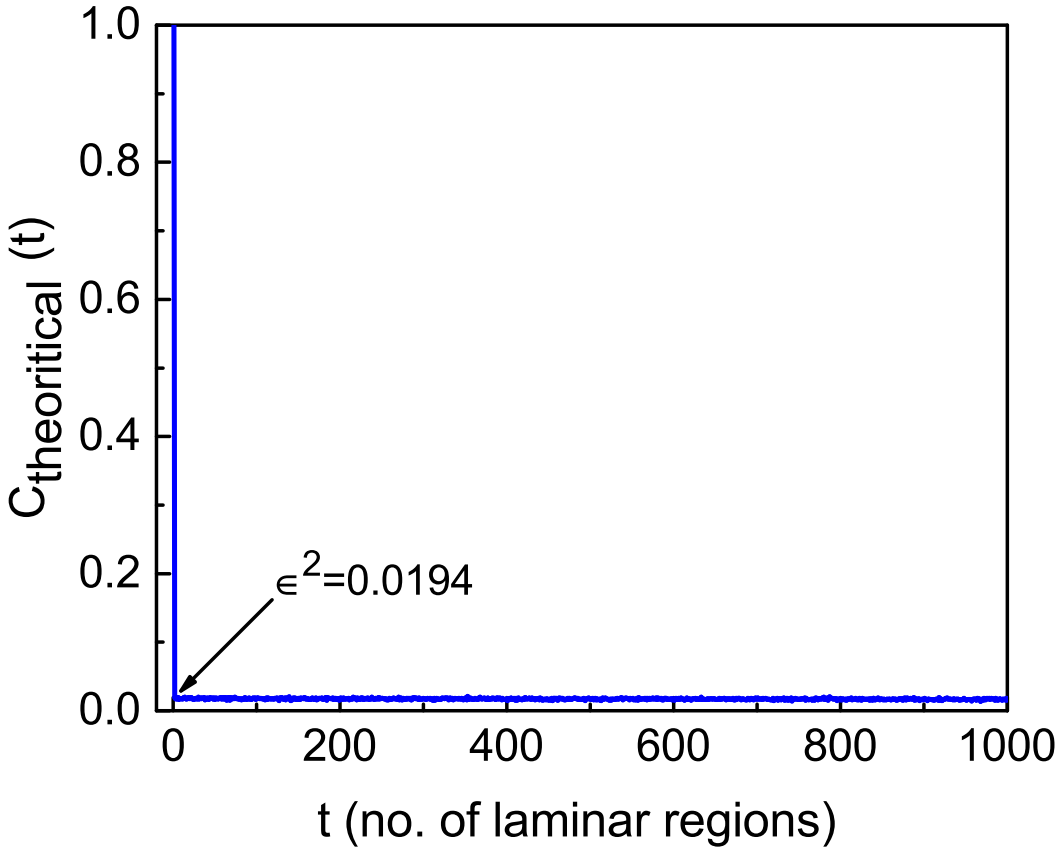

FIGURE 4.6. Correlation function C(t) for the surrogate data in the case of strong randomness. We utilize the prescription creating dressed crucial events.

from $C(0) = 1$. Fig. 4.6 demonstrates a theoretical correlation function utilizing a surrogate sequence for strong randomness. Fig. 4.7 demonstrates a theoretical correlation function utilizing a surrogate sequence for weak randomness.

It is important to address that the selection of $\Delta T = 1/30$ sec is not random. In fact, investigators [61] determine that the estimation of ΔT prompts the maximal intensity of $\in^2$ for all patients, both healthy and pathological, except for the transplanted hearts. This widespread property appears to infer the action of the autonomic system [61].

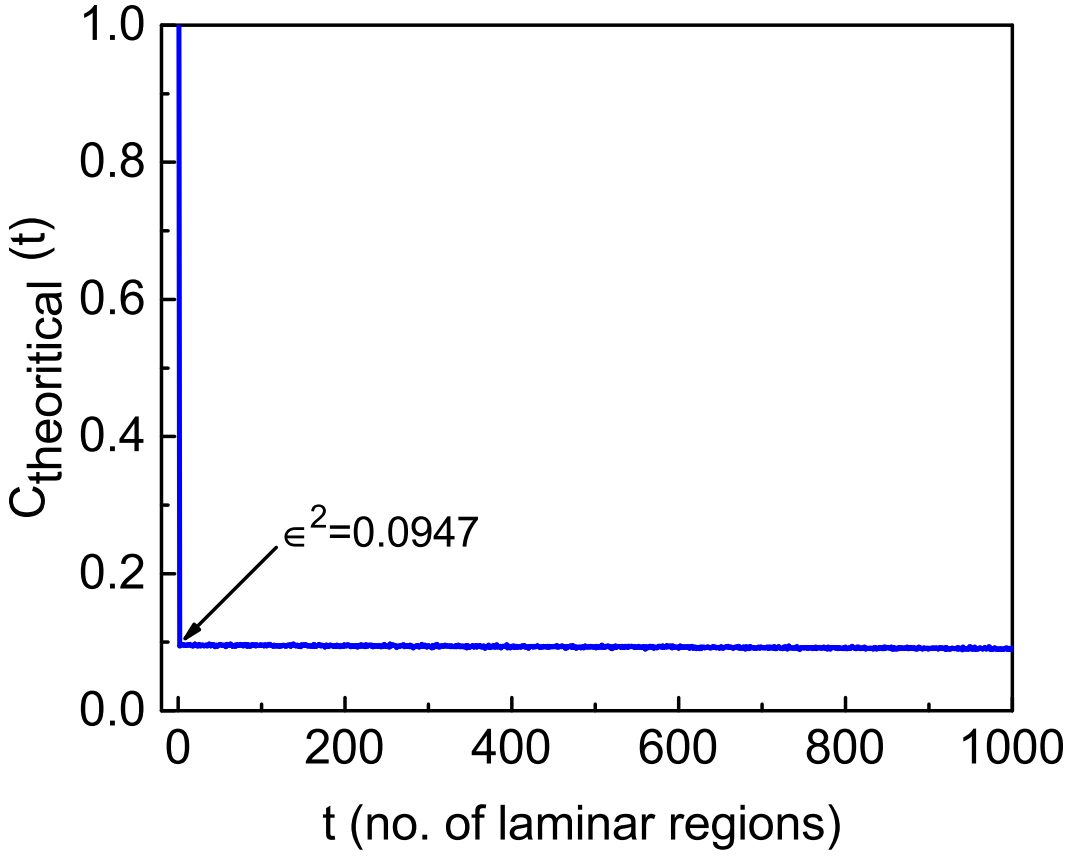

FIGURE 4.7. Correlation function C(t) for the surrogate data in the case of weak randomness. We utilize the prescription producing dressed crucial events.

4.7. Joint Use of DEA and C(t)

Here, we retrieve the main result of [28], which was based on the joint use of DEA and the correlation function $C(t)$. For each subject we evaluate both δ and $\in^2$.

Fig. 4.8 is virtually identical to the main result discovered by the investigators of [28], which determines a measure to recognize pathological patients from healthy patients using HRV time series. We see that the ideally healthy condition compares to $\in= 1$ and $\delta = 1$. This implies that the crucial events should not host any uncorrelated Poisson-like event and must have $\mu = 2$, which is the border between the region of perennial aging, $\mu < 2$, and the region where the rate of randomness production becomes constant in the long-time limit,

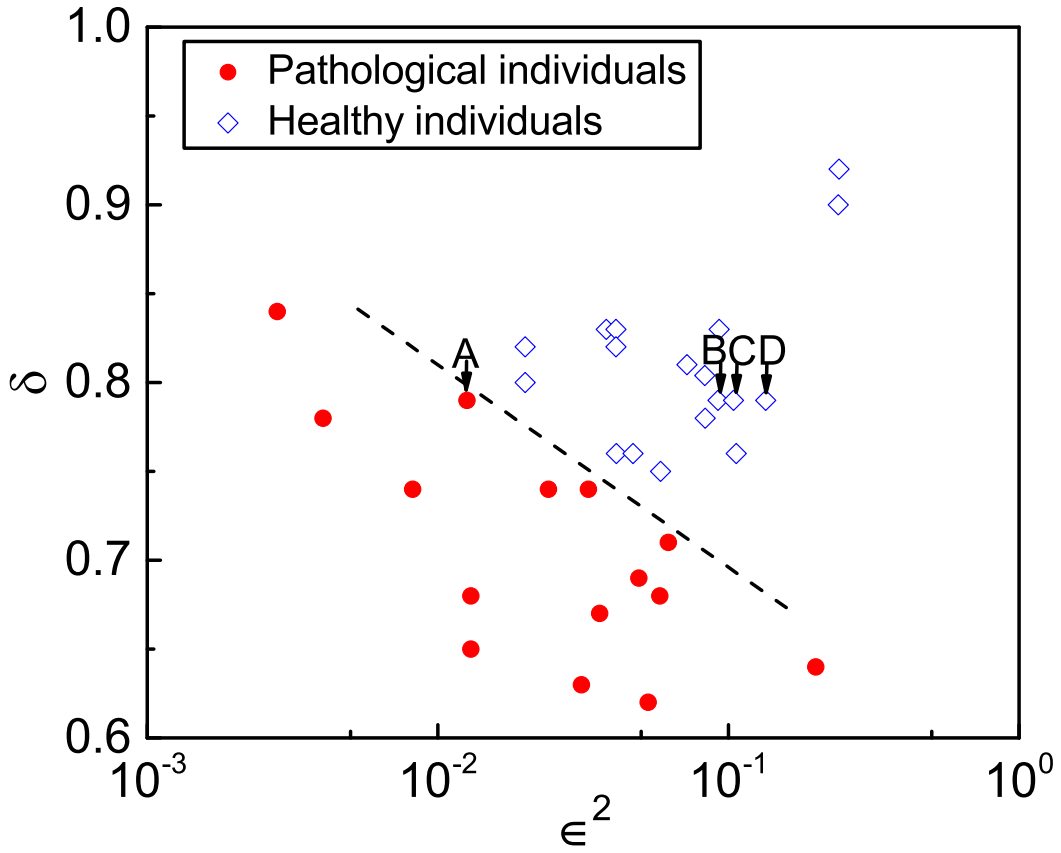

FIGURE 4.8. Distinguishing subjects with healthy from those with pathological HRV.

$\mu > 2$ [12]. The individuals' HRVs advance toward the pathological condition as their scaling turns out to be nearer to the scaling of ordinary diffusion $\delta = 0.5$, to be specific nearer to the border between the region of crucial events, $\mu < 3$, and the Gaussian basin of attraction, $\mu > 3$.

It is important to note that the work of [11] built up that the brain, producing perfect $1/f$-noise, is situated at the outskirt between the region of perennial aging and the region of crucial events hosted by heartbeats, as per the investigation of this study and prior work [28].

The investigation done in the new field of network medicine [62] concentrates on the

communication between the diverge organs of the human body, the brain and heart being a unique instance of this intercommunication [63]. As per the *principle* of *complexity matching* [12], based on the assumption that the synchronization of complex networks is encouraged by the networks having the same complexity, $\mu = 2$, in the case of brain-heart correspondence, we make the conceivable assumption that the right-top corner of Fig. 4.8 refers to a suitable condition for brain-heart communication in the ideal case of healthy patients. However, the recent literature on complexity matching stresses the correspondence between the two complex networks through their multi-fractal spectra [34]. Along these lines, building up a relation between crucial events and multi-fractal spectra is an objective of this study. The most essential property of Fig. 4.8 is to contribute to achieve that objective by building up a relation between [28] and [27, 29].

We concentrate our attention on the patients marked A, B, C and D in Fig. 4.8. These patients have the same δ and as indicated by the prior analysis [28] the distinction amongst sick and healthy patients is due to the fact that the heartbeat of the sick patients is influenced by excessive randomness. Moreover, as per some investigators [27, 29] the difference is because of the fact that healthy patients have more wider multi-fractal spectra.

The focal result of this investigation is acquired by applying the MFDFA to the patients A, B, C and D to prove the relation between the diagnostic approach of [28] and that of [29, 27].

Fig. 4.9 fully confirms this connection. We observe that , moving from the sick (A) to the healthy patients (B,C,D) has the impact of broadening of the multi-fractal spectrum. Note that Fig. 4.10 presents additional confirmation of this relation through the utilization of surrogate sequences.

4.8. Concluding Remarks

The diagnostic technique produced by following prior work [28] provides extra advantages compared to the method of [29]. One of these advantages is that the distinction amongst healthy and pathologic patients is built up through the two-dimensional portrayal

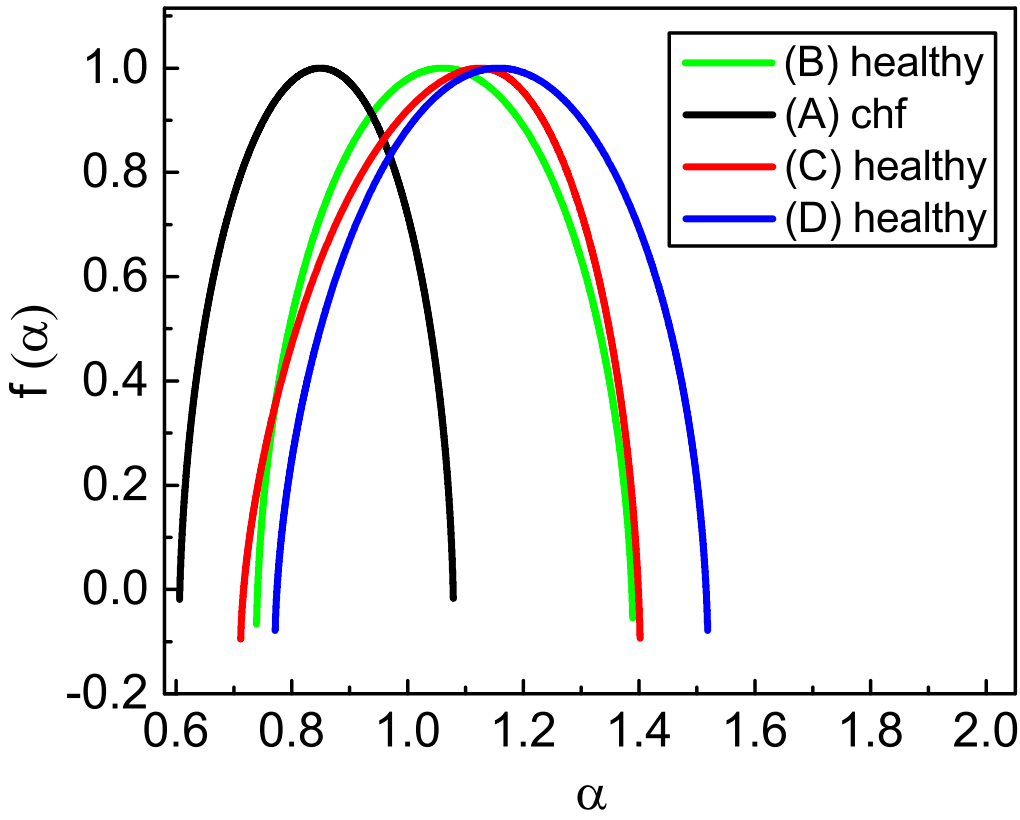

s

FIGURE 4.9. Multi-fractal spectra of HRV as a function of $\in$ (see Fig. 4.8) keeping constant the scaling index $\delta = 0.79$.

of Fig. 4.8 instead of the three-dimensional portrayal of [29]. Another significant outcome of this investigation is its contribution to an enhanced vision of variability and multi-fractality. To welcome this noticable improvement let us concentrate on the outcomes obtained by applying the MFDFA to the surrogate series in the limiting case of a SOTC [38] process, unperturbed by uncorrelated Poisson-like fluctuations $\in= 1$, and of a mere sequence of uncorrelated fluctuations, $\in= 0$.

The outcome of this investigation is illustrated in Fig. 4.11. In the top panel of this figure we adopt the prescription to create bare crucial events and in the base we adopt

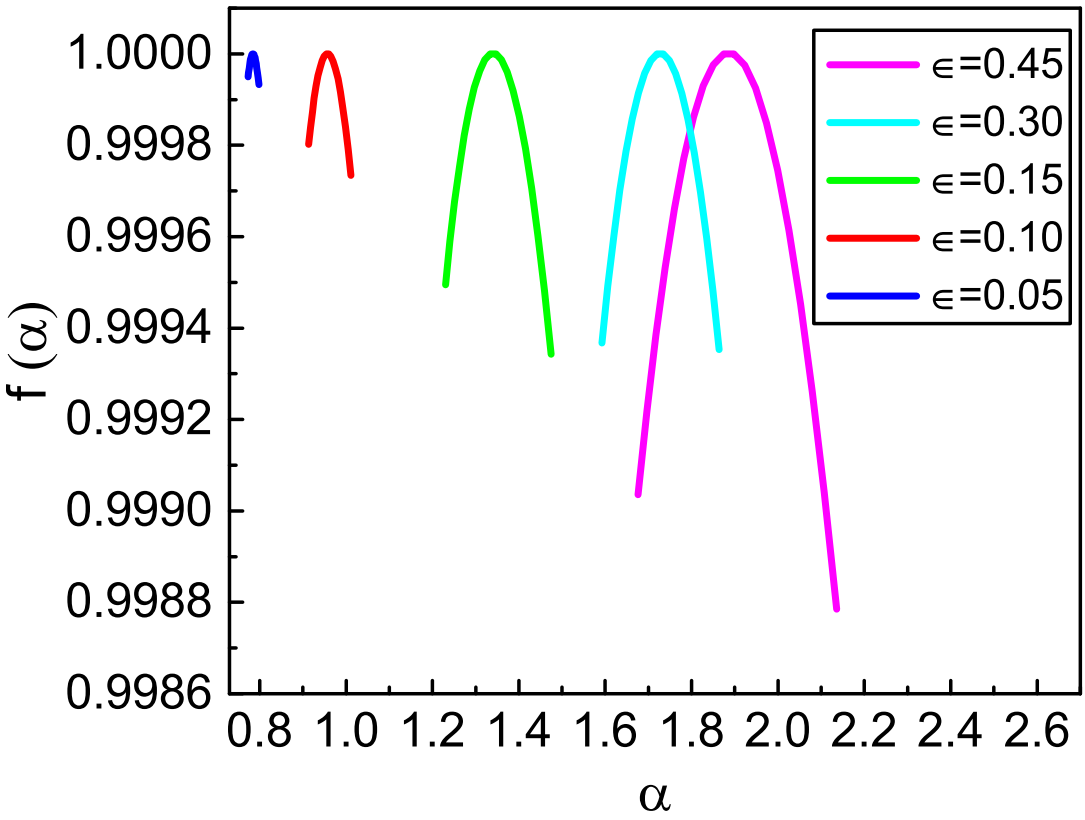

FIGURE 4.10. Multi-fractal spectra of surrogate data, based on the prescription creating bare crucial events, as a function of $\in$ with constant the scaling index $\delta = 0.83$.

the prescription to produce dressed crucial events. Obviously, for the situation $\in= 0$ both procedures create a very sharp multifractal distribution centered at $\alpha = 0.5$.

The narrowest multi-fractal spectrum is obtained by setting $\in= 0$. The broadest multi-fractal spectrum is obtained without Poisson-like random events, $\in= 1$, with a slight difference between bare crucial events (top panel of Fig. 4.11) and dressed crucial events (bottom panel of Fig. 4.11). The dressed crucial events are appeared to yield a more extensive multi-fractal spectrum.

We restate that, as per SOTC [38], crucial events are portrayed by three different

time regimes, a transient initial regime, the intermediate asymptotics time regime, and a last tempered time regime with exponential truncation. The transient time regime turns out to be increasingly stretched out with reducing $\in$. However, the extended transient regime produced by a very small value of $\in$ must not be mistaken with a wide transient regime relating to the occurrence of an adequate number of crucial events to realize the prescription $\delta = 1/(\mu - 1)$ of the GCLT [23, 60]. The GCLT transient regime is the smaller scale advancement towards the IPL regime anticipated by SOTC [38]. This transient regime, the intermediate asymptotic time regime and the last tempering time regime are the creators of the wide variability that the multi-fractal DFA proficiently identifies. The uncorrelated Poisson-like events with $\mu > 3$ produce a stretched out transient regime that has the contrary impact of yielding a very narrow spectrum around the ordinary scaling index $\alpha = 0.5$.

Taking everything into account, the outcomes of this study set up a connection between the multi-fractal spectrum and SOTC fluctuations, subsequently managing a promising tool to get further advancements in the field of network medicine [62], where broad multi-fractal spectra are transferred, as indicated by [12], starting with one network onto another by means of crucial events.

The exploration program laid out in this chapter isn't finished, since we have not, so far, addressed the brain-heart correspondence and the impact of periodicity [63]. It is vital to mention that SOTC [38] can be applied to create a self-organization phenomenon combining crucial events and periodicity, so as to change the black line of Fig. 4.4 into fluctuations that affected by either therapeutic action [64] or meditation [51] may turn out to be relatively coherent oscillations.

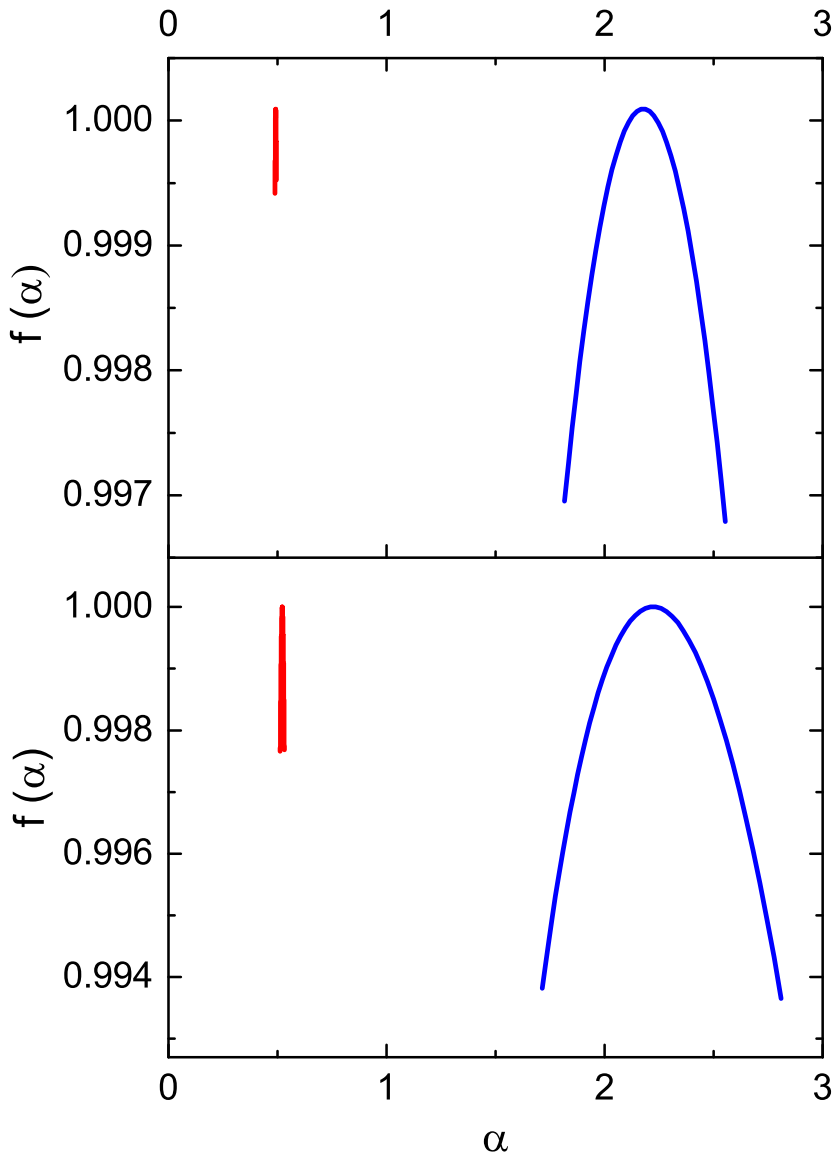

FIGURE 4.11. Extreme cases of very narrow, $\in = 0$, and very broad, $\in = 1$, multi-fractal spectra. The top panel is based on the prescription creating bare crucial events and the base panel is based on the prescription creating dressed crucial events. Numerical constants used in the calculation are $T = 0.5$, $L = 1.5(10^5)$, window sizes $(500 : 500 : 30000)$. Other parameters are moments range $q = -0.4 : 0.001 : 0.4$ for $\mu = 5$ and $q = -0.02 : 0.001 : 0.02$ for $\mu = 2.2$.

CHAPTER 5

MEDITATION AND HEARTBEAT DYNAMICS

Results obtained in Chapter 4 led us to focus our analysis on the statistical properties of crucial events. We have adopted the same statistical analysis to study the statistical properties of the heartbeat dynamics of subjects practicing meditation. The heartbeats of people doing meditation are known to produce coherent fluctuations. In addition to this effect, we made the surprising discovery that meditation makes the heartbeat depart from the ideal condition of 1/f noise. Also, this method of statistical analysis quantifies the level of stress reduction realized by the practice of Kundalini Yoga Meditation.

5.1. Introduction

Stress is known to disturb the ordinary HRV spectrum and figuring out how to evade the debilitating impact of stress is one of the motivation of meditation. The origin of meditation is unknown, yet researchers agree that it has been part of civilized culture for thousands of years, with the earliest records, around 1,500 BCE, involving Vedantism, a Hindu custom in Nepal and India. As specified by Chow [66] the *Yoga Sutras of Patanjali*, illustrating the eight limbs of yoga, was incorporated between 400-100 BCE. Contemporaneously, the *Bhagavad Gita* was composed, which talks about the philosophy of yoga and meditation.

From a physiological point of view meditation constitutes a coupling of the functionality of the heart with that of the brain and has been investigated and grown for centuries. However, we are just now starting to apply the techniques of science and data analysis to this brain-heart coupling. The fundamental purpose of this investigation is to give a measure of decrease in the level of stress provided by meditation, which is to evaluate, through the

statistical analysis of HRV time series before and during meditation, precisely how much stress is reduced by control through meditation of the heart-brain coupling.

5.2. Statistics

The crucial events are described by the fundamental property that the time interval between the occurrence of consecutive crucial events is described by the waiting-time probability density function (PDF):

$$\psi(\tau) \propto \frac{1}{\tau^{\mu}}, \tag{5.1}$$

As indicated by Watkins [67, 68] the non-ergodic fractional renewal model of Mandelbrot [69, 70] yields the inverse power law (IPL) spectrum as function of the frequency f:

$$S(f) \propto \frac{1}{f^{\gamma}}, \tag{5.2}$$

with

$$\gamma = 3 - \mu. \tag{5.3}$$

The dynamics creating crucial events are renewal, which implies that the sequence of waiting times $\{\tau_i\}$ between successive events are totally independent of one another. This renewal property can also be expressed by the assumption that the probability of occurrence of both τ_i and τ_j, $\Pi(\tau_i, \tau_j)$, when $i \neq j$ is given by,

$$\Pi(\tau_i, \tau_j) = P(\tau_i) * P(\tau_j), \tag{5.4}$$

where $P(\tau_i)$ and $P(\tau_j)$ are the probability of occurrence of τ_i and τ_j, respectively.

Also, the times τ_i should not be correlated. This property is expressed by the mathematical relation of the two-point correlation function

$$C(t) = \frac{\sum\limits_{|i-j|=t} \overline{(\tau_i - \overline{\tau})\,(\tau_j - \overline{\tau})}}{\sum\limits_{i} \overline{(\tau_i - \overline{\tau})^2}}. \tag{5.5}$$

This correlation function is properly normalized, thereby yielding $C(0) = 1$, and in the case of genuine renewal events should satisfy the condition $C(t) = 0$ for $t > 0$. Here, we focus on $C(1)$ defined as $C(1) = C(t = |i - j| = 1)$.

The physical significance of this mathematical property is that the occurrence of a renewal crucial event creates a rejuvenation of the system. Therefore, the system develops towards the occurrence of the upcoming renewal event as if the occurrence of the earlier crucial event made the system brand new.

We found that meditation shifts the IPL index μ of Eq. (5.1) with perfect $1/f$ condition, $\mu = 2$, to the index values close to the Gaussian basin of attraction, $\mu = 3$.

5.3. Subordination of Harmonic Oscillations

Ascolani [71] investigated the subordination of a dynamic process to harmonic motion in 2009. We assume that the clock's hour-hand completes a rotation from twelve to twelve through M clicks. The time interval between two consecutive clicks Δt is normalized to 1. The frequency of the regular oscillator is given by

$$\Omega = \frac{2\pi}{M}. \tag{5.6}$$

The regular oscillation is deterministic motion given by the rate equation

$$\frac{d\xi}{dt} = i\Omega\xi \tag{5.7}$$

Being insigthful of the decision $\Delta t = 1$, we set $\Omega \ll 1$ in order for the dynamics to be as close as possible to the coherent behavior of a regular clock. Each time duration between back to back clicks is changed over into an operational time τ whose statistics are given by the hyperbolic PDF;

$$\psi(\tau) = (\mu - 1)\frac{T^{\mu-1}}{(\tau + T)^{\mu}}, \tag{5.8}$$

. This is identical to realizing the time duration between crucial events given by Eq. (5.1). Numerically these statistics are generated [72] by drawing a random number y with a uniform

PDF on the interval $[0,1]$ $(0 < y < 1)$ and changing over it into the operational time using

$$\tau = T\left[\frac{1}{y^{\frac{1}{\mu-1}}} - 1\right]. \tag{5.9}$$

The outcome of this process yields a stochastic trajectory which for the simplicity of the discussion is illustrated in Fig. 5.1. Here we concentrate our attention on $\mu > 2$, a condition making the average value $\langle\tau\rangle$ finite, where the brackets denote an average taken using Eq.(5.8):

$$\langle\tau\rangle = \frac{T}{(\mu-2)}. \tag{5.10}$$

The quantity of crucial events generated moving from noon to the long-time limit t is equal to $t/ < \tau >$. Thus, the frequency of the subordinated signal is equal to that of the coherent oscillator.

It is vital to point out that the theoretical arguments using diffusion entropy analysis (DEA) [28, 65], in the long-time limit the crucial events yield a scaling index

$$\delta = \frac{1}{\mu-1}, \tag{5.11}$$

We need to average the solution of Eq.(5.7) over an ensemble of realizations to obtain the spectrum. Therefore, we define

$$Y(t) = Re\left[\langle\xi(t)\rangle\right], \tag{5.12}$$

where $\xi(t)$ is a single realization and the brackets denote an ensemble average.

Also, we adopt the prescription

$$\langle S(\omega)\rangle = \frac{1}{L}\left\langle |\int_0^L dt e^{i\omega t}\xi(t)|^2 \right\rangle, \tag{5.13}$$

to evaluate the spectrum $S(\omega)$ with a time series of length L, which is equivalent to

$$\langle S(\omega)\rangle = 2ReA, \tag{5.14}$$

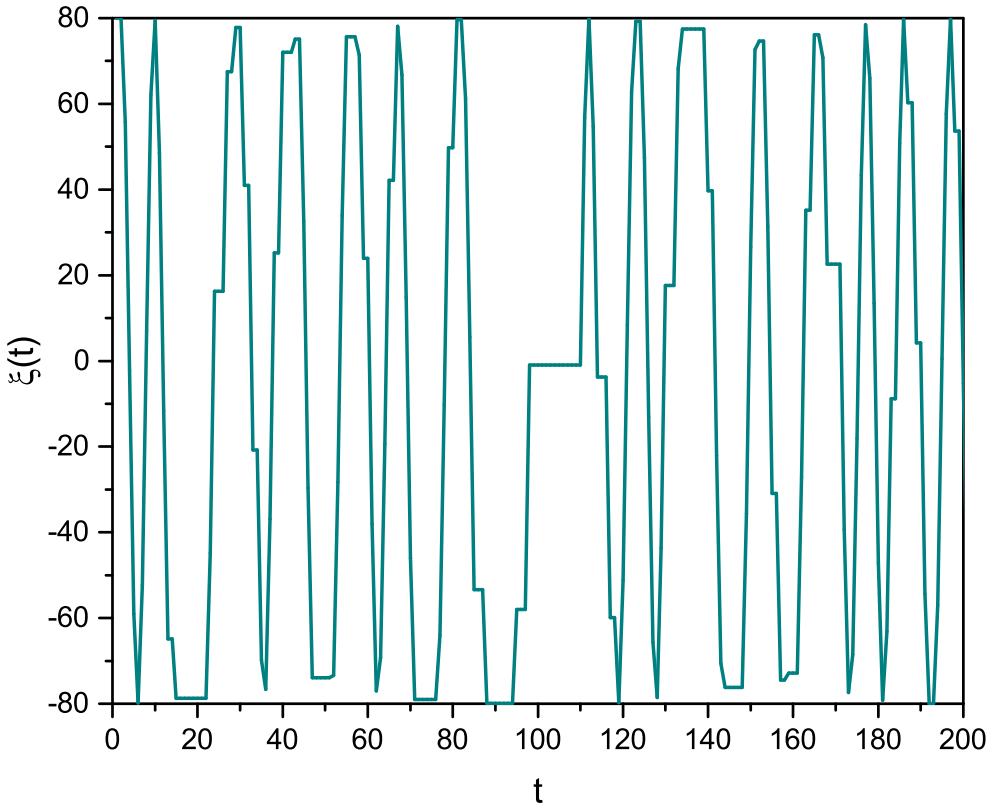

FIGURE 5.1. Subordinated cosine wave with $\Omega = 0.8$ and $\mu = 2.8$

where

$$A \equiv \frac{1}{L}\int_0^L dt_1 \int_0^{t_1} dt_2 e^{i\omega(t_1-t_2)} \langle \xi(t_1)\xi^*(t_2)\rangle \,. \tag{5.15}$$

It is helpful to notify that the correlation function, under the integral in Eq.(5.15), isn't stationary, yet it becomes stationary in the long-time limit. We expect that if the length L of the time series is adequately large, the spectrum characterized by Eq.(5.13) reduces to the ordinary Wiener-Khinchin prescription

$$S(\omega) = \frac{1}{2\pi}\int_{-\infty}^{+\infty} \Phi_\xi(t) exp(-i\omega t) dt, \tag{5.16}$$

where $\Phi_\xi(t)$ is the aged correlation function. The aged correlation function is a damped oscillatory function, with a tail portrayed by the aged survival probability, specifically an

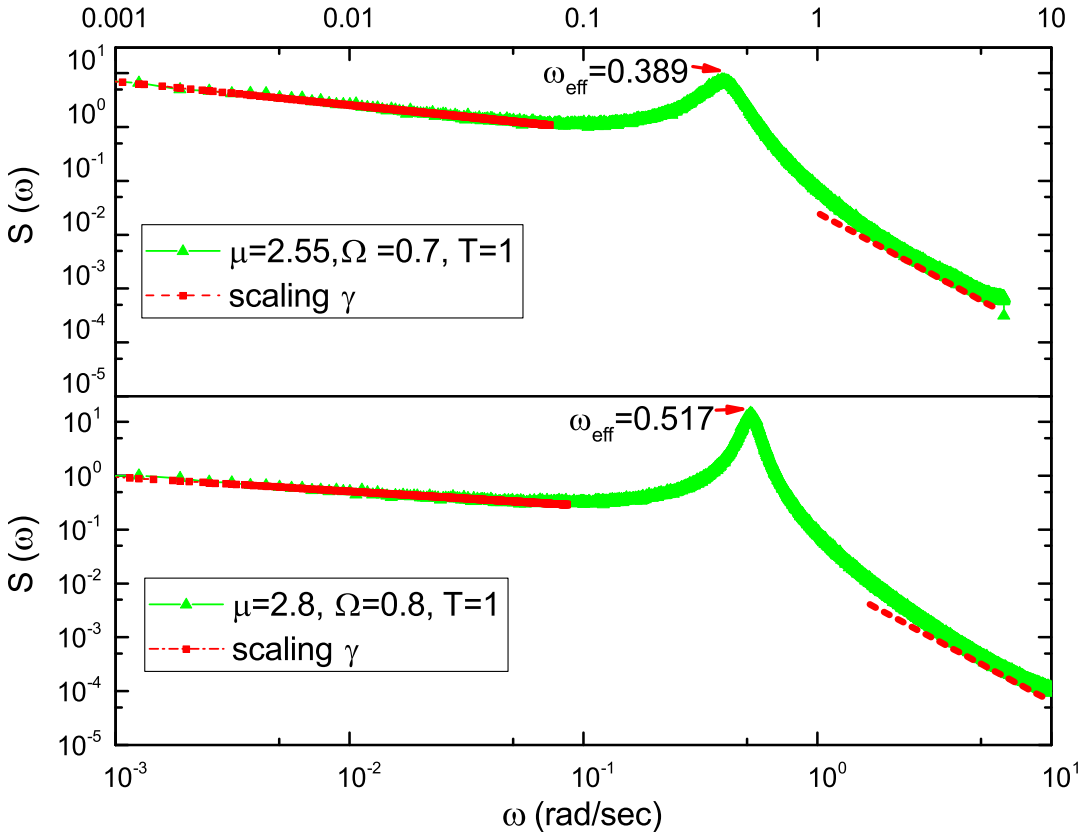

FIGURE 5.2. Spectra corresponding to $\mu = 2.55$ (top) and $\mu = 2.8$ (bottom).The red lines are the fitting to the numerical results. Top panel: The red lines at the left of periodicity bumps yield $\gamma = 0.43$ to be compared to the theoretical prediction $\gamma = 3 - \mu = 0.45$. The red lines at the right of the periodicity bump correspond to the prediction $\gamma = 2$. Bottom panel: The red lines at the left of periodicity bumps yield $\gamma = 0.26$ to be compared to the theoretical prediction $\gamma = 3 - \mu = 0.2$. The red lines at the right of the periodicity bump correspond to the prediction $\gamma = 2$.

IPL with index $\mu - 2$. We expect, in this manner that for $f \to 0$ the results of Eq. (5.2) and Eq. (5.3) are recovered.

The numerical outcomes of Fig. 5.2 satisfy our heuristic arguments. Indeed, we find that in the region of low frequency the theoretical prediction $\gamma = 3 - \mu$ is satisfactorily confirmed. In the less exact case portrayed on the bottom of the figure, we run $\mu = 2.8$ and

the numerical outcomes correspond to an effective $\mu = 2.74$. In the region of very high values of ω, the exponential decay of the damped oscillations produce $\gamma = 2$. Between the two IPL regions a bump shows up, this being a clear mark of the effective frequency that becomes lower by decreasing μ. Actually, decreasing μ diminishes the rate of event production, which corresponds to the effective frequency $\omega_{eff} = r\Omega$. Decreasing the rate of event production r decreases the effective frequency.

5.4. Power Spectra from Real Data

Here, we show the power spectrum of Eq. (5.13) of two individuals, C1 and C2, practicing Chi meditation and two individuals, Y1 and Y2 practicing Kundalini Yoga mediation. We present samples of the HRV time series in Fig. 5.3 referring to individuals Y1 and C2 to understand our procedure in a more clear way. The data is taken from Physionet, previously analyzed by Peng et al. [73] using completely different techniques than ours. Among the meditators, Chi meditators are novices and the Kundalini Yoga meditators are advanced practitioners. We observe that the main qualitative difference between Kundalini Yoga and Chi meditation is that the rate of heartbeats in the former case significantly increases, whereas in the latter it does not. However, coherent-like oscillations appear during both types of mediation.

The power spectrum $S(\omega)$ for the case of Chi mediation is shown in Fig. 5.4. We find that for both Chi meditators, C1 and C2, the transition from the pre-meditation to the meditation condition produces visible periodicity bumps. Comparing from right to the left panels, a bump appears at $\omega \approx 0.34$ radians per second for C1 and at $\omega \approx 0.38$ for C2, each induced by meditation.

With the technique of scaling analysis presented in Section 5.5 the IPL index μ of C1 is found to change from 2.4, before meditation, to 2.55, during meditation. Similarly, the IPL index μ of C2 is seen to change from 2.28, before meditation, to 2.54, during meditation. Similar properties can be seen in the case of Kundalini Yoga meditation, Fig. 5.5. In the latter case the periodicity bump during meditation for Y1 appears at $\omega \approx 0.4$ and for Y2

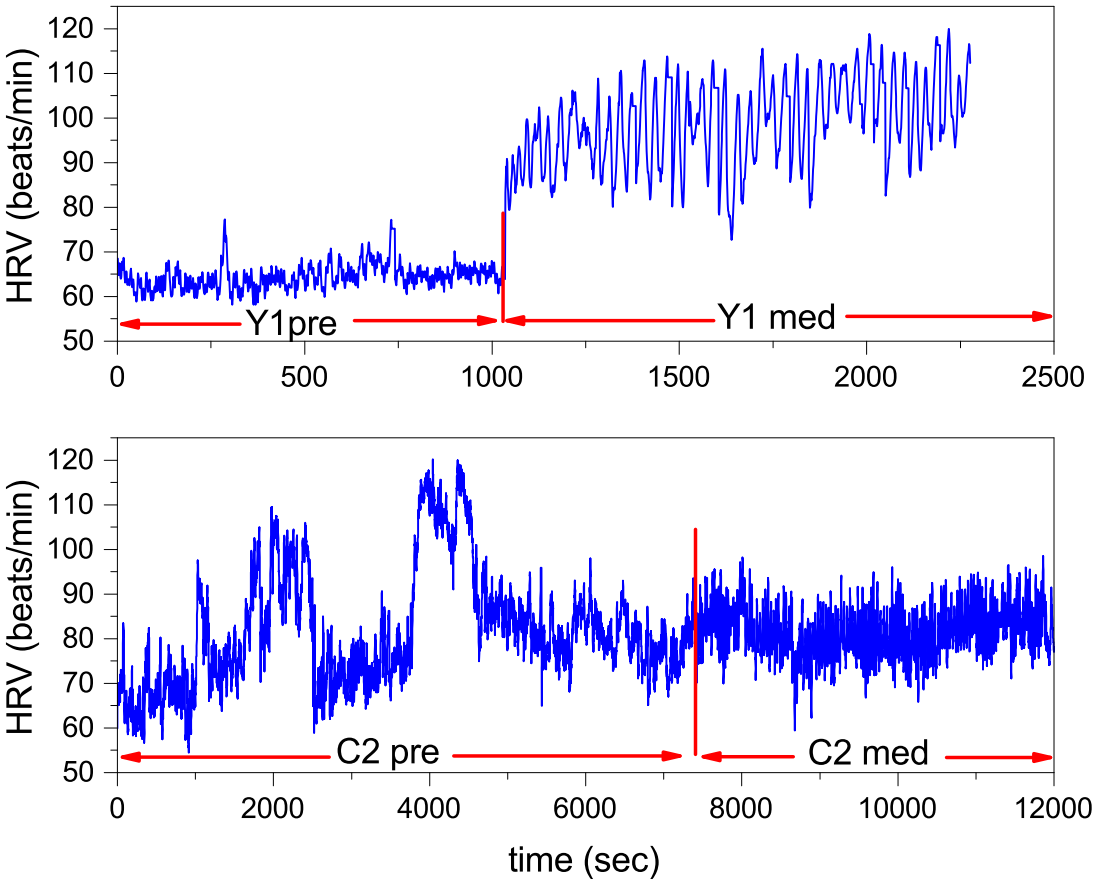

FIGURE 5.3. HRV time series of Yoga meditator (Y1), at the top, and the Chi meditator (C2), at the bottom. The vertical red lines denote the time at which the two meditations start.

at $\omega \approx 0.65$. Note that in the case of both Y1 and Y2 meditators there exists periodicity bumps before meditation. From the observation of these two experienced practitioners we find that periodicity bumps exist, even before meditation, this suggest that the long term practice of meditation yields permanent physiological effects. Regarding IPL index μ, the evaluation done in Section 5.5 depicts that the individual $Y1$, before meditation, has the IPL index $\mu = 2.64$, which moves to $\mu = 2.68$. The individual $Y2$ has the IPL index $\mu = 2.66$ before meditation and the IPL index $\mu = 2.72$, during meditation. We shall discuss this shift in more detail in Section 5.6.

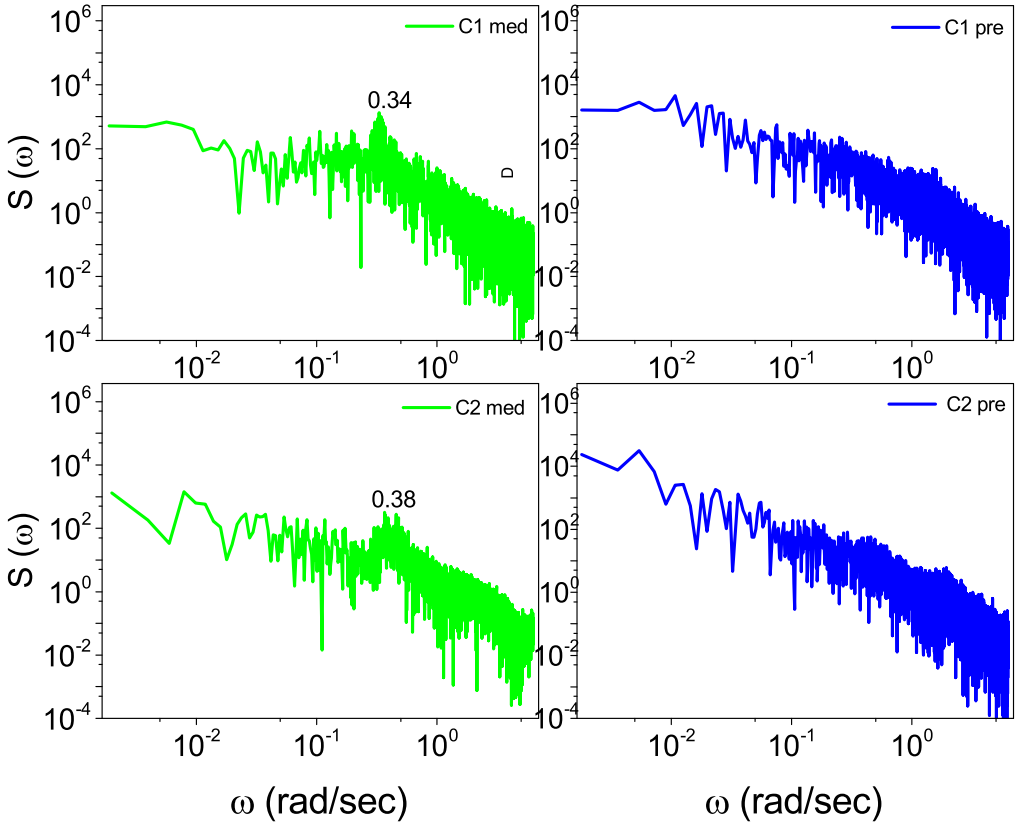

FIGURE 5.4. The Power spectra $S(\omega)$ of Chi meditators (C1,C2) before, on the right, and during meditation, on the left.

The spectrum of real data shown in Fig. 5.5 with the idealized surrogate spectrum of Fig. 5.2 has impressive similarity. The top panel of Fig. 5.2 has been obtained using subordination process with the IPL index $\mu = 2.55$, which is the mean value of the IPL index corresponds to Chi meditation and the bottom panel with the value $\mu = 2.8$, is the average value corresponds to the Kundalini Yoga meditation. More detail is presented in Section 5.5.

We again take note that the spectral analysis had been previously examined by Peng *et al* [73], and observed the meditation-induced bump first time. However, they didn't talk about the frequency region to the left of the bump, which from our analysis is theoretically

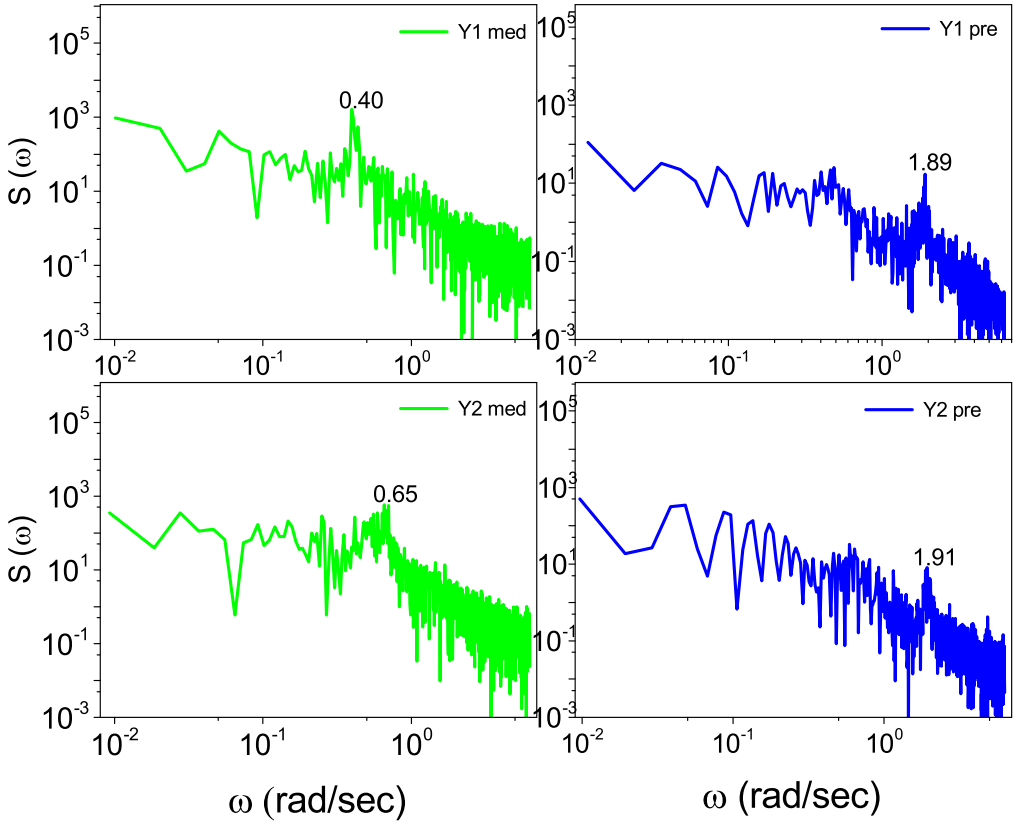

FIGURE 5.5. The power spectra $S(\omega)$ of Kundalini Yoga meditators (Y1,Y2) before, on the right, and during meditation, on the left.

obtained by crucial events. It is vital to say that Fig. 5.2 is produced by evaluating averages of many numerical realizations. IPL index μ corresponding to the spectrum to the left of the periodicity bump cannot be derived from the experimental spectrum because of single realization. This information can be obtained by adopting the technique [28, 65] used by us in Section 5.5.

5.5. Search of Crucial Events

As mentioned earlier, the search for crucial events is carried out using the method of stripes, developed earlier [28, 65].

Fig. 5.6 and Fig. 5.7 are obtained applying the analysis procedure of Refs. [28, 65] to the HRV meditation data of Ref. [73]. We see the different effects with different forms of meditation. Let us compare the Chi meditation Fig. 5.6, to the Kundulini Yoga meditation Fig. 5.7. In both meditations we see the IPL index μ increases significantly. Among Chi meditators only subject not changing μ is C7. For the rest, δ moves from above the dashed line to below it. The change in μ is little low, for C1 and C5, moving from $\mu = 2.47$ to $\mu = 2.54$ where as the higher change, for C2, moving from $\mu = 2.28$ to $\mu = 2.54$. In case of Kundalini Yoga meditators the minimal change is for Y1, from $\mu = 2.64$ to $\mu = 2.68$ where as the maximal change is for Y4, moving from $\mu = 2.66$ to $\mu = 2.85$.

Yoga meditators surprisingly have an effect of noticable increasing of $\in$ in addition to changing μ. Allegrini et al. [28] conjectured that $1- \in$ is an indicator of stress level that will eventually lead to heart failure. According to this interpretation, we can say that yoga is an efficient technique to reduce stress. It seems that Chi meditation is not as efficient as Kundulini Yoga, since for some meditators, $C3$, $C4$ and $C8$, $\in^2$ is decreasing rather than increasing.

5.6. Concluding Remarks

Here we oberved that meditation does not suppress the occurrence of crucial events alongwith the well known fact that it creates "exaggerated heart rate oscillations" [73]. We already figured out in an earlier publication [65] that these crucial events are often embedded in a billow of uncorrelated and irrelevant events. This leads us to introduce the notion of dressing. Meaning of dressed crucial event is that the time interval between the crucial events are filled with poisson events. The exaggerated heart rate oscillations are the type of dressing induced by meditation. The selection of the strip method [65] facilitated the evaluation of the level of dressing by means of the measure $\in^2$. This allowed to illustrate $1- \in$ is the percent of Poisson events which affect the HRV time series. Allegrini et al. [28] conjectured that the Poisson events are the source of stress and the large quantity of such events as quantified by $\in^2$, i.e., stress, might be the reason for heart failure. According to this interpretation,

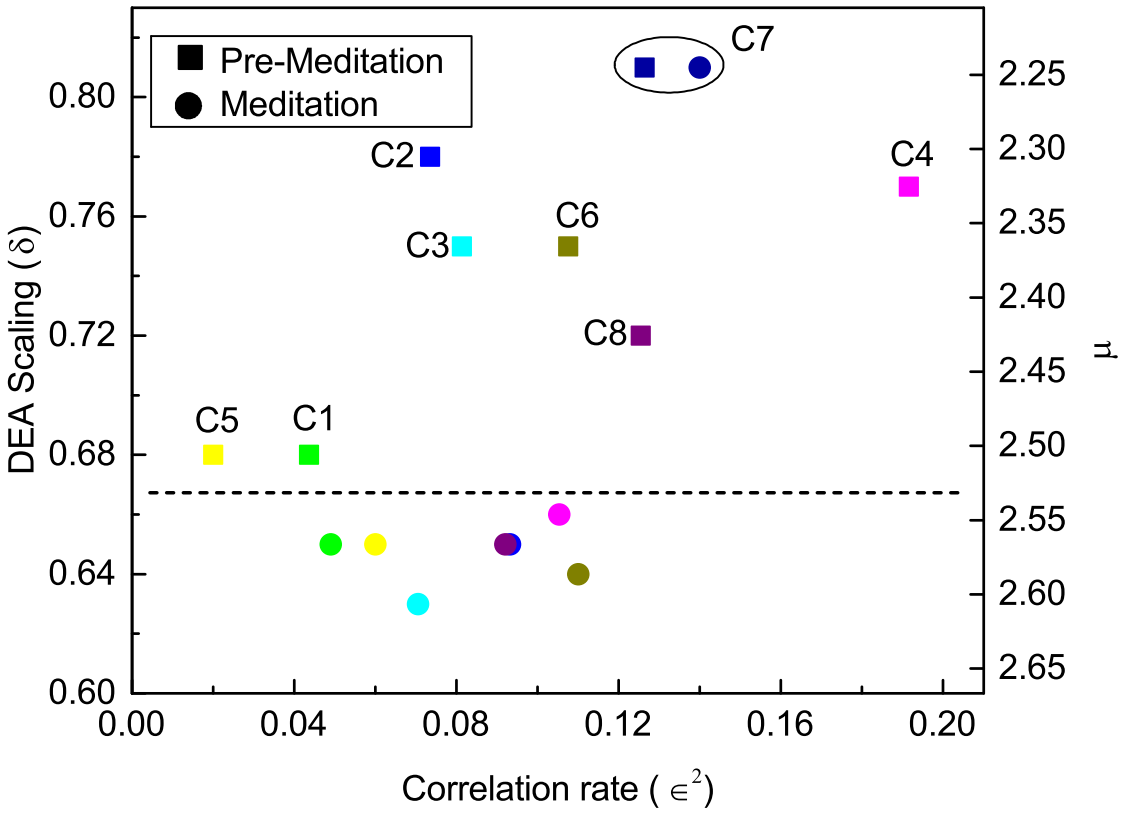

FIGURE 5.6. DEA scaling δ, IPL index μ and $\in^2$ of the HRV time series of eight different participants before and during Chi meditation

one can conclude that the results of Fig. 5.7 demonstrate that Kundalini Yoga meditation significantly diminish the level of stress. Therefore, this study provides a method of analysis of HRV that might be utilized directly to evaluate the advantage of meditation, which are currently examined indirectly, through the observation of psychological health [74].

Gard et al. [74] portrayed a fascinating remarks on the bottom-up and top-down processes induced by yoga. We discover that the meditation-enhanced cognition mentioned by them has the vital impact of changing the IPL index μ from a region near to the border $\mu = 2$, which is the ideal $1/f$-noise, see Eq. (5.2), to a region nearer to the Gaussian basin of attraction, $\mu = 3$ [75].

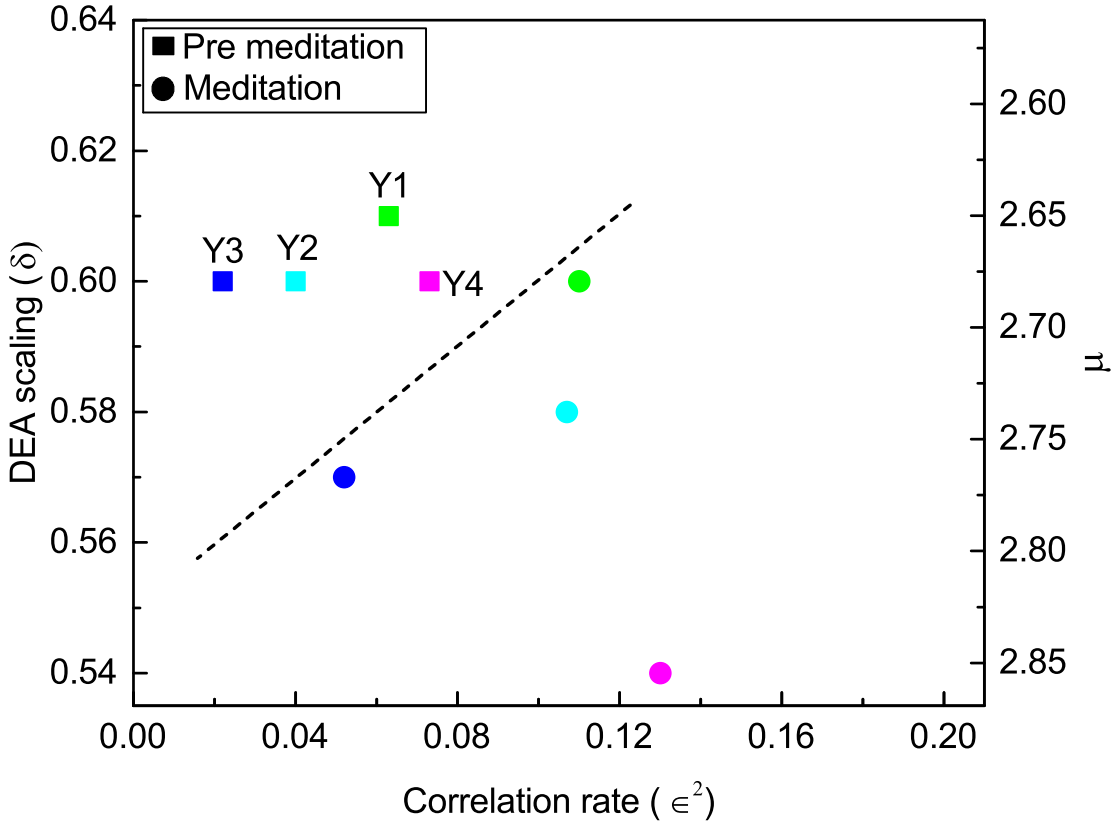

FIGURE 5.7. DEA scaling δ, IPL index μ and $\in^2$ of the HRV time series of four different participants before and during Kundalini Yoga meditation

Does meditation make physiological processes more complex, or less complex? We posit the plausible conjecture that meditation makes physiology more complex [51] through the observation made in this study where we found the value of IPL index μ increasing signifying a tendency towards the Gaussian basin of attraction. The increase of $\in^2$, with significantly lessening the amount of Poisson events, facilitates the generation of regular oscillations.

The shift taking place from a region near to $\mu = 2$ to nearer to $\mu = 3$ is a signature of departure from the ideal $1/f$-noise condition which fits the examination done by psychologists [76] in line with the phenomenological philosopher Heidegger [77], according to which

cognition is activated by performing a difficult task. This fits with the examination done by Correll [78] that the fast reaction to a difficult social identification task often results unconscious bias; one measure of the task's difficulty being the profound cognitive transition from $1/f$ - noise to white noise, corresponding to $\mu \gg 1$. Meditation, generating a shift from the ideal $1/f$-noise to the Gaussian basin of attraction, which in the Poisson limit $\mu \to \infty$ results white noise, is a form of a difficult task that yields relaxation and stress reduction, where as the difficult task of bypassing the unconscious bias might be a source of stress.

According to [79] and [80] phenomena such as dreamless deep sleep and brain dynamics under anesthesia respectively result a shift from the criticality condition, and this is considered as favoring a lack of sensitivity to perturbation [81] in line with other recent results [82]. There is another important literature written by Varela and his co-workers according to which Buddhist philosophy, a source of meditation techniques is of fundamental importance in dealing with the ambitious field of cognition [83], which is similar to those examined in this study. Therefore we believe that this research approach plays an important role to the advancement of cognition science.

CHAPTER 6

DYNAMICS OF THE BRAIN

In this chapter we discuss how to combine the wave-like nature of the dynamics of the brain with the existence of crucial events that are responsible for the $1/f$ noise. Crucial events correspond to abrupt transitions in the wave-like structure of EEG's, requiring a complex procedure for their detection. We show that the anomalous scaling generated by the crucial events can be established by means of a direct analysis of raw data. The efficiency of the direct analysis procedure is made possible by the fact that periodicity and crucial events are the product of a spontaneous process of self-organization. We argue that the results of this study can be used to shed light on the nature of this process of self-organization.

6.1. Introduction

The dynamics of the brain are a challenging issue that is forcing researchers to go beyond the conventional forms of non-equilibrium statistical physics [85] and is expected to contribute to reshaping the emerging field of complex networks [86]. The dynamics of the brain, as those of biological processes more in general, are characterized by homeodynamics [87], thereby implying the analysis of the dynamics of the brain to be done taking into account that they are driven by rhythms and waves.

A parallel line of inquiry has been developing in the past years focusing on the connection between the dynamics of the brain and criticality [88, 89, 90]. Allegrini et al. [91] using a technique proposed by Kaplan and co-workers [92] proved that the Rapid Transition Processes (RTP) host crucial events.

Crucial events are defined in terms of their statistical properties as follows. The time intervals between consecutive crucial events are described by a waiting time probility density function (PDF) $\psi(\tau)$ with the inverse power law (IPL) structure

$$\psi(\tau) \propto \frac{1}{\tau^{\mu}}, \tag{6.1}$$

with an IPL index in the interval

$$1 < \mu < 3. \tag{6.2}$$

The crucial events are renewal and consequently the times τ_i should not be correlated. If a sequence of crucial events are defined by the time intervals τ_1,τ_2,τ_3,..... then the time-average correlation function is a Kronecker delta function where the time average is indicated by an overbar

$$C(t) = \frac{\sum\limits_{|i-j|=t} \overline{(\tau_i - \overline{\tau})(\tau_j - \overline{\tau})}}{\sum\limits_i \overline{(\tau_i - \overline{\tau})^2}}. \tag{6.3}$$

This correlation function is properly normalized, thereby yielding $C(0) = 1$, and in the case of genuine renewal events should satisfy the condition $C(t) = 0$ for $t > 0$. This renewal property can also be expressed by the assumption that the probability of occurrence of both τ_i and τ_j, $\Pi(\tau_i, \tau_j)$, when $i \neq j$ is given by,

$$\Pi(\tau_i, \tau_j) = P(\tau_i) * P(\tau_j), \tag{6.4}$$

where $P(\tau_i)$ and $P(\tau_j)$ are the probability of occurrence of τ_i and τ_j, respectively. Allegrini et al. [91] conjectured that these crucial events are a signature of criticality and addressed the important tasks of detecting them from the observation of EEG [93]. The criticality hypothesis is in line with the views of many other researchers [94, 95, 96, 97]. However, it is not yet clear what kind of criticality, either that determined by externally tunning a control parameter (Ising-like) or that achieved spontnneously through the internal system dynamics i.e., Self-Organized Criticality (SOC), is expected to afford sufficient theoretical picture. We discuss the open issue of the proper form of criticality to use to increase our understanding of the brain dynamics in Section 6.5 and Section 6.6 .

The adoption of the RTP method is very attractive but, as shown in Section 6.2 its adoption does not make it possible for us to measure the complexity of brain dynamics directly and in addition requires a filtering process. Herein we propose a technique of analysis of EEG data not require the detection of RTPs, and leads to the detection of scaling directly

from raw data. We show that the resulting scaling is identical to that obtained in earlier work using RTP's. More importantly , we argue that the present technique may help to establish a bridge between EEG waves [98] and crucial events. In fact, as shown in Section 6.3, this result may lead us to understand more about what form of criticality to apply to study the dynamics of the brain.

In section 6.2 we review the procedure adopted to detect RTP events. We devote Section 6.3 to an intuitive introduction to the process of self-organization combining periodicity and crucial events and in Section 6.4 we analyze the spectrum of one EEG to point out the interesting qualitative agreement with the predictions of Section 6.3. In Section 6.5 we illustrate a technique of detection of crucial events that will facilitate the analysis of EEG's. Finally, in Section 6.6 we make concluding remarks and plans for future work.

6.2. Detection of Rapid Transition Events

The efficacy of the RTP method in the study of brain dynamics has previously been demonstrated by Allegrini and co-workers [91]. However, for the sake of clarity we sketch the method here to emphasize the importance of recovering the same results for detecting the same scaling, using a very different technique. We base our analysis on data derived from Ref. [99], which are available in Ref. [27]. These EEG data have been filtered between 0.15-28 Hz and the sampling rate (F_s) is 2048 Hz. We select one healthy subject, from the dataset, and the top panel of Fig. 6.1 shows the raw data of this subject. The second panel displays one intrinsic mode function, obtained adopting the method of Hilbert-Huang Transformation (HHT) illustrated in [100]. The HHT method decomposes the original EEG signal into many intrinsic mode functions, with different structures. We select a structure with a kind of sausage-like pattern suggested by the theoretical results of Bologna et al. [101]. They proved that a set of infinitely many three-state oscillators, cooperatively interacting with an interaction parameter K, at criticality generate a coherent non-harmonic oscillation. When the number of oscillators is finite the regular non-harmonic oscillations generate a sausage-like structure similar to the second panel of Fig. 6.1. In Section 6.6.1 we shall make

additional remarks on the criticality-induced sausage-like structure.

The third panel of Fig. 6.1 from the top is the module of the second panel. The green curve in the fourth panel is the envelope of the curve of the third panel, called Testing Sequence (TS). The blue curve in the fourth pannel of Fig. 6.1 is the Level Sequence (LS) obtained from the TS via a running-average smoothing. Finally, the red crosses denote the crucial events.

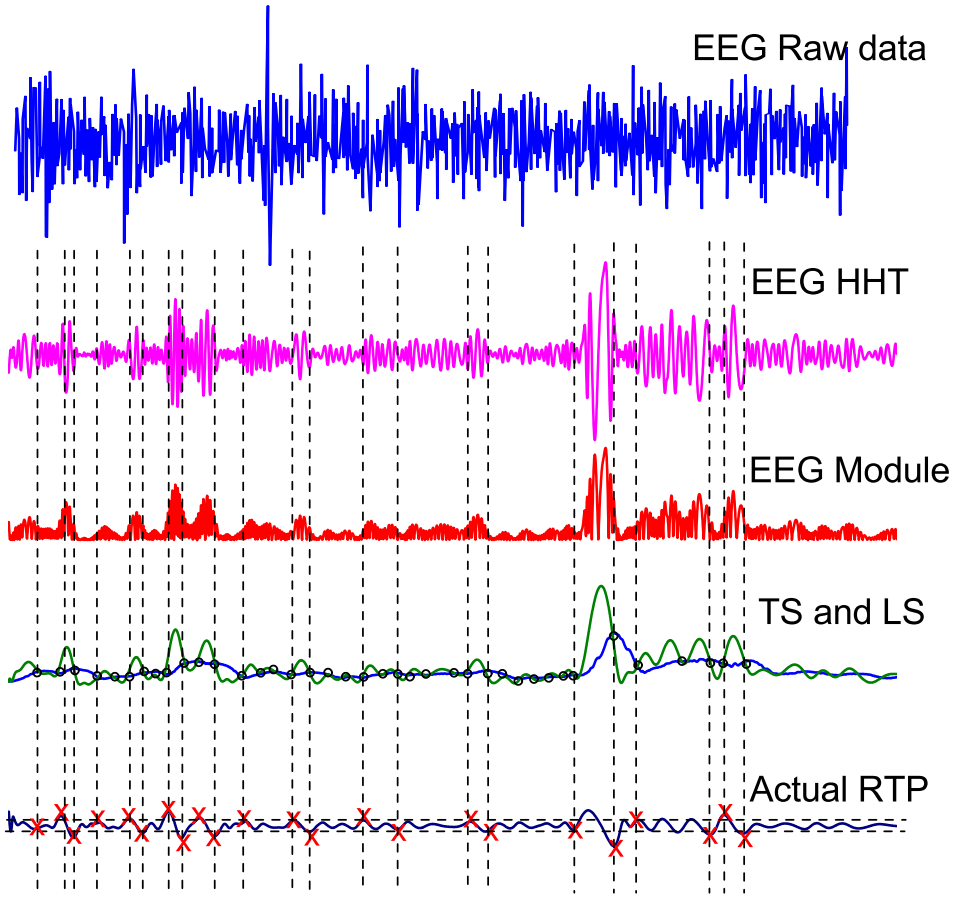

FIGURE 6.1. Illustration of the RTP procedure

Note that this procedure to find the crucial events is not sufficiently accurate to be restricted to detecting only renewal events. It is known that the events revealed by this analysis are a mixture of crucial events and ordinary Poisson events [102]. However, the presence of Poisson events does not prevent us from detecting the anomalous scaling generated by the crucial events. The desired scaling is detected in the following way. The

authors of [103] make the detected events generate a diffusion process $x(t)$ using the rule that the random walker makes a jump ahead when event, either crucial or Poisson, occurs. The scaling generated by the Poisson events has a power-law index $\delta = 0.5$, whereas the scaling power-law index δ of the crucial events is given by the important relation

$$\delta = \frac{1}{\mu - 1}, \tag{6.5}$$

Note that the latter scaling dominates asymptotically in the time due to Eq. (6.5) resulting in $\delta > 0.5$ when the condition $2 < \mu < 3$ applies [103]. When $1 < \mu < 2$ crucial events yield the scaling $\delta = (\mu - 1)$, but the EEG's studied in this paper and the subordination theory of Section 6.3 adopted to explain their complexity show that we have to focus on $\mu > 2$.

To be explicit, since in this paper as far as the scaling detection is concerned, we adopt the same procedure as that proposed by Grigolini *et al* [103], we generate a fluctuation $\xi(t)$ holding the value 1 when an event, either crucial or Poisson, occurs, and the vanishing value when no event occurs. The diffusion variable $x(t)$ is obtained from the following equation of motion

$$\frac{d}{dt}x = \xi(t). \tag{6.6}$$

Using a moving window of size t, we generate a PDF $p(x,t)$ and the Shannon information entropy

$$S(t) = -\int_{-\infty}^{+\infty} dx p(x,t) ln[p(x,t)]. \tag{6.7}$$

The PDF constructed from the diffusion process has the scaling form

$$p(x,t) = \frac{1}{t^{\delta}} F\left(\frac{x}{t^{\delta}}\right). \tag{6.8}$$

Then inserting Eq. (6.8) into Eq. (6.7), after a simple algebra yields

$$S(t) = A + \delta ln(t), \tag{6.9}$$

where A is the entropy constant

$$A \equiv -\int_{-\infty}^{+\infty} dy F(y) ln[F(y)]. \tag{6.10}$$

To make this treatment compatible with the hereby discussed arguments about intermediate asymptotics, we rewrite Eq. (6.7) in the following way

$$S(t) = C + \delta(t) ln(t), \tag{6.11}$$

where C denotes a constant that may different from A, when, as in the case of this paper, the proper complexity scaling emerges only in the intermediate asymptotics.

It is important to stress that a significant advance on regarding the theoretical justification of Eq. (6.11) based on an extension of the theory of SOC, incorporating complexity in the time domain, is called Self-Organized Temporal Criticality (SOTC) [38, 104, 105]. This new theory leads us to strongly support the adoption of this method to define the crucial IPL index μ. In fact, according to SOTC the processes of spontaneous self-organization, in general, and especially those behind the statistical analysis used herein, namely physiological processes, naturally evolves to a state generating the crucial events defined in Section 6.1. These events emerge in the intermediate time scale, called intermediate asymptotics [106, 53]. As a consequence of temporal complexity emerging in the intermediate time scale, $S(t)$ is not a straight line when expressed as a function of $ln(t)$. As shown in Fig. 6.2, it is a straight line in the intermediate time scale and its slope is used to define the statistics of crucial events occurring in that intermediate time scale through the power law index μ established by Eq. (6.5).

To explain using an intuitive interpretation the intermediate asymptotics, we notice that the short-time region corresponds to the time scale where the self-organization is not yet perceived by the interacting units. According to SOTC [38], the intermediate time scale with temporal complexity becomes more and more extended with an increasing number of units cooperatively interacting. However, the fluctuation intensity becomes smaller and the long-time scale is a sort of Poisson shoulder that, however, does not affect the communication efficiency of the complex system that is determined by the intermediate time region. The exponential truncation favors the transmission of information because the flexibility of the complex system to the environmental influence requires that the system explores a sufficiently

high number of crucial events (*free-will states*) to adapt itself to the external influence and the exponential truncation has the effect of making the mean value of the mean time interval between consecutive crucial events finite, even in the case $\mu < 2$. We remind the reader that the theoretical mean time between crucial events is $< \tau > \propto 1/(\mu - 2)$, if $\mu > 2$ and it is divergent if $\mu < 2$ and the inverse power law distribution density is not truncated.

The events generated by SOTC are renewal thereby explaining the adoption of Eq. (6.5) for the connection between δ and μ, which is based in fact on the renewal assumption [103].

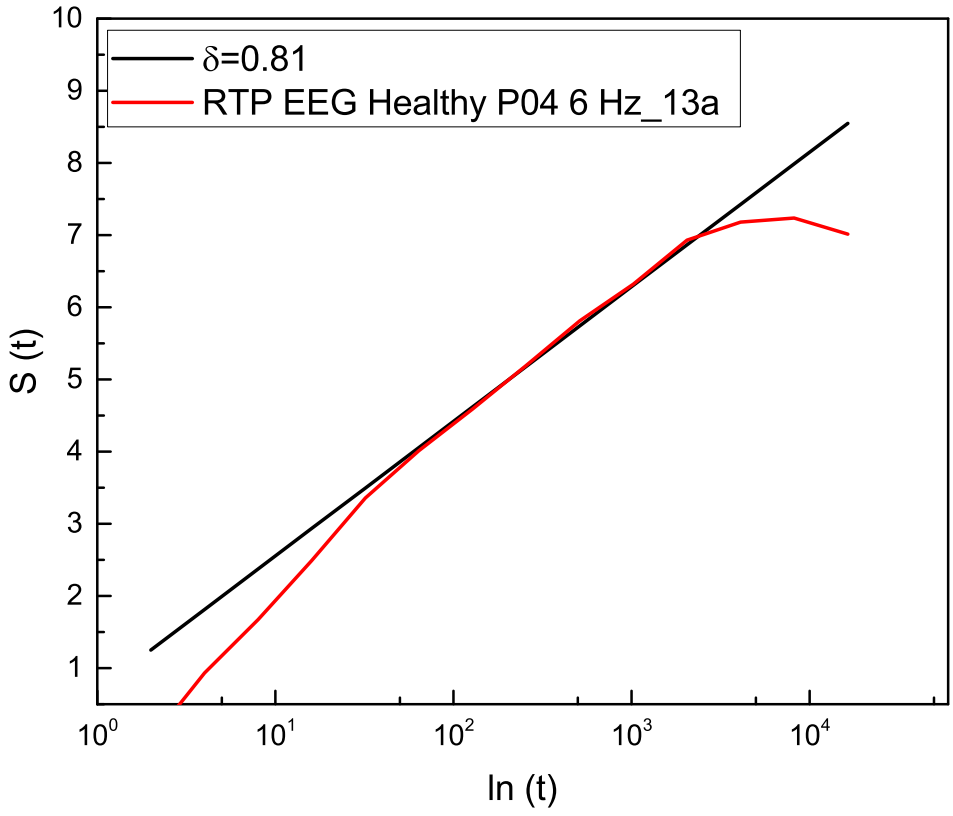

FIGURE 6.2. Detection of the scaling δ applying DEA to the diffusion process generated by a random walker making a jump ahead when a crucial event occurs.

We see from Fig. 6.2 that the subject examined with DEA procedure yields $\mu = 2.2$.

It is convenient to stress the fact that the choice of the RTP method, illustrated in Fig. 6.1, has been motivated by the intuitive assumption that crucial events have physical effects. With reference to the second panel from the top of Fig. 6.1, an event may be located in the short time region of weak fluctuations separating an ending sausage from the beginning of a new one. Actually, the theoretical approach outlined in Section 6.3 suggests that many more crucial events exist, thereby leading to a scaling method evaluation resting on a much larger number of crucial events, even if, as in the case of the method of Kaplan *et al* [92], not all the events adopted to generate the diffusion process analyzed with DEA, are crucial.

6.3. Subordination

Establishing the statistics of the crucial events hosted by EEG's by means of the detection of RTP, unfortunately, does not help us to build a bridge between the wavelike nature of EEG's and crucial events. To establish the theoretical connection between the periodicity of EEG's and crucial events, we adopt the SOTC of units with an individual periodicity, for instance the SOTC [38] as applied to the Kuramoto model [107]. This computationally demanding approach has not yet been converted into an analytical approach to bridging waves and crucial events. We believe that the theoretical remarks of this Section are a fair account of this form of SOTC.

The research work done in the recent past on the brain with the help of the RTP method led the authors of Ref. [108] to conclude that the crucial events are characterized by values of μ very close to $\mu = 2$, according to the prescription

$$S(\omega) \propto \frac{1}{\omega^{3-\mu}}. \tag{6.12}$$

The derivation of this spectrum was done by the authors of Refs. [109, 72] assuming that the time regions between consecutive crucial events are filled with either $+1's$ or $-1's$, values

generated by a coin tossing algorithm. No direct evaluation of the EEG spectrum was done. Herein we see that if the EEG spectrum is evaluated, the frequency region for $\omega \to 0$ is affected by strong fluctuations making it difficult to assess the IPL property of Eq. (6.12). However, we are able to shed light into the overall structure of the spectrum and we argue that this is compatible with Eq. (6.12).

To establish a bridge between crucial events and periodicity, as done by Ascolani *et al.* [71], we make an extension of the well known Continuous Time Random Walk (CTRW) [110, 111, 112]. The subordination to a coherent process with frequency Ω is a mathematical simple way of simulating a genuine process of self-organization. We have a clock with frequency Ω the hands of which move clockwise from noon to noon making T_{RR} clicks with an interval of Δt. Thus,

$$\Omega = \frac{2\pi}{T_{RR*\Delta t}}. \tag{6.13}$$

The crucial events, some of which have been detected by Allegrini et al. [91] through the search of RTP, are imbedded into this regular motion, by assuming that the time interval between consecutive clicks is derived from a waiting-time PDF $\psi(\tau)$ with the temporal complexity of Eq. (6.1). The explicit analytical form of $\psi(\tau)$ is

$$\psi(\tau) = (\mu - 1)\frac{T^{\mu-1}}{(\tau + T)^{\mu}}, \tag{6.14}$$

corresponding to the survival probability

$$\Psi(\tau) = \left(\frac{T}{\tau + T}\right)^{\mu-1}. \tag{6.15}$$

The parameter T serves the purpose of properly defining the short-time scale and setting the normalization condition $\Psi(0) = 1$. The temporal complexity becomes important at times $\tau \gg T$.

This procedure of infusing the original perfect coherence of the clock with complex randomness establishes a bridge between waves and crucial events. This has the effect of

turning the frequency Ω into an effective frequency Ω_{eff}, thereby modeling a process of self-organization of interacting oscillators, each of which is characterized by its own frequency, into a collective homeodynamic process.

According to the theoretical treatment of Ref. [113], valid for $\mu > 2$,

$$\Omega_{eff} = \frac{\Omega(\mu - 2)}{T}. \tag{6.16}$$

This theoretical prediction suggests, in agreement with Fig. 6.3, that the frequency peak is evident for $\mu > 2$ and that, in addition to that, it also depends on the parameter T of the waiting time distribution density $\psi(\tau)$ of Eq. (6.14). This property is used in Section 6.4 to shed light into the meaning of the HHT components of the method adopted to detect RTP events [100]. In the range $\mu > 2$, when both the first and second moment of τ are finite, $\Omega_{eff} = \Omega$ [113].

This illustration of subordination makes it evident that crucial events are not only at the border between consecutive pieces of the sausage but the oscillatory-like behavior within a sausage hosts crucial events. This observation suggests that it should be possible to design a method of statistical analysis for extracting information from a larger set of crucial events even if they remain invisible.

Fig. 6.3 illustrates spectra generated by surrogate sequences obtained using the subordination method with $\Delta t = 1$ unit. We keep the frequency Ω fixed and change the power law index μ. We note that a spectrum consists of three parts. There exists a peak corresponding to the effective frequency Ω_{eff} that shifts to the right upon decreasing μ and disappears for $\mu < 2$. At the left of the Ω_{eff} the slope of the spectrum β obeys the prescription

$$\beta = 3 - \mu. \tag{6.17}$$

We see that the spectrum becomes flat at $\mu = 3$ and remains flat for higher values of μ, as clearly shown in Fig. 6.3.

Note that due to the average of many realizations, which is not possible with a real EEG, the region of small frequencies is regular and is not affected by the fluctuations that would appear when evaluating the spectrum with only one time series. For this reason,

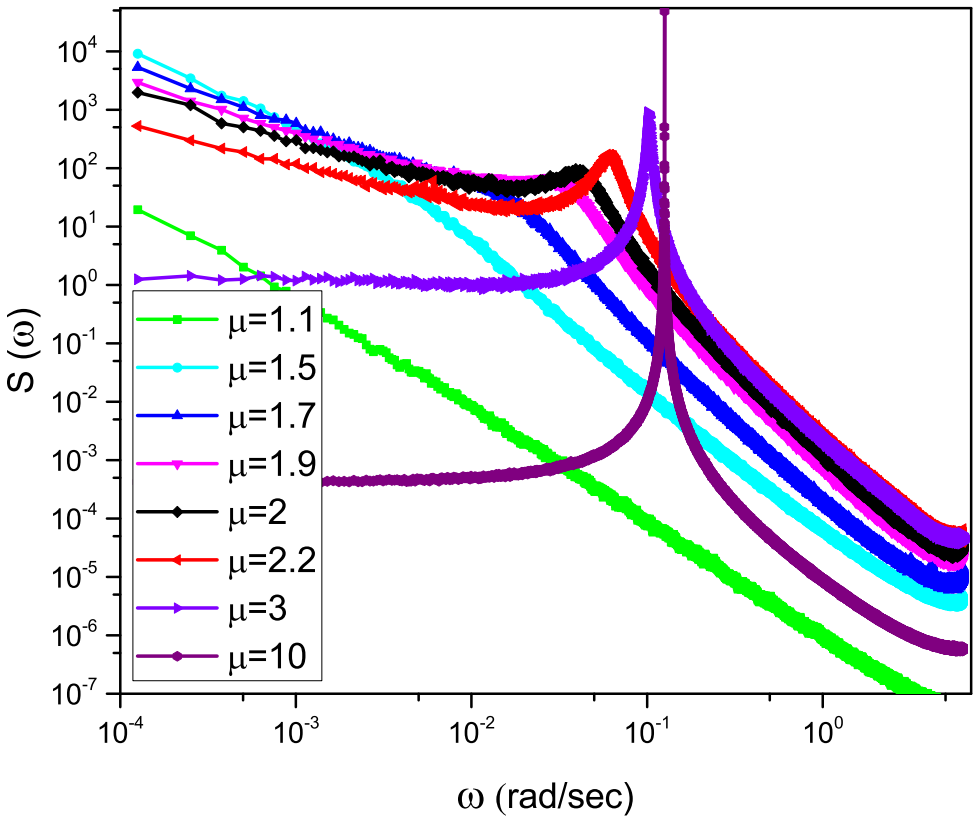

FIGURE 6.3. Spectra obtained averaging over 300 trajectores with numerical parameters $T = 0.5$ and the regular oscillation before subordination has the frequency $\Omega = 0.77$.

the adoption of surrogate time series makes it possible for us to prove that, as expected, subordination is compatible with the emergence of $1/f$ noise in the ideal case $\mu = 2$.

6.4. Spectra from Raw Data

In this section we discuss the spectrum generated by real EEG fluctuations as shown in Fig. 6.4. We see that the region of low frequencies is very erratic, due to the fact that, as mentioned earlier, the use of only one time series makes it impossible to generate a smooth curve. There exists a sign of a frequency bump, generated by periodicity, and for frequencies

larger than this bump the slope $\beta = 2$ is recovered. This real spectrum depends on a wide set of frequencies.

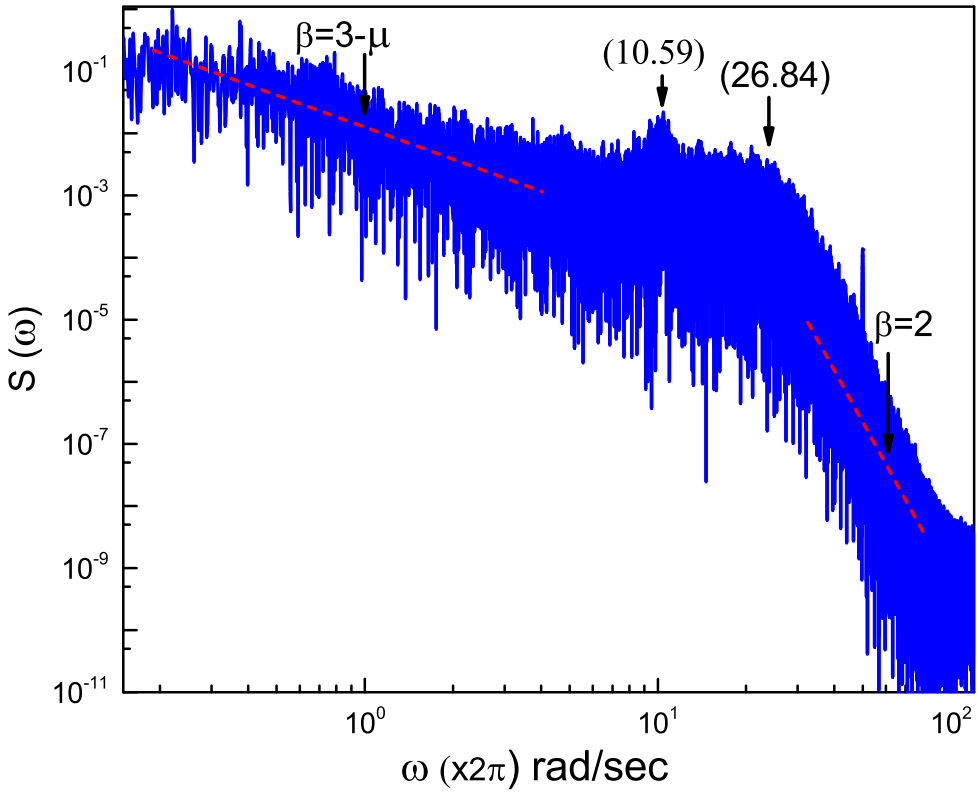

FIGURE 6.4. Spectrum obtained from raw data

To stress the multi-frequency nature of the real spectrum, using again the HHT method [100] we evaluate six intrinsic mode functions of the EEG raw data corresponding to the spectrum of Fig. 6.4. These different components of the whole signal correspond to six different frequencies of decreasing value. They are the frequencies: 26.84 Hz; 18.97 Hz, 10.59 Hz; 5.406 Hz and 2.438 Hz and 1.031 Hz, which are shown in Fig. 6.5.

In Fig. 6.6 we use the subordination prescription described in Section 6.3 with Δt as a inverse of sampling frequency of real data ($\Delta t = \frac{1}{2048} sec$) to generate surrogate spectra that should help clarify the meaning of the different spectra in Fig. 6.5. We assign to the

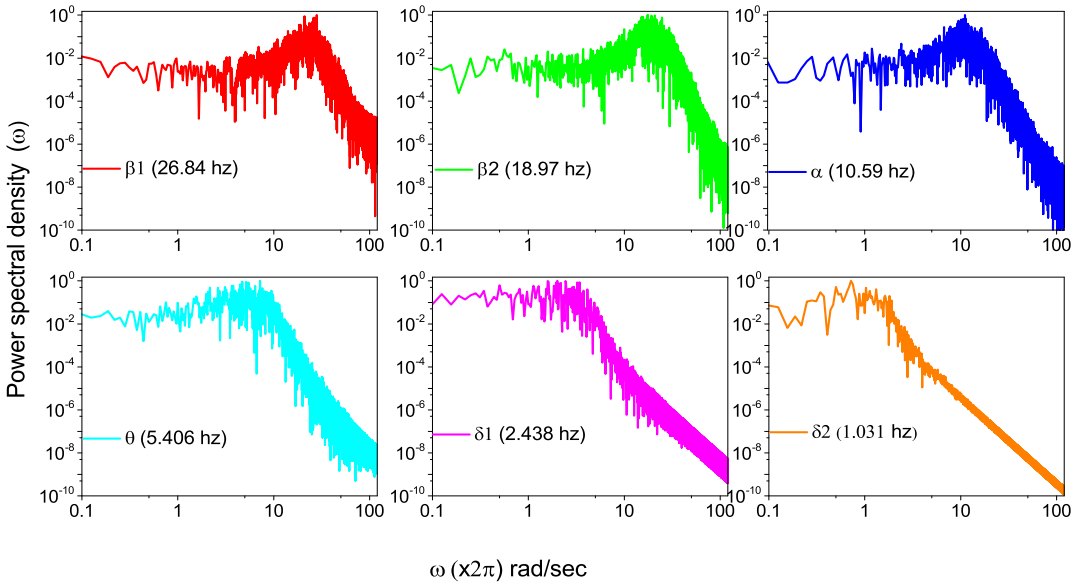

FIGURE 6.5. Power Spectra of the same subject with different frequency components.

monochromatic frequency 62 Hz with six different values of the parameters T, mimicking the dominant frequencies of the six HHT components illustrated in Fig. 6.5. The real spectrum of Figure 6.4 is interpreted as a superposition of the spectra illustrated in Fig. 6.6. In fact all these spectra share the property $\beta = 3-\mu$ in the small frequency region and the property $\beta = 2$ in the large frequency regions and intermediate region where the change of slope occurs is significantly more extended than in the monochromatic case.

6.5. Method of Stripes

The stripe method was originally adopted to detect the scaling of crucial events hosted by heartbeats [28] and was not used in the case of EEG's probably because of a lack of a proper theoretical understanding of the connection between crucial events and periodicity. The same method was more recently applied by Bohara et al. [65] to establish a connection between the occurrence of crucial events and multifractality.

In Section 6.3 we used an intuitive illustration of the process of self-organization,

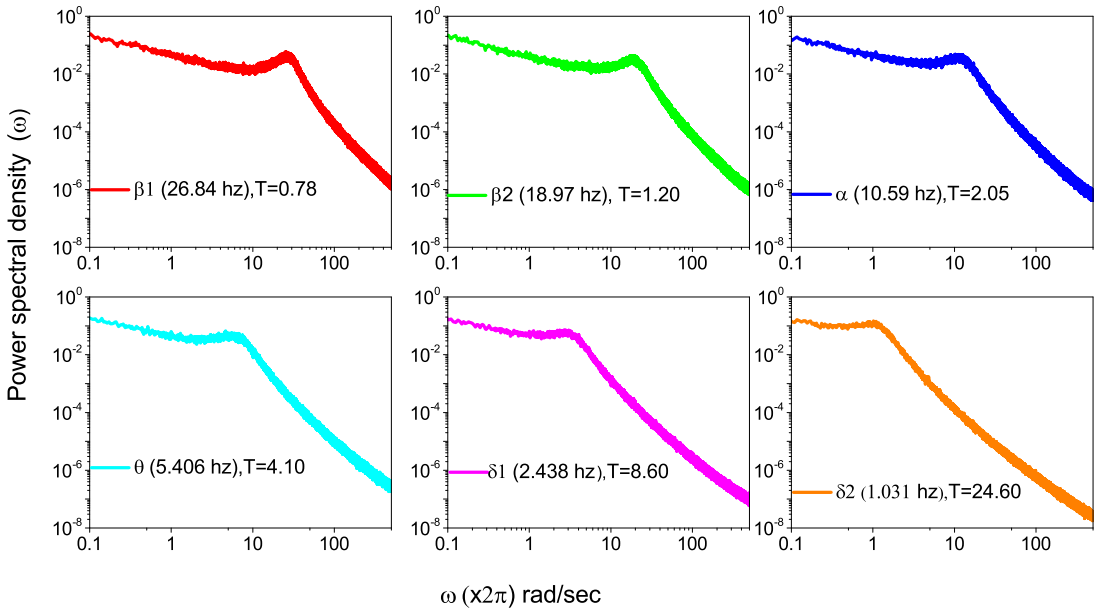

FIGURE 6.6. Power Spectra generated according to subordination of Section 6.3 .

based on subordination that affords theoretical support for the adoption of the method of the stripes. The central idea is that the RTP method detects only a small fraction of crucial events, whereas real EEG's, and subordination theory with them, host a much larger number of crucial events, even if they remain invisible.

Fig. 6.7 shows how the method of stripes works. As is well known [93], an EEG measures Event Related Potentials (ERPs) which, in turn, measures the rate of firing neurons. The method divides the vertical axis into many stripes of size ΔE, here assumed to have the value $\Delta E = 1/30$ μv, and we record the times at which the raw signal crosses the line separating two adjacent stripes. The level of the stripe is determined by the number of neuron firings at a given time, and we record for how long that firing rate remains constant.

The change from one firing rate to another is an event. Of course this event is not necessarily a crucial event. As a consequence, the time distance between consecutive events cannot be used to define the important parameter μ. This lack of precision in determining the occurrence of crucial events applies also to the RTP method. Let us call N_T the total

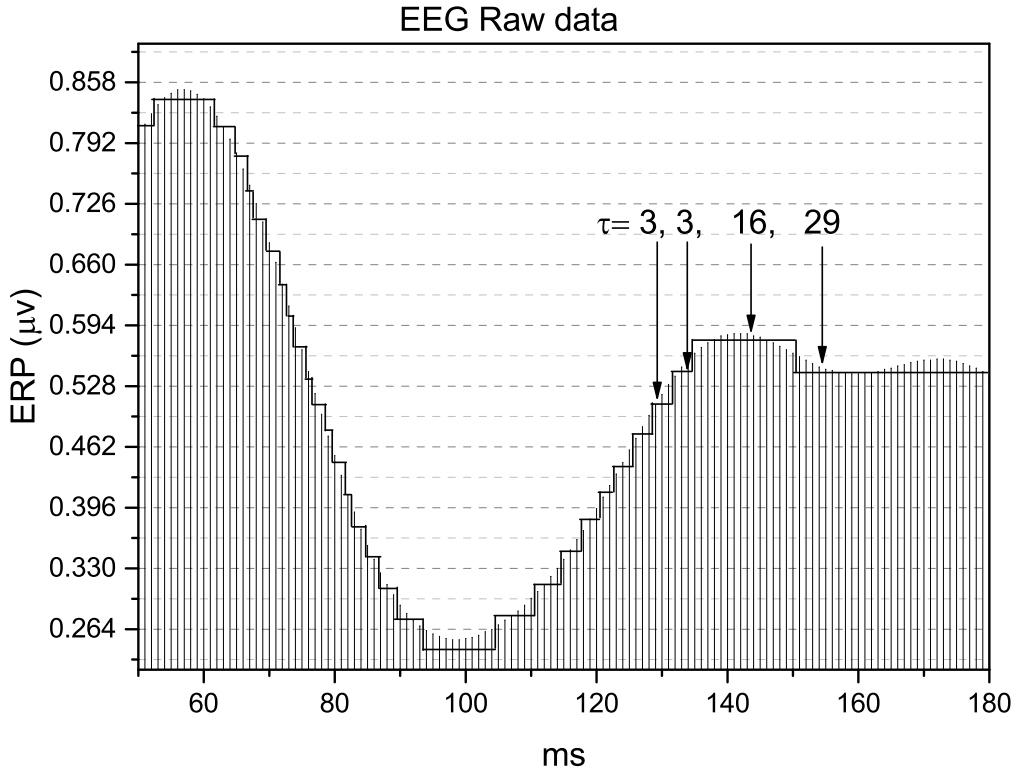

FIGURE 6.7. Illustration of the method of the stripes. The size of stripes is $\Delta E = 1/30$ μv.

number of events detected, N_c the total number of (unknown) crucial events and N_{nc} the total number of non-crucial, possibly Poisson events. The intermediate asymptotics, revealing the complex scaling δ of Eq. (6.5), begins earlier upon increase of the ratio

$$r_c \equiv \frac{N_c}{N_T}. \tag{6.18}$$

In both cases, the adoption of the DEA method is essential. In fact, after recording events with the method of the stripes, as done with the method of RTP, we adopt the prescription of Ref.[103]. We turn again the sequence of detected events, either crucial or not, into a diffusion signal $x(t)$ by making the random walker jumping ahead by a fixed quantity, equal to 1. As pointed out in Section 6.2, the non-crucial events generates a diffusion process with scaling $\delta = 0.5$ and the crucial events, on the contrary, generate the

scaling of Eq. (6.5) that for $\mu > 2$ is larger than 1/2, thereby making it possible for DEA to establish the correct scaling of Eq. (6.5) at long times.

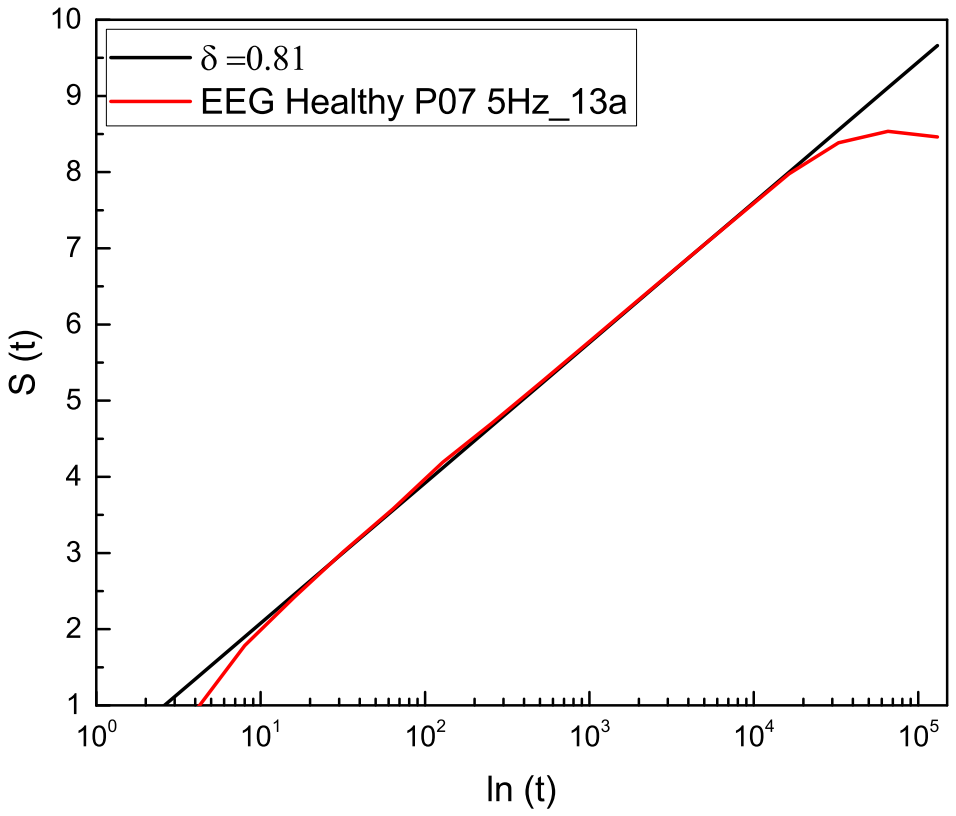

FIGURE 6.8. DEA applied to the diffusion process generated by the stripe-crossing events.

The result illustrated in Fig. 6.8 shows that the scaling detected with this method is virtually identical to the result obtained with the use of RTP method. In both cases the complex scaling of Eq. (6.5) appears in the intermediate time regime, but it appears that the present method is somewhat more accurate, since the slope covers three decades of scale, see Fig. 6.8, while the RTP method is limited to only two decades (Fig. 6.2). This is a clear indication that the method of stripes makes the ratio r_c of Eq. (6.18) significantly larger than the RTP method.

6.6. Concluding Remarks

The adoption of the RTP method makes it easy to establish the non-local nature of the brain criticality [91]. This is a consequence of the fact that it is sufficient to count how many electrodes undergo RTP's at the same times. However, the detailed illustration of Section 6.2 shows that the procedure to establish the occurrence of an RTP is not straightforward and we think that it may be replaced by the adoption of a cross-correlation function between the EEG generated by different electrodes. But this remains to be verified.

6.6.1. Self-Organized Temporal Criticality (SOTC)

The sausage-like structure of the model studied by Bologna *et al* [101] has a surprising similarity to the second panel from the top of Fig. 6.1. This is not accidental. In fact, the theory adopted by Bologna *et al* [101] is a phase transition obtained by assigning to the control parameter K the critical value $K = 1.5$. At criticality the oscillators are no longer independent of the others and as a result of highly correlated motion they generate a regular non-harmonic oscillation.

The SOTC is a new form of self-organization suggested by the observation Beig et al. [114]. When a system at criticality is assigned a distribution different from the equilibrium distribution, the system is expected to relax back towards equilibrium with infinitely slow motion, referred to as critical slowing down. At equilibrium, however, the mean field retains a fixed mean value. These observation apply when the system has an infinitely large number of units. When the number of units is finite the mean field fluctuates around the mean value. In the special case studied by Bologna et al. [101], when the mean field has a regular oscillation, the intensity of these oscillations and their frequency are modulated in time generating the sausage-like structure of the second panel from the top of Fig. 6.1. Subordination theory affords a simple way of mimicking this process of organization, introducing *ad hoc* the crucial events, which actually are the results of a spontaneous self-organization.

The processes of phase transitions are characterized by power laws with indices expressing the universality of criticality. The construction of renormalization group theory

made it possible to determine without a detailed knowledge of the the micro-interactions of the system, the scaling nature of phase transitions. In the case of the brain the micro-units, whose dynamics depart from the erratic behavior of independent units to collective behavior at criticality, are neurons. However, in spite of the frequent use of the term SOC these model rest on tuning a control parameter to critical value that establishes global properties making the micro-dynamics unimportant in favor the macro-dynamics of criticality. If a neuron fires all the neurons linked to it makes a step ahead towards the firing level. Criticality is a condition generated by a suitable value of the control parameter that establishes a complex dynamics characterized by temporal complexity, namely, the crucial events defined in Section 6.1. An interesting example of "Self-organized criticality" is given by Levina et al. [97]. They propose a very interesting model generating super-criticality and sub-criticality as well as criticality, a puzzling result because we expect that a process of self-organization may lead only to criticality. We make the conjecture that SOTC may realize this wide set of condition depending on how the process of self-organization is realized.

This work has been submitted to Frontiers in Physiology for the publication.

CHAPTER 7

CONCLUSION AND FUTURE WORKS

In conclusion, we have analyzed the human heartbeat time series and established that in fact the heartbeats are characterized by the occurrence of crucial and Poisson events. An increase in the percentage of crucial events makes the multifractal spectrum broader, thereby establishing the connection between crucial events and multifractality.

These results led us to focus our analysis on the statistical properties of crucial events. We have adopted the same statistical analysis to study the statistical properties of the heartbeat dynamics of subjects practicing meditation. The heartbeats of people doing meditation are known to produce coherent fluctuations. In addition to this effect, we made the surprising discovery that meditation makes the heartbeat depart from the ideal condition of 1/f noise.

We oberved that meditation does not suppress the occurrence of crucial events alongwith the well known fact that it creates "exaggerated heart rate oscillations" [73]. We already figured out in an earlier publication [65] that these crucial events are often embedded in a billow of uncorrelated and irrelevant events. This leads us to introduce the notion of dressing. Meaning of dressed crucial event is that the time interval between the crucial events are filled with poisson events. The exaggerated heart rate oscillations are the type of dressing induced by meditation. The selection of the strip method [65] facilitated the evaluation of the level of dressing by means of the measure $\in^2$. This allowed to illustrate $1- \in$ is the percent of Poisson events which affect the HRV time series. Allegrini et al. [28] conjectured that the Poisson events are the source of stress and the large quantity of such events as quantified by $\in^2$, i.e., stress, might be the reason for heart failure. According to this interpretation, one can conclude that the results of Fig. 5.7 demonstrate that Kundalini Yoga meditation significantly diminish the level of stress. Therefore, this study provides a method of analysis of HRV that might be utilized directly to evaluate the advantage of meditation, which are currently examined indirectly, through the observation of psychological health [74]. We

found also that the long-term practice of meditation has the effect of making permanent the meditation-induced physiological changes.

We also discussed how to combine the wave-like nature of the dynamics of the brain with the existence of crucial events that are responsible for the $1/f$ noise using subordination theory. Crucial events correspond to abrupt transitions in the wave-like structure of EEG's, requiring a complex procedure for their detection. We showed that that the anomalous scaling generated by the crucial events can be established by means of a direct analysis of raw data. The efficiency of the direct analysis procedure is made possible by the fact that periodicity and crucial events are the product of a spontaneous process of self-organization. We argue that the results of this study can be used to shed light into the nature of this process of self-organization.

Based on this examination, we intend to address the issue of heart-brain communication. We would bring up that our theoretical approach may make it conceivable to clarify why meditation has the impact of enhancing the energy of EEG alpha waves, as per observation [115], using Kriya Yoga, which is not the same as Kundalini Yoga.

Kundalini Yoga is known to be an efficient way to treat certain psychiatric disorders [116], but the therapists using this technique are looking for further improvements [117]. Varela and his co-workers according to which Buddhist philosophy, a source of meditation techniques is of fundamental importance in dealing with the ambitious field of cognition [83], which is similar to those examined in this study. Therefore we believe that this research approach plays an important role to the advancement of cognition science.

BIBLIOGRAPHY

[1] Sunny Y Auyang, *Foundations of complex-system theories: in economics, evolutionary biology, and statistical physics*, Cambridge University Press, 1999.

[2] Byron Hawk, *A counter-history of composition: Toward methodologies of complexity*, University of Pittsburgh Pre, 2007.

[3] Eric Bertin, *Statistical physics of complex systems*, Springer, 2016.

[4] Yaneer Bar-Yam, *Dynamics of complex systems*, vol. 213, Addison-Wesley Reading, MA, 1997.

[5] Shaun Bullett, Tom Fearn, and Frank Smith, *Dynamical and complex systems*, vol. 5, World Scientific, 2016.

[6] L Douglas Kiel, *Knowledge management, organizational intelligence and learning, and complexity*, Paris: Unesco (EOLSS), 2008.

[7] Ralph H Abraham, *The genesis of complexity*, World Futures 67 (2011), no. 4-5, 380–394.

[8] W Ross Ashby, *Principles of the self-organizing dynamic system*, The Journal of general psychology 37 (1947), no. 2, 125–128.

[9] J Schnakenberg, *G. nicolis und i. prigogine: Self-organization in nonequilibrium systems. from dissipative structures to order through fluctuations. j. wiley & sons, new york, london, sydney, toronto 1977. 491 seiten, preis*, vol. 82, Wiley Online Library, 1978.

[10] Jason Merritt, *Cellular automata as emergent systems and models of physical behavior*, (2012).

[11] Paolo Allegrini, Danilo Menicucci, Remo Bedini, Leone Fronzoni, Angelo Gemignani, Paolo Grigolini, Bruce J West, and Paolo Paradisi, *Spontaneous brain activity as a source of ideal 1/f noise*, Physical Review E 80 (2009), no. 6, 061914.

[12] Bruce J West, Elvis L Geneston, and Paolo Grigolini, *Maximizing information exchange between complex networks*, Physics Reports 468 (2008), no. 1, 1–99.

[13] Per Bak, Chao Tang, and Kurt Wiesenfeld, *Self-organized criticality: An explanation of the 1/f noise*, Physical review letters 59 (1987), no. 4, 381.

[14] Jerzy Letkowski, *Sa 12083 applications of the poisson probability applications of the poisson probability distribution*, 2012.

[15] C. Schulze, K. H. Hoffmann, and P. Sibani, *Aging phenomena in complex systems: A hierarchical model for temperature step experiments*, EPL (Europhysics Letters) 15 (1991), no. 3, 361.

[16] Mark EJ Newman, *Power laws, pareto distributions and zipf's law*, Contemporary physics 46 (2005), no. 5, 323–351.

[17] Adrian Drăgulescu and Victor M Yakovenko, *Exponential and power-law probability distributions of wealth and income in the united kingdom and the united states*, Physica A: Statistical Mechanics and its Applications 299 (2001), no. 1, 213–221.

[18] J Doyne Farmer and John Geanakoplos, *Power laws in economics and elsewhere*, Santa Fe Institute, 2008.

[19] Zoubin Ghahramani and Zoubin Ghahramani, *Entropy and mutual information*, (2007).

[20] J Borwein and M Rose, *Explainer: what is chaos theory*, Retrieved October 22 (2012), 2014.

[21] Joseph Klafter, Michael F Shlesinger, and Gert Zumofen, *Beyond brownian motion*, Physics today 49 (1996), no. 2, 33–39.

[22] Howard M Taylor and Samuel Karlin, *An introduction to stochastic modeling*, Academic press, 2014.

[23] Nicola Scafetta and Paolo Grigolini, *Scaling detection in time series: diffusion entropy analysis*, Physical Review E 66 (2002), no. 3, 036130.

[24] C-K Peng, Shlomo Havlin, H Eugene Stanley, and Ary L Goldberger, *Quantification of scaling exponents and crossover phenomena in nonstationary heartbeat time series*, Chaos: An Interdisciplinary Journal of Nonlinear Science 5 (1995), no. 1, 82–87.

[25] SM Ossadnik, SV Buldyrev, AL Goldberger, S Havlin, RN Mantegna, CK Peng, M Si-

mons, and HE Stanley, *Correlation approach to identify coding regions in dna sequences*, Biophysical Journal 67 (1994), no. 1, 64–70.

[26] Jan W Kantelhardt, Stephan A Zschiegner, Eva Koscielny-Bunde, Shlomo Havlin, Armin Bunde, and H Eugene Stanley, *Multifractal detrended fluctuation analysis of nonstationary time series*, Physica A: Statistical Mechanics and its Applications 316 (2002), no. 1, 87–114.

[27] Ary L Goldberger, Luis AN Amaral, Leon Glass, Jeffrey M Hausdorff, Plamen Ch Ivanov, Roger G Mark, Joseph E Mietus, George B Moody, Chung-Kang Peng, and H Eugene Stanley, *Physiobank, physiotoolkit, and physionet*, Circulation 101 (2000), no. 23, e215–e220.

[28] Paolo Allegrini, Paolo Grigolini, P Hamilton, Luigi Palatella, and G Raffaelli, *Memory beyond memory in heart beating, a sign of a healthy physiological condition*, Physical Review E 65 (2002), no. 4, 041926.

[29] Plamen Ch Ivanov, Luis A Nunes Amaral, Ary L Goldberger, Shlomo Havlin, Michael G Rosenblum, Zbigniew R Struzik, and H Eugene Stanley, *Multifractality in human heartbeat dynamics*, Nature 399 (1999), no. 6735, 461–465.

[30] A John Camm, Marek Malik, JT Bigger, G Breithardt, Sergio Cerutti, RJ Cohen, P Coumel, EL Fallen, HL Kennedy, RE Kleiger, et al., *Heart rate variability: standards of measurement, physiological interpretation and clinical use. task force of the european society of cardiology and the north american society of pacing and electrophysiology*, Circulation 93 (1996), no. 5, 1043–1065.

[31] Andrea Bravi, André Longtin, and Andrew JE Seely, *Review and classification of variability analysis techniques with clinical applications*, Biomedical engineering online 10 (2011), no. 1, 90.

[32] C-K Peng, Sergey V Buldyrev, Shlomo Havlin, Michael Simons, H Eugene Stanley, and Ary L Goldberger, *Mosaic organization of dna nucleotides*, Physical review e 49 (1994), no. 2, 1685.

[33] Giovanni Paladin and Angelo Vulpiani, *Anomalous scaling laws in multifractal objects*, Physics Reports 156 (1987), no. 4, 147–225.

[34] Didier Delignières, Zainy MH Almurad, Clément Roume, and Vivien Marmelat, *Multifractal signatures of complexity matching*, Experimental brain research 234 (2016), no. 10, 2773–2785.

[35] Stefano Zapperi, Kent Bækgaard Lauritsen, and H Eugene Stanley, *Self-organized branching processes: mean-field theory for avalanches*, Physical review letters 75 (1995), no. 22, 4071.

[36] Matteo Martinello, Jorge Hidalgo, Serena di Santo, Amos Maritan, Dietmar Plenz, and Miguel A Muñoz, *Neutral theory and scale-free neural dynamics*, arXiv preprint arXiv:1703.05079 (2017).

[37] Eugenio Lippiello, Lucilla de Arcangelis, and Cataldo Godano, *Memory in self-organized criticality*, EPL (Europhysics Letters) 72 (2005), no. 4, 678.

[38] Korosh Mahmoodi, Bruce J West, and Paolo Grigolini, *Self-organizing complex networks: individual versus global rules*, Frontiers in physiology 8 (2017), 478.

[39] Cai Shi-Min, Peng Hu, Yang Hui-Jie, Zhou Tao, Zhou Pei-Ling, and Wang Bing-Hong, *Scaling behaviour and memory in heart rate of healthy human*, Chinese Physics Letters 24 (2007), no. 10, 3002.

[40] Petr Jizba and Jan Korbel, *Multifractal diffusion entropy analysis: Optimal bin width of probability histograms*, Physica A: Statistical Mechanics and its Applications 413 (2014), 438–458.

[41] Jingjing Huang, Pengjian Shang, and Xiaojun Zhao, *Multifractal diffusion entropy analysis on stock volatility in financial markets*, Physica A: Statistical Mechanics and its Applications 391 (2012), no. 22, 5739–5745.

[42] A Yu Morozov, *Comment on ?multifractal diffusion entropy analysis on stock volatility in financial markets?[physica a 391 (2012) 5739–5745]*, Physica A: Statistical Mechanics and its Applications 392 (2013), no. 10, 2442–2446.

[43] Huijie Yang, Fangcui Zhao, Longyu Qi, and Beilai Hu, *Temporal series analysis approach to spectra of complex networks*, Physical Review E 69 (2004), no. 6, 066104.

[44] Yang Yujun, Li Jianping, and Yang Yimei, *Multiscale multifractal multiproperty analysis of financial time series based on rényi entropy*, International Journal of Modern Physics C 28 (2017), no. 02, 1750028.

[45] Jingjing Huang and Pengjian Shang, *Multiscale multifractal diffusion entropy analysis of financial time series*, Physica A: Statistical Mechanics and its Applications 420 (2015), 221–228.

[46] Daniel Mirman, Julia R Irwin, and Damian G Stephen, *Eye movement dynamics and cognitive self-organization in typical and atypical development*, Cognitive neurodynamics 6 (2012), no. 1, 61–73.

[47] James A Dixon, John G Holden, Daniel Mirman, and Damian G Stephen, *Multifractal dynamics in the emergence of cognitive structure*, Topics in Cognitive Science 4 (2012), no. 1, 51–62.

[48] Damian G Kelty-Stephen, Kinga Palatinus, Elliot Saltzman, and James A Dixon, *A tutorial on multifractality, cascades, and interactivity for empirical time series in ecological science*, Ecological Psychology 25 (2013), no. 1, 1–62.

[49] Damian G Stephen and Alen Hajnal, *Transfer of calibration between hand and foot: Functional equivalence and fractal fluctuations*, Attention, Perception, & Psychophysics 73 (2011), no. 5, 1302–1328.

[50] Salvatore Scellato, Mirco Musolesi, Cecilia Mascolo, and Vito Latora, *On nonstationarity of human contact networks*, Distributed Computing Systems Workshops (ICDCSW), 2010 IEEE 30th International Conference on, IEEE, 2010, pp. 105–111.

[51] A Sarkar and P Barat, *Effect of meditation on scaling behavior and complexity of human heart rate variability*, Fractals 16 (2008), no. 03, 199–208.

[52] Grigory Isaakovich Barenblatt, *Scaling, self-similarity, and intermediate asymptotics: dimensional analysis and intermediate asymptotics*, vol. 14, Cambridge University Press, 1996.

[53] Nigel Goldenfeld, *Lectures on phase transitions and the renormalization group*, CRC Press, 2018.

[54] Rosario N Mantegna and H Eugene Stanley, *Stochastic process with ultraslow convergence to a gaussian: the truncated lévy flight*, Physical Review Letters 73 (1994), no. 22, 2946.

[55] Ismo Koponen, *Analytic approach to the problem of convergence of truncated lévy flights towards the gaussian stochastic process*, Physical Review E 52 (1995), no. 1, 1197.

[56] Arijit Chakrabarty and Mark M Meerschaert, *Tempered stable laws as random walk limits*, Statistics & Probability Letters 81 (2011), no. 8, 989–997.

[57] Mark M Meerschaert, Parthanil Roy, and Qin Shao, *Parameter estimation for exponentially tempered power law distributions*, Communications in Statistics-Theory and Methods 41 (2012), no. 10, 1839–1856.

[58] Ravitej Uppu and Sushil Mujumdar, *Exponentially tempered lévy sums in random lasers*, Physical review letters 114 (2015), no. 18, 183903.

[59] S Burov, R Metzler, and E Barkai, *Aging and nonergodicity beyond the khinchin theorem*, Proceedings of the National Academy of Sciences 107 (2010), no. 30, 13228–13233.

[60] William Feller, *Fluctuation theory of recurrent events*, Transactions of the American Mathematical Society 67 (1949), no. 1, 98–119.

[61] Paolo Allegrini, Rita Balocchi, Santi Chillemi, Paolo Grigolini, Luigi Palatella, and Giacomo Raffaelli, *Short-and long-term statistical properties of heartbeat time-series in healthy and pathological subjects*, International Symposium on Medical Data Analysis, Springer, 2002, pp. 115–126.

[62] Plamen Ch Ivanov, Kang KL Liu, and Ronny P Bartsch, *Focus on the emerging new fields of network physiology and network medicine*, New Journal of Physics 18 (2016), no. 10, 100201.

[63] Gert Pfurtscheller, Andreas R Schwerdtfeger, Annemarie Seither-Preisler, Clemens Brunner, Christoph Stefan Aigner, Joana Brito, Marciano P Carmo, and Alexandre Andrade, *Brain–heart communication: Evidence for ?central pacemaker? oscillations*

with a dominant frequency at 0.1 hz in the cingulum, Clinical Neurophysiology 128 (2017), no. 1, 183–193.

[64] Rollin McCraty and Maria A Zayas, *Cardiac coherence, self-regulation, autonomic stability, and psychosocial well-being*, Frontiers in psychology 5 (2014).

[65] Gyanendra Bohara, David Lambert, Bruce J West, and Paolo Grigolini, *Crucial events, randomness, and multifractality in heartbeats*, Physical Review E 96 (2017), no. 6, 062216.

[66] Chow Susan, *Meditation history*, November 2015, [Online; posted 22-Nov-2015].

[67] Nicholas W Watkins, *On the continuing relevance of mandelbrot's non-ergodic fractional renewal models of 1963 to 1967*, The European Physical Journal B 90 (2017), no. 12, 241.

[68] Nicholas Wynn Watkins, *Mandelbrot's 1/f fractional renewal models of 1963–67: The non-ergodic missing link between change points and long range dependence*, International Work-Conference on Time Series Analysis, Springer, 2016, pp. 197–208.

[69] Benoit Mandelbrot, *Some noises with i/f spectrum, a bridge between direct current and white noise*, IEEE transactions on Information Theory 13 (1967), no. 2, 289–298.

[70] BB Mandelbrot, *Time varying channels, 1/f noises, and the infrared catastrophe: or why does the low frequency energy sometimes seem infinite*, Proceedings of the the 1st IEEE Annual Communications Convention, Boulder, CO, USA, 1965, pp. 7–9.

[71] Gianluca Ascolani, Mauro Bologna, and Paolo Grigolini, *Subordination to periodic processes and synchronization*, Physica A: Statistical Mechanics and its Applications 388 (2009), no. 13, 2727–2740.

[72] Mirko Lukovic and Paolo Grigolini, *Power spectra for both interrupted and perennial aging processes*, The Journal of chemical physics 129 (2008), no. 18, 184102.

[73] C-K Peng, Joseph E Mietus, Yanhui Liu, Gurucharan Khalsa, Pamela S Douglas, Herbert Benson, and Ary L Goldberger, *Exaggerated heart rate oscillations during two meditation techniques*, International journal of cardiology 70 (1999), no. 2, 101–107.

[74] Tim Gard, Jessica J Noggle, Crystal L Park, David R Vago, and Angela Wilson, *Po-*

tential self-regulatory mechanisms of yoga for psychological health, Frontiers in human neuroscience 8 (2014), 770.

[75] Mario Annunziato and Paolo Grigolini, *Stochastic versus dynamic approach to lévy statistics in the presence of an external perturbation*, Physics Letters A 269 (2000), no. 1, 31–39.

[76] Dobromir Dotov, Lin Nie, Kevin Wojcik, Anastasia Jinks, Xiaoyu Yu, and Anthony Chemero, *Cognitive and movement measures reflect the transition to presence-at-hand*, New Ideas in Psychology 45 (2017), 1–10.

[77] Martin Heidegger, *Being and time (j. macquarrie & e. robinson, trans.)*, 1962.

[78] Joshua Correll, *1/f noise and effort on implicit measures of bias.*, Journal of personality and social psychology 94 (2008), no. 1, 48.

[79] Paolo Allegrini, Paolo Paradisi, Danilo Menicucci, Marco Laurino, Andrea Piarulli, and Angelo Gemignani, *Self-organized dynamical complexity in human wakefulness and sleep: Different critical brain-activity feedback for conscious and unconscious states*, Physical Review E 92 (2015), no. 3, 032808.

[80] Sebastiano Stramaglia, Mario Pellicoro, Leonardo Angelini, Enrico Amico, Hannelore Aerts, JM Cortés, Steven Laureys, and Daniele Marinazzo, *Ising model with conserved magnetization on the human connectome: Implications on the relation structure-function in wakefulness and anesthesia*, Chaos: An Interdisciplinary Journal of Nonlinear Science 27 (2017), no. 4, 047407.

[81] Guillermo Solovey, Leandro M Alonso, Toru Yanagawa, Naotaka Fujii, Marcelo O Magnasco, Guillermo A Cecchi, and Alex Proekt, *Loss of consciousness is associated with stabilization of cortical activity*, Journal of Neuroscience 35 (2015), no. 30, 10866–10877.

[82] Dominik Krzemiński, Maciej Kamiński, Artur Marchewka, and Michał Bola, *Breakdown of long-range temporal correlations in brain oscillations during general anesthesia*, NeuroImage 159 (2017), 146–158.

[83] Francisco J Varela, Evan Thompson, and Eleanor Rosch, *The embodied mind: Cognitive science and human experience*, MIT press, 2017.

[84] Rohisha Tuladhar, Gyanendra Bohara, Paolo Grigolini, and Bruce J. West, *Meditation-induced coherence and crucial events*, Frontiers in Physiology 9 (2018), 626.

[85] David Papo, *Time scales in cognitive neuroscience*, Frontiers in Physiology 4 (2013), 86.

[86] David Papo, Massimiliano Zanin, José Angel Pineda-Pardo, Stefano Boccaletti, and Javier M. Buldú, *Functional brain networks: great expectations, hard times and the big leap forward.*, Philosophical transactions of the Royal Society of London. Series B, Biological sciences 369 1653 (2014).

[87] F Eugene Yates, *Order and complexity in dynamical systems: homeodynamics as a generalized mechanics for biology*, Mathematical and computer modelling 19 (1994), no. 6-8, 49–74.

[88] Tjeerd Boonstra, Biyu He, and Andreas Daffertshofer, *Scale-free dynamics and critical phenomena in cortical activity*, Frontiers in Physiology 4 (2013), 79.

[89] Enzo Tagliazucchi, Pablo Balenzuela, Daniel Fraiman, and Dante Chialvo, *Criticality in large-scale brain fmri dynamics unveiled by a novel point process analysis*, Frontiers in Physiology 3 (2012), 15.

[90] Matthew J Aburn, CA Holmes, James A Roberts, Tjeerd W Boonstra, and Michael Breakspear, *Critical fluctuations in cortical models near instability*, Frontiers in physiology 3 (2012), 331.

[91] Paolo Allegrini, P Paradisi, Danilo Menicucci, and Angelo Gemignani, *Fractal complexity in spontaneous eeg metastable-state transitions: New vistas on integrated neural dynamics*, 1 (2010), 128.

[92] Alexander Ya Kaplan, Andrew A Fingelkurts, Alexander A Fingelkurts, Sergei V Borisov, and Boris S Darkhovsky, *Nonstationary nature of the brain activity as revealed by eeg/meg: methodological, practical and conceptual challenges*, Signal processing 85 (2005), no. 11, 2190–2212.

[93] Michael D Rugg, *Erp studies of memory.*, Oxford University Press, 1995.

[94] Ariel Haimovici, Enzo Tagliazucchi, Pablo Balenzuela, and Dante R Chialvo, *Brain organization into resting state networks emerges at criticality on a model of the human connectome*, Physical review letters 110 (2013), no. 17, 178101.

[95] Enzo Tagliazucchi, Pablo Balenzuela, Daniel Fraiman, and Dante R Chialvo, *Criticality in large-scale brain fmri dynamics unveiled by a novel point process analysis*, Frontiers in physiology 3 (2012), 15.

[96] Anna Levina, J Michael Herrmann, and Theo Geisel, *Dynamical synapses causing self-organized criticality in neural networks*, Nature physics 3 (2007), no. 12, 857.

[97] ———, *Phase transitions towards criticality in a neural system with adaptive interactions*, Physical review letters 102 (2009), no. 11, 118110.

[98] Serena di Santo, Pablo Villegas, Raffaella Burioni, and Miguel A Muñoz, *Landau–ginzburg theory of cortex dynamics: Scale-free avalanches emerge at the edge of synchronization*, Proceedings of the National Academy of Sciences 115 (2018), no. 7, E1356–E1365.

[99] Ana Matran-Fernandez and Riccardo Poli, *Towards the automated localisation of targets in rapid image-sifting by collaborative brain-computer interfaces*, PloS one 12 (2017), no. 5, e0178498.

[100] Norden Eh Huang, *Hilbert-huang transform and its applications*, vol. 16, World Scientific, 2014.

[101] Mauro Bologna, Elvis Geneston, Paolo Grigolini, Malgorzata Turalska, and Mirko Lukovic, *Coherence and complexity*, Decision Making: A Psychophysics Application of Network Science, World Scientific, 2011, pp. 119–134.

[102] Paolo Allegrini, Danilo Menicucci, Remo Bedini, Angelo Gemignani, and Paolo Paradisi, *Complex intermittency blurred by noise: theory and application to neural dynamics*, Physical Review E 82 (2010), no. 1, 015103.

[103] Paolo Grigolini, Luigi Palatella, and Giacomo Raffaelli, *Asymmetric anomalous dif-*

fusion: an efficient way to detect memory in time series, Fractals 9 (2001), no. 04, 439–449.

[104] Korosh Mahmoodi, Bruce J West, and Paolo Grigolini, *Self-organized temporal criticality: Bottom-up resilience versus top-down vulnerability*, Complexity 2018 (2018).

[105] K Mahmoodi, P Grigolini, and BJ West, *On social sensitivity to either zealot or independent minorities*, Chaos, Solitons & Fractals 110 (2018), 185–190.

[106] Grigory Isaakovich Barenblatt, *Scaling, self-similarity, and intermediate asymptotics: dimensional analysis and intermediate asymptotics*, vol. 14, Cambridge University Press, 1996.

[107] Yoshiki Kuramoto, *Self-entrainment of a population of coupled non-linear oscillators*, International symposium on mathematical problems in theoretical physics, Springer, 1975, pp. 420–422.

[108] Paolo Allegrini, Danilo Menicucci, Remo Bedini, Leone Fronzoni, Angelo Gemignani, Paolo Grigolini, Bruce J West, and Paolo Paradisi, *Spontaneous brain activity as a source of ideal 1/f noise*, Physical Review E 80 (2009), no. 6, 061914.

[109] Gennady Margolin and Eli Barkai, *Nonergodicity of a time series obeying lévy statistics*, Journal of statistical physics 122 (2006), no. 1, 137–167.

[110] Elliott W Montroll and George H Weiss, *Random walks on lattices. ii*, Journal of Mathematical Physics 6 (1965), no. 2, 167–181.

[111] Michael F Shlesinger, *Origins and applications of the montroll-weiss continuous time random walk*, The European Physical Journal B 90 (2017), no. 5, 93.

[112] IM Sokolov, *Lévy flights from a continuous-time process*, Physical Review E 63 (2000), no. 1, 011104.

[113] R. Tuladhar B. J. West P. Grigolini D. Lambert, M. Bologna, *Joint action of periodicity and ergodicity breaking crucial events: Spectrum evaluation*, J. Math. Phys. (208).

[114] MT Beig, A Svenkeson, M Bologna, BJ West, and P Grigolini, *Critical slowing down in networks generating temporal complexity*, Physical Review E 91 (2015), no. 1, 012907.

[115] Sushil Chandra, Amit Kumar Jaiswal, Ram Singh, Devendra Jha, and Alok Prakash

Mittal, *Mental stress: Neurophysiology and its regulation by sudarshan kriya yoga*, International journal of yoga 10 (2017), no. 2, 67.

[116] David S Shannahoff-Khalsa, *An introduction to kundalini yoga meditation techniques that are specific for the treatment of psychiatric disorders*, The Journal of Alternative & Complementary Medicine 10 (2004), no. 1, 91–101.

[117] Manjit K Khalsa, Julie M Greiner-Ferris, Stefan G Hofmann, and Sat Bir S Khalsa, *Yoga-enhanced cognitive behavioural therapy (y-cbt) for anxiety management: a pilot study*, Clinical psychology & psychotherapy 22 (2015), no. 4, 364–371.